Distribution Agreement

In presenting this thesis or dissertation as a partial fulfillment of the requirements for an advanced degree from Emory University, I hereby grant to Emory University and its agents the non-exclusive license to archive, make accessible, and display my thesis or dissertation in whole or in part in all forms of media, now or hereafter known, including display on the world wide web. I understand that I may select some access restrictions as part of the online submission of this thesis or dissertation. I retain all ownership rights to the copyright of the thesis or dissertation. I also retain the right to use in future works (such as articles or books) all or part of this thesis or dissertation.

Signature:

_____ _____

Joel Eggert Date

Adaptations to Tonic T Cell Receptor Signaling in
Naive T Cells

By

Joel Eggert
Doctor of Philosophy

Graduate Division of Biological and Biomedical Sciences
Immunology and Molecular Pathogenesis

_____

Byron Au-Yeung, Ph.D.
Advisor

_____

Luisa Cervantes-Barragan, Ph.D.
Committee Member

_____

Arash Grakoui, Ph.D.
Committee Member

_____

Haydn Kissick, Ph.D.
Committee Member

_____

Chrystal Paulos, Ph.D.
Committee Member

Accepted:

_____

Kimberly Jacob Arriola, Ph.D, MPH
Dean of the James T. Laney School of Graduate Studies

_____

Date

Adaptations to Tonic T Cell Receptor Signaling in Naive T Cells

By

Joel Eggert

B.S. Uppsala University, 2015
M.Sc. Ludwig Maximilian University of Munich, 2017

Advisor: Byron Au-Yeung, Ph.D.

An abstract of
A dissertation submitted to the Faculty of the
James T. Laney School of Graduate Studies of Emory University
In partial fulfillment of the requirements for the degree of
Doctor of Philosophy
In Graduate Division of Biological and Biomedical Science
Immunology and Molecular Pathogenesis
2023

Abstract

Adaptations to Tonic T Cell Receptor Signaling in Naive T Cells

By Joel Eggert

Naive T cells experience recurrent TCR:self-pMHC signals in the steady state, termed tonic signaling. Such signals are generally inadequate to promote canonical T cell activation. Still, they are sufficient to modulate proximal TCR signaling and induce gene expression changes and epigenetic modifications of naive T cells. Therefore, tonic TCR signals have implications for the responsiveness and differentiation of naive T cells following canonical T cell activation. However, how extensive tonic TCR signaling affects naive $CD8^+$ T cells upon subsequent agonist TCR stimulation remains unresolved. We investigated the heterogeneity and functional implications of tonic TCR signal strength in naive $CD8^+$ T cells by utilizing a transcriptional reporter of *Nr4a1* (Nur77-GFP) reflective of TCR signaling. We found that naive $CD8^+$ T cells experience highly variable levels of tonic TCR signaling strength as measured by Nur77-GFP fluorescence intensity. Consistent with Nur77-GFP expression as an indicator of TCR signaling, GFP^{HI} cells exhibited a gene expression profile more indicative of T cell activation than GFP^{LO} cells. However, the cells that experienced the most extensive tonic TCR signaling (GFP^{HI} cells) exhibited diminished IFN-γ and IL-2 secretion in response to agonist TCR ligand stimulation relative to GFP^{LO} cells. The attenuated responsiveness of GFP^{HI} cells correlated with increased protein levels of Cbl-b, a negative regulator of TCR signaling. Deficiency of *Cbl-b* partly restored the responsiveness of naive $CD8^+$ GFP^{HI} cells. Our data suggests that extensive tonic TCR signaling induces adaptations of naive $CD8^+$ T cells that attenuate the responsiveness to agonist TCR stimulation. Furthermore, negative regulation induced by strong TCR:self-pMHC signals partly depends on Cbl-b expression. We propose that this de-sensitization of naive T cells may allow the immune system to limit the autoreactive potential of the most self-reactive naive $CD8^+$ T cells.

Adaptations to Tonic T Cell Receptor Signaling in Naive T Cells

By

Joel Eggert

B.S. Uppsala University, 2015
M.Sc. Ludwig Maximilian University of Munich, 2017

Advisor: Byron Au-Yeung, Ph.D.

A dissertation submitted to the Faculty of the
James T. Laney School of Graduate Studies of Emory University
In partial fulfillment of the requirements for the degree of
Doctor of Philosophy
In Graduate Division of Biological and Biomedical Science
Immunology and Molecular Pathogenesis
2023

Acknowledgments

First and foremost, I would like to thank my supervisor, **Byron Au-Yeung**, for never-ending support and encouragement. I have learned such a great deal from you. You are a brilliant scientist, a great mentor, but much more importantly, one of the kindest people I have ever met. I will work on my Checkers game for a few years to have a fighting chance next time.

I want to thank **Wendy Zinzow-Kramer** for being the best lab mate I could ever ask for. You are greatly missed, but I am excited to see what you come up with in your new scientific home (Matt is lucky to have you on his team). **Anting Chen**, you are an incredibly talented and inspiring person. I have zero doubt that you will accomplish amazing things in the future.

I would also like to acknowledge and thank my thesis committee, **Luisa Cervantes-Barragan**, **Arash Grakoui**, **Haydn Kissick**, and **Chrystal Paulos**, for great discussions and helpful suggestions. I am truly grateful for all the advice and support I have received over the years.

I also thank the Pediatrics/Winship Flow Cytometry Core, the most extraordinary core facility I have ever utilized (sorry, Wichtl). Thank you to all current and past members of the core, such as **Aaron Rae**, **Lisa Bixby**, **Prasanthi Chappa**, **Juan Bustamente**, and **Erich Williams**, who helped out so extensively. Without the countless hours spent here, there would (almost) be no experiments in the first place.

I am also grateful for all the excellent scientists and people I had the opportunity to work with in Uppsala and Munich. I want to thank **Dirk Busch** for letting me be part of his outstanding research

group and for further support after I left. I will forever be grateful to my extraordinary mentors at the time: **Kilian Schober** and **Simon Grassmann**. I thank **Nicolas Gompel** for being such a great mentor at LMU and **Reinhard Obst** for introducing me to Behring and Kitasato's 1898 paper in the magnificent seminar course that propelled me in the direction of immunology. I am grateful to **Dan Larhammar** for the opportunity to train in his lab and for his continued support. I want to especially thank **Xesús Abalo**, for without his passion and excitement for any experiment, big or small, I am not sure I would have pursued scientific research.

Finally, I would like to thank my family and friends. To **Mom**, **Dad**, **Björn**, **Ami**, **Gabriel**, **Simon**, **Anders**, **Vick**, and everyone else (ingen nämnd, ingen glömd) for enormous support. **Tony** and **Abhinav**, I am so grateful and happy you could make it this summer. To **my new family**, for being so great. To **Peter**, **Oliver**, and **Asaada**, for keeping me more busy with the important stuff of life instead of the busy stuff of life. How I found you is beyond my understanding.

Table of Contents

Table of Figures

Chapter 1: Introduction

Sections of this chapter have been published:

Eggert, J., and B.B. Au-Yeung. 2021. Functional heterogeneity and adaptation of naive T cells in response to tonic TCR signals. *Curr Opin Immunol* 73:43-49.

T cells are part of the adaptive immune response and are a crucial component of the host response to infections and cancer (1). Infants born with primary immunodeficiencies resulting in the absence of T cells illustrate the importance of T cells for the human immune system. Such patients are susceptible to opportunistic infections, and survival depends on immune reconstitution during their first few months of age (2). Likewise, the loss of a subset of T cells due to human immunodeficiency viruses leads to impaired cellular immunity and susceptibility to opportunistic infections (3). While T cells help protect the host against exogenous threats such as pathogens or endogenous ones such as aberrant host cells, dysregulation of the T cell response is associated with several autoimmune diseases (4). Hence, the activation of T cells must be strictly controlled to prevent any responses to non-malignant self.

The composition of T cells in secondary lymphoid organs (SLOs) in both mice and humans is primarily composed of T cells expressing a T cell receptor (TCR) consisting of an α-chain and a β-chain (5, 6). The TCR αβ heterodimer linked by a disulfide bond associates with the CD3 complex consisting of CD3ζ homodimers and CD3γε and CD3δε heterodimers (7-10). The CD3 complex is essential for initiating TCR signaling, whereas the αβ heterodimer mediates antigen recognition and thus provides the specificity of the T cell (11-14). T cells recognize peptides derived from foreign or host proteins situated in a binding cleft of host glycoproteins termed Major Histocompatibility Complex (pMHC) (15-17). Two main subsets of T cells harbor distinctive

surface phenotypes (18-20). T cells expressing the surface protein CD4 recognize peptides presented by MHC class II whereas T cells expressing CD8 recognize peptides in the context of MHC class I (21-24).

All αβ T cells are positively selected in the thymus for weak reactivity to self-peptide antigens presented by self-pMHC during development (25-28). Naive $CD4^+$ and $CD8^+$ T cells continue to experience low-level T cell receptor (TCR) signaling in response to self-pMHC in the periphery, termed *basal* or *tonic* signaling (29, 30). Tonic TCR signaling is sufficient to induce constitutive tyrosine phosphorylation of immunoreceptor tyrosine-based activation motifs (ITAMs) in the TCR CD3 complex and ZAP-70 recruitment to phosphorylated ζ-chains (31-33). ZAP-70-bound phosphorylated ζ-chains are detectable in $CD4^+$ T cells isolated from lymph nodes but not from peripheral blood (33). Conditional depletion of conventional dendritic cells (cDCs) also reduces the phosphorylated ζ-chains associated with ZAP-70 in $CD4^+$ T cells during steady-state conditions with ~50% (34). Moreover, $CD4^+$ T cells from germ-free mice exhibit ζ-chain phosphorylation similar to T cells isolated from specific-pathogen-free mice (35). This finding indicates that antigens from commensal bacteria are not a primary driver of tonic TCR signaling. Together, these studies thus suggest that tonic TCR signaling occurs in SLOs mediated mainly by interactions with self-pMHC presented by DCs.

The phosphorylation of ZAP-70 is an early signal transduction step of canonical TCR signaling rapidly induced after agonist TCR stimulation (36, 37). Although ZAP-70 associates with phosphorylated ζ-chains in T cells isolated from steady-state conditions, ZAP-70 phosphorylation is below the limit of detection by western blotting, contrary to cells that experienced canonical TCR signaling (32). Weak-affinity pMHC stimulation of T cells likewise induces phosphorylation

of ζ-chains but not detectable phosphorylation of ZAP-70 and the resulting production of IL-2 or clonal expansion (38). Although tonic TCR signaling does not induce ZAP-70 phosphorylation and the subsequent initiation of the downstream signaling cascade, multiple studies illustrate how self-pMHC:TCR signals during steady-state conditions can modulate T cell responsiveness. For instance, total deprivation of tonic TCR signals mediated by adoptive transfer of T cells into MHC deficient recipients or antibody-blocking of MHC affects T cell responsiveness (33, 39-42). For $CD8^+$ T cells, deprivation of MHC I signals leads to enhanced sensitivity to weak affinity pMHC:TCR signals (39). However, such studies on $CD4^+$ T cells have reached conflicting results. For example, transferring $CD4^+$ T cells into T cell- and MHC II-deficient mice resulted in enhanced calcium flux upon TCR ligation (40). On the other hand, antibody-mediated blocking of MHC II in lymphoreplete mice resulted in reduced proliferation and IL-2 secretion upon activation (33). Whether the different lymphopenic versus lymphoreplete experimental environments or the distinct readouts of T cell activation drive the conflicting results from these studies is unclear. In either case, these studies on $CD4^+$ and $CD8^+$ T cells suggest that the complete absence of tonic TCR signals affects T cell reactivity to subsequent stimulation.

More recent studies have focused on how self-pMHC:TCR signal strength influences T cell responses. For instance, the strength of tonic signaling naive T cells experience correlates with epigenetic modifications, transcriptional and protein gene expression changes, and metabolic activity (43, 44). A growing body of evidence suggests that tonic TCR signal strength experienced before cognate antigen exposure influence primary and secondary responses of T cells (30). Here, we discuss recent advances in our understanding of how tonic TCR signaling is detected, how naive T cells adapt to varying tonic TCR signal strengths, and the impact on effector responses.

Markers of tonic signaling

CD5

CD5 is a scavenger receptor expressed on the surface of T cells, certain B cell lymphomas and B cell subsets, and various DCs in mice and humans (45). Studies in vitro have shown that several ligands can bind CD5, such as CD72, antibody framework regions, fungal cell wall components, and CD5 itself (46-49). However, the physiological relevancy in vivo of these reported ligands identified in vitro remains inconclusive (50). Regardless of CD5-ligand interactions, TCR stimulation can induce tyrosine phosphorylation of the cytoplasmic tail of CD5 (51). Moreover, recruitment of CD5 to the immune synapse occurs upon T cell activation (52). Initial studies that characterized the function of CD5 in T cells reported that cells stimulated with anti-CD3 and anti-CD5 antibodies exhibited enhanced T cell activation compared to cells stimulated with only anti-CD3 (53, 54). Hence, the interpretation from these studies was that CD5 acts as a positive regulator of TCR signaling. However, subsequent studies utilizing CD5-deficient transgenic mice found that $CD5^{-/-}$ thymocytes were hyperresponsive to TCR stimulation (55). CD5-deficient thymocytes, or T cell hybridomas expressing a mutated CD5 protein with a truncated cytoplasmic domain, were similarly hyperresponsive to TCR stimulation (56, 57). These results suggest that signaling events mediated by CD5 upon TCR engagement can inhibit TCR signaling in thymocytes. Although some uncertainty remains about whether CD5 could modulate TCR signaling differently in thymocytes versus mature T cells, CD5 is mainly considered a negative regulator of TCR signals in developing and mature T cells (45). For instance, the E3 ubiquitin ligases and negative regulators of TCR signaling, c-Cbl, and Cbl-b, are recruited to the cytoplasmic domain of CD5 upon T cell activation (58-62). The role of CD5 as a regulator of TCR signaling is discussed in more detail in later sections.

An elegant study by Paul Love's laboratory first described the positive correlation between TCR

signal strength and CD5 surface expression in thymocytes by generating transgenic ζ-chain-deficient mice reconstituted with a full-length ζ-chain versus a truncated ζ-chain with no ITAM domains (63). In this system, thymocytes exhibiting attenuated TCR signaling due to the reduced number of ITAMs of the CD3 complex expressed lower surface levels of CD5 (63). Likewise, studies utilizing TCR transgenic T cells in systems that modulated TCR signal strength in developing T cells by altering MHC haplotypes or restricting the peptide repertoire found a positive correlation between the affinity of the self-pMHC:TCR interaction and CD5 expression (57, 64). Hence, these studies showed that CD5 expression is a correlate marker of TCR signal strength during development. Later studies also revealed that surface expression of CD5 positively correlates with the strength of tonic TCR signaling naive, mature T cells experience (35). Naive $CD4^+$ and $CD8^+$ T cells expressing the highest levels of CD5 exhibit increased ζ-chain phosphorylation compared to $CD5^{LO}$ cells (35). The magnitude of CD5 expression can vary between T cells with different TCR specificities, as demonstrated by comparing TCR transgenic populations (35). However, CD5 expression and TCR specificity are not strictly linked, as two TCR transgenic strains can recognize the same *Listeria monocytogenes* epitope with similar affinity but exhibit different surface levels of CD5 (65, 66). In sum, CD5 has been a useful marker to identify T cells that experience relatively weak or strong tonic signaling.

Reporters of *Nr4a*

The immediate early gene *Nr4a1* (encoding Nur77) is an orphan nuclear receptor in the same family as *Nr4a2* (encoding Nurr1) and *Nr4a3* (encoding Nor1) (67). The DNA binding domains of Nurr1 and Nor1 share over 90% sequence homology to the Nur77 counterpart, and all three transcription factors bind similar DNA motifs (68, 69). Proposedly, *Nr4a* receptors may be transcriptionally active constitutively, independent of any ligand binding (70). Antigen-receptor

stimulation, but not cytokine stimulation, induces expression of *Nr4a1* in T and B cells (71, 72). Two Nur77-GFP reporter transgenes have been independently generated (71, 72). Like CD5, Nur77-GFP expression is initiated during thymic development and maintained in mature peripheral T cells (71, 73). The level of basal Nur77-GFP in naive T cells is relatively stable short-term, as the majority of sorted cells retain similar Nur77-GFP intensity ten days after adoptive transfer into WT recipients, but not in MHC II-deficient hosts (71, 73). Stimulation with cognate pMHC or TCR crosslinking antibodies leads to rapid upregulation of Nur77-GFP expression (71, 74). While Nur77-GFP expression is sensitive to TCR stimulation induced by self-pMHC interactions, Bending and colleagues recently showed that *Nr4a3* reporter expression is two- to threefold less sensitive to TCR stimulation and is selectively activated by cognate pMHC stimulation (75).

Beyond inducing transcription, Nur77, and Nor1 can also promote apoptosis by translocating to the mitochondria and inducing a conformational change of Bcl-2 that uncovers a Bcl-2 pro-apoptotic domain (76-79). Induced constitutive expression of WT Nur77 or Nor1 sensitizes thymocytes to activation-induced apoptosis (68, 80). In contrast, the constitutive expression of a dominant-negative Nur77 mutant leads to impaired negative selection and clonal deletion of developing T cells (80-82). These studies thus suggest that extensive TCR signaling in thymocytes induces Nur77 and Nor1 expression that promotes apoptosis and the negative selection of highly self-reactive thymocytes during development. Even mixed bone marrow chimeras consisting of WT and $Nr4a1^{-/-}$ $Nr4a3^{-/-}$ bone marrow develop systemic autoimmunity over time despite having a WT T_{reg} compartment (83). When CD4 expression drives the Cre-recombinase-driven deletion of Nr4a1 and Nr4a3 in these chimeras, the deletion event occurs in thymocytes at the double-positive (DP) stage (84). Such chimeras exhibit a peripheral $CD8^+$ T cell compartment primarily

consisting of $CD44^{HI}$ antigen-experienced $CD8^+$ T cells (83). However, CD8-cre-mediated deletion of Nr4a1 and Nr4a3 in CD8 single-positive (SP) thymocytes results in a CD8 T cell compartment mainly consisting of naive T cells similar to WT animals (83, 85). Such targeted Cre-expression is attainable due to a CD8α enhancer that is active and drives Cre-expression in mature $CD8^+$ T cells and CD8 SP but not in DP thymocytes (85). The absence of Nur77 and Nor1 during the negative selection of DP thymocytes severely hinders the deletion of highly self-reactive thymocytes leading to a more self-reactive TCR repertoire with a majority of naive $CD8^+$ T cell clones becoming activated by strong self-pMHC:TCR signaling during steady-state conditions. On the contrary, deletion of Nr4a1 and Nr4a3 at the CD8 SP stage enables Nur77 and Nor1 expression in DP thymocytes, facilitating negative selection of highly self-reactive $CD8^+$ T cells and thus restoring central tolerance.

The *Nr4a* transcription factors are also crucial for the differentiation of CD4 helper cells into regulatory T cells (T_{regs}) (86). Single knockout *Nr4a1*$^{-/-}$, *Nr4a2*$^{-/-}$, and *Nr4a3*$^{-/-}$ mice exhibit no reduction of thymic and peripheral T_{reg} populations and do not develop autoimmune disease (86, 87). However, mice with *Nr4a1*- and *Nr4a3*-deficient T cells have severely reduced T_{reg} frequencies and die within a month of birth due to systemic autoimmune pathology (86). Other double knockout combinations in T cells (*Nr4a1*$^{-/-}$ *Nr4a2*$^{-/-}$ or *Nr4a2*$^{-/-}$ *Nr4a3*$^{-/-}$) do not promote apparent autoimmunity in mice (86). These studies suggest that *Nr4a1* and *Nr4a3* have critical but redundant roles in T_{reg} development. Moreover, *Nr4a* factors also promote a T_{reg} fate in highly self-reactive thymocytes that have avoided negative selection (88). By utilizing a CD4 TCR transgenic T cell clone that exhibits minimal signs of negative selection, Sekiya and colleagues could identify thymocytes that expressed phenotypic markers associated with T_{reg} precursor cells in *Nr4a1*$^{-/-}$ *Nr4a2*$^{-/-}$ *Nr4a3*$^{-/-}$ (TKO) thymocytes (88, 89). However, T_{reg}-fated TKO thymocytes

failed to upregulate Foxp3 protein expression and could not mount sustained Foxp3 mRNA expression in response to IL-2 stimulation (88). Furthermore, polyclonal T_{reg} precursors from *Nr4a* TKO mice induced wasting disease in lymphopenic recipients, contrary to the WT counterparts (88). These studies suggest that the *Nr4a* family of genes is essential for directing highly self-reactive thymocytes that have escaped negative selection into the T_{reg} lineage, thus mitigating their differentiation into pathogenic and autoreactive T cells.

The expression of Nr4a transcription factors is also crucial for the function of mature T_{regs}. While mice that harbor a T_{reg}-specific deletion of all three *Nr4a* genes exhibit regular T_{reg} frequencies, they die within four months of birth due to systemic autoimmunity (90). *Nr4a* TKO T_{regs} exhibit attenuated suppressive function and are more likely to turn off Foxp3 expression (90). Hence, the *Nr4a* factors play an essential role beyond T_{reg} development in ensuring T_{reg} suppression and the maintenance of Foxp3 expression and commitment to the T_{reg} lineage. Thus, these studies indicate that the *Nr4a* family genes contribute to central and peripheral tolerance in several ways. First, by promoting highly self-reactive thymocytes to undergo apoptosis and negative election. Second, by fostering self-reactive thymocytes that escape negative selection to differentiate into T_{regs}, and third, by ensuring mature T_{regs}' functional capabilities and commitment in the periphery. The role of the *Nr4a* genes as a regulator of TCR signaling in the context of peripheral tolerance is discussed in later sections.

Ly6C

Ly6C1 and Ly6C2 are two homologous GPI-linked receptors with unknown functions that are currently not distinguishable from each other with monoclonal antibodies and are often collectively referred to as Ly6C (91). Various murine immune cells express Ly6C, such as $CD4^+$ and $CD8^+$ T cells, NK cells, neutrophils, subsets of monocytes, DCs, and stromal cells like

medullary thymic epithelial cells (92, 93). A subpopulation of naive $CD4^+$ T cells upregulates Ly6C expression shortly after thymic egress (94). In contrast to CD5 and Nur77-GFP, Ly6C expression *inversely* correlates with $CD4^+$ T cell reactivity to self-pMHC, as demonstrated by decreased ζ-chain phosphorylation in $Ly6C^+$ naive $CD4^+$ T cells (**Fig. 1.1**) (94). Moreover, the adoptive transfer of naive $Ly6C^-$ $CD4^+$ T cells into MHC II-deficient recipients leads to upregulation of Ly6C (73). Hence, Ly6C surface levels in naive $CD4^+$ T cells depend on the exposure to TCR:self-pMHC signals. Mechanistically, the downregulation of Ly6C expression depends on TCR-induced Ca^{2+} signaling (95). Within the T_{reg} population, Ly6C expression also marks a subset of $Foxp3^+$ cells that experience weaker tonic signaling and exhibit decreased

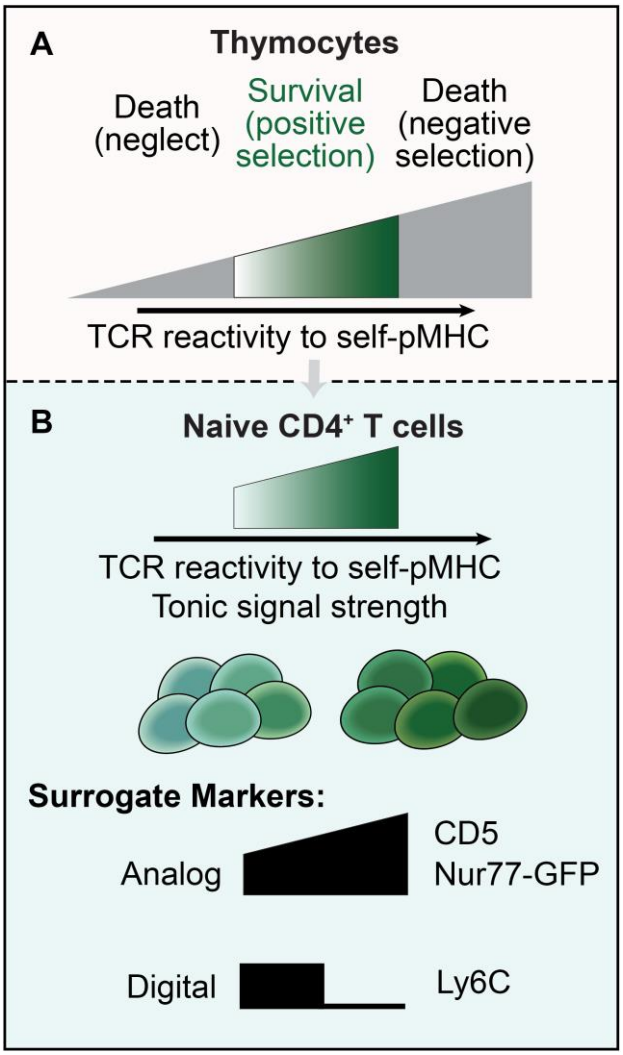

Fig. 1.1. TCR reactivity to self-pMHC during development and in the periphery.

(**A**) There is a broad range of self-reactivity in the immature $CD4^+$ $CD8^+$ double-positive population. Positively selected thymocytes (in green) exhibit self-reactivity that is neither too weak nor too strong. (**B**) Self-reactivity persists in the periphery, and naive $CD4^+$ T cells experience varying strengths of tonic TCR signaling. Surrogate markers of tonic signal strength in mice include CD5, Ly6C, and the Nur77-GFP transgene.

suppressive activity (96, 97). Furthermore, effector $CD4^+$ T cells are heterogeneous regarding Ly6C expression (98-102). Briefly, T follicular helper cells are $Ly6C^-$ whereas subsets of Th1 cells are both $Ly6C^-$ and $Ly6C^+$ (99, 102, 103). As effector $CD4^+$ T cells that experience strong TCR signaling during an acute infection exhibit bimodal Ly6C expression, TCR signaling strength does not seem to correlate strongly with Ly6C expression on effector $CD4^+$ T cells.

For $CD8^+$ T cells, Ly6C upregulation can occur at the CD8 SP stage in the thymus but is more noticeable in the periphery among naive $CD8^+$ T cells (104, 105). Contrary to $CD4^+$ T cells, deprivation of tonic TCR signals in naive $CD8^+$ T cells upon adoptive transfer to recipients with nearly absent MHC class I expression correlates with Ly6C downregulation (104). Thus, for naive $CD8^+$ T cells, tonic TCR signals are crucial for Ly6C surface expression. Furthermore, naive $CD8^+$ T cells expressing low CD5 levels are almost exclusively Ly6C-negative (104, 105). Therefore, LyC6 expression in naive $CD8^+$ T cells may positively correlate with tonic TCR signal strength, whereas the opposite is true for naive $CD4^+$ T cells. Consistent with these findings, T cell activation induced by TCR crosslinking in vitro induces upregulation of Ly6C in $CD8^+$ but not in $CD4^+$ T cells (106).

For both $CD4^+$ and $CD8^+$ naive T cells, modulation of surface Ly6C expression can occur in the absence of TCR agonist stimulation. Naive $CD4^+$ and $CD8^+$ T cells treated with type I interferon (IFN) upregulate Ly6C (104-106). Moreover, $CD8^+$ T cells deficient in the type I IFN receptor or the downstream transcription factor STAT1 exhibit severely reduced frequencies of $Ly6C^+$ cells during steady-state conditions suggesting that type I IFN signaling contributes either directly or indirectly to Ly6C expression in $CD8^+$ T cells (104, 105). One caveat with these studies is that general rather than T cell-specific knockout mice were used to study animals with defective type I IFN-signaling (104, 105). As type I IFNs can induce increased MHC I expression on stromal

cells in lymph nodes, one possibility is that type I IFNs enhance MHC expression even during steady-state conditions (105). Hence, increased MHC expression could facilitate stronger tonic TCR signals in naive $CD8^+$ T cells, reflected by modulated Ly6C expression. In support of this hypothesis, antibody-mediated blocking of MHC I mitigates the induced Ly6C expression by adding type I IFNs to in vitro cultures of purified naive $CD8^+$ T cells (105). These results thus suggest that type I IFNs either modulate MHC expression and thus promote increased tonic TCR signaling strength or STAT1-induced signaling contributes synergistically to induce Ly6C expression on naive $CD8^+$ T cells in the presence of tonic TCR signals.

Ly6C expression on naive $CD5^{HI}$ $CD8^+$ T cells positively correlates with T cell effector functions independently of TCR specificity (104, 105). TCR transgenic $Ly6C^+$ $CD5^{HI}$ naive $CD8^+$ T cells exhibit an increased proliferative response than $Ly6C^-$ $CD5^{HI}$ cells upon competitive transfer experiments during an acute viral infection (104). However, the function of Ly6C does seemingly not contribute to the competitive advantage of $Ly6C^+$ over $Ly6C^-$ naive $CD8^+$ T cells. Mice deficient of both *Ly6c1* and *Ly6c2* exhibit no defects in T cell development, no altered composition of peripheral T cell subsets, and *Ly6c1*$^{-/-}$ *Ly6c2*$^{-/-}$ T cells proliferate similarly to WT T cells in response to TCR agonist stimulation (107). Hence, Ly6C expression presumably identifies a naive $CD8^+$ T cell subset with an altered gene expression profile that may enhance the recruitment and expansion of T cells independently of Ly6C function (104, 105).

Combination of markers

Our laboratory investigated whether a combination of markers could improve the dynamic range of tonic signaling that can be detected (73). The combination of Nur77-GFP plus Ly6C exhibited a broader dynamic range compared to GFP plus CD5 or Ly6C plus CD5. In this scheme, Nur77-GFP^{LO} $Ly6C^+$ cells experience the weakest tonic signaling, and Nur77-GFP^{HI} $Ly6C^–$ cells

experience the strongest tonic signals, as shown by ζ-chain phosphorylation (73). While Nur77-GFP^{HI} Ly6C$^{–}$ cells express high levels of CD5, high CD5 expression alone does not solely mark the Nur77-GFP^{HI} Ly6C$^{–}$ subset. These data raise the possibility that the range of tonic signal strength extends further than previously thought. Future studies with new markers or combinations of markers may improve the "resolution" to detect tonic signal strength.

Role of tonic signaling in CD4^{+} T cells

Paul Allen's laboratory generated an elegant experimental system where the researchers investigated naive CD4^{+} T cells from two different TCR transgenic mouse lines specific to the same epitope with similar affinity (65, 66). These two TCR clonotypes exhibited differential CD5 expression and thus marked naive CD4^{+} T cells that experienced different basal TCR signaling strength but with similar cognate antigen-specificity and affinity. T cell clones from the CD5^{HI} TCR transgenic exhibited greater ERK phosphorylation and IL-2 production in response to acute stimulation (66). However, at the late stages of the primary response, higher percentages of CD5^{HI} TCR transgenic cells underwent apoptosis than CD5^{LO} cells, and T cell clones from the CD5^{LO} TCR transgenic dominated the acute phase of the primary immune response (65). A model based on these studies suggests that strong tonic signaling correlates with a robust acute response that is not sustained due to increased cell death (108). Hence, one potential consequence of naive CD4^{+} T cell heterogeneity is that different clones may engage in primary responses to foreign antigens with different kinetics. However, for naive CD4^{+} T cells, the relationship between CD5 expression and the responsiveness toward subsequent cognate antigen stimulation is complex. Germain and colleagues showed that upon co-transfer of CD5^{HI} and CD5^{LO} naive polyclonal CD4^{+} T cells, CD5^{HI} cells were present in greater numbers than CD5^{LO} cells at the late stages of the primary response in different infection models (35). As CD5^{HI} cells exhibit an increased susceptibility to

activation-induced cell death relative to $CD5^{LO}$ cells at the height of the acute immune response, the increased abundance of polyclonal $CD5^{HI}$ relative to $CD5^{LO}$ cells is likely the result of increased clonal expansion (66, 104). The discrepancies in the studies between the Allen and the Germain laboratories are presumably due to comparing polyclonal T cells versus T cell clones of similar specificity and cognate antigen affinity. For example, when adoptively transferring polyclonal T cells, it is impossible to control for the precursor frequencies or the affinity of antigen-specific T cells, which might differ between the $CD5^{LO}$ and $CD5^{HI}$ populations.

Studies from our laboratory revealed that weak tonic signal strength, experienced by naive $CD4^{+}$ T cells with a Nur77-GFP^{LO} $Ly6C^{+}$ phenotype, consistently correlated with the most robust activation, as reflected by IL-2 secretion, cell division, and ERK phosphorylation (73). Nur77-GFP^{MED} $Ly6C^{+}$ and Nur77-GFP^{MED} $Ly6C^{-}$ cells, which experience moderate tonic signal strength, mounted IL-2 responses comparable to Nur77-GFP^{LO} $Ly6C^{+}$ cells early (four hours post-stimulation). Still, the IL-2 responses of GFP^{LO} $Ly6C^{+}$ cells were consistently higher at later time points. These findings are compatible with the concept that strong tonic signaling correlates with short-lived acute responses. However, Nur77-GFP^{HI} $Ly6C^{-}$ cells, which experience extensive tonic signaling, consistently exhibited decreased responsiveness to stimulation. This result is congruent with a "tunable" model where lymphocytes adapt to the amount of tonic signaling they experience (109). Consequently, cells that experience strong tonic TCR signaling shift their activation threshold and effectively become de-sensitized to subsequent TCR stimulation (**Fig. 1.2**). Additionally, the Allen laboratory has demonstrated similar results in transgenic mice that experience stronger tonic signaling due to the expression of a voltage-gated sodium channel that facilitates sustained calcium signaling (110, 111). In this system, TCR transgenic T cells that experience heightened tonic TCR signaling exhibit an impaired primary immune response. Hence,

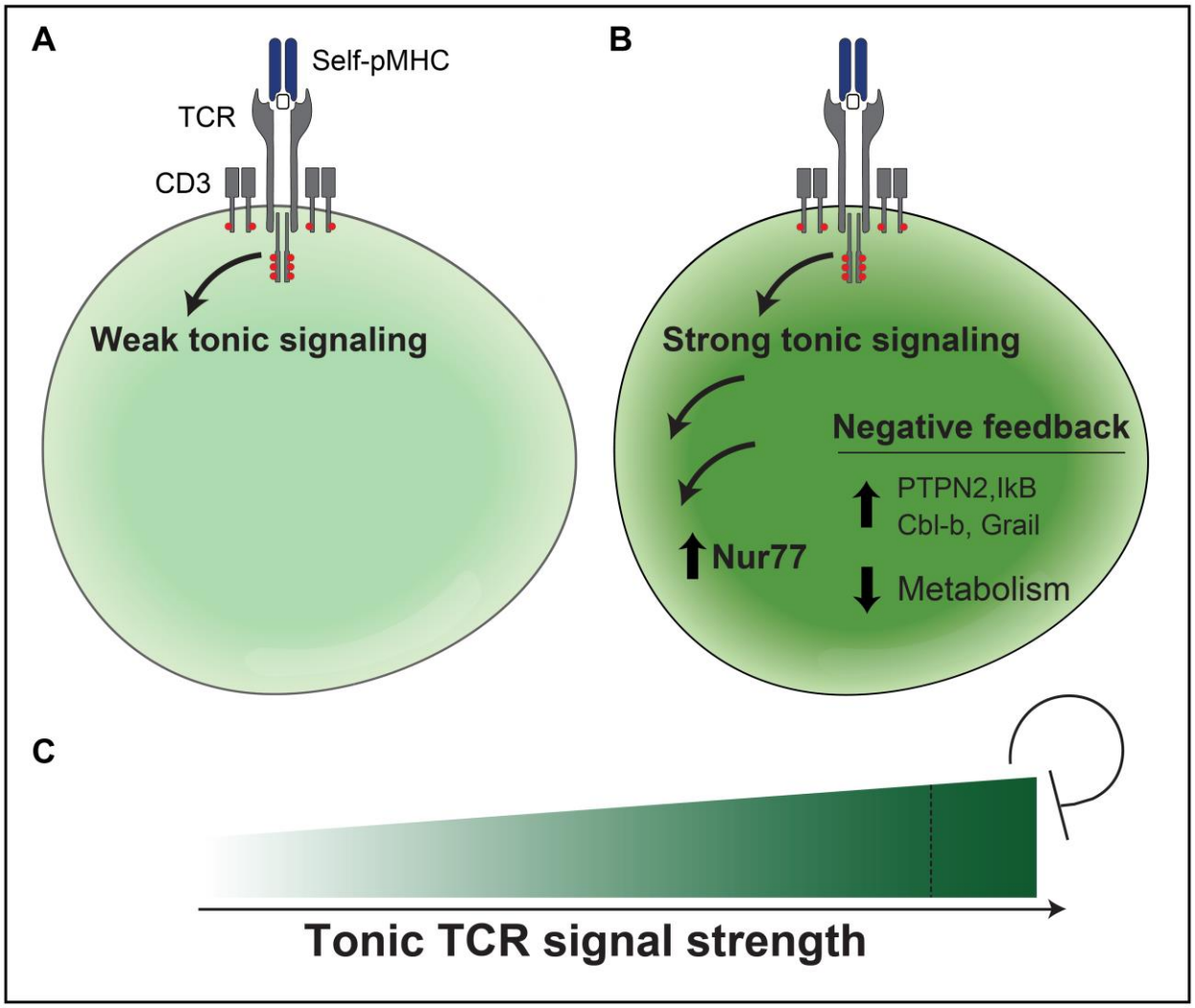

Fig. 1.2. Adaptation to tonic TCR signals through negative feedback.

(**A**) Individual naive T cells that exhibit relatively weak reactivity to self-pMHC induce weak tonic TCR signals. (**B**) $CD4^+$ T cells that exhibit strong reactivity to self-pMHC induce more extensive tonic TCR signaling, which results in higher expression of Nur77, and correlates with higher expression of negative regulators of TCR signaling and decreased basal metabolism. (**C**) Naive $CD4^+$ T cells that experience the most extensive tonic signal strength have attenuated responsiveness.

these studies suggest that for naive $CD4^+$ T cells, when normalized for TCR specificity and affinity to cognate antigen, extensive tonic TCR signaling correlates with an attenuated primary immune

response. Finally, while some of the correlations identified using CD5 and Nur77-GFP as correlate markers of tonic TCR signaling strength overlap, differences remain. Further research is needed to clarify how tonic TCR signaling impacts $CD4^+$ T cells at various stages of primary responses.

The molecular pathways tonic TCR signaling activates remain incompletely understood (29). A major challenge in studying the basal TCR signaling machinery has been the lack of an in vitro model. However, studies have highlighted how tonic signal strength can impact $CD4^+$ T cells. For instance, in a mouse model with impaired NF-κβ signaling, naive T cells express lower levels of the IL-7 receptor α-subunit and exhibit reduced cell survival compared to WT cells (112), suggesting that the downstream effects of basal TCR signaling may affect cell survival. More recent studies add to the complexity and suggest that tonic TCR signaling could have both positive and negative effects on T cell effector function and influence T cell differentiation.

Tonic signal strength influences effector functions and cell fate decisions

Th1-polarized $CD5^{HI}$ cells express lower levels of Tbet and produce less IFNγ relative to $CD5^{LO}$ cells upon stimulation (113). Similarly, strong tonic signaling correlates with impaired T follicular helper cell differentiation (114). In contrast, naive $CD4^+$ T cells that experience increased tonic signaling, such as $CD5^{HI}$, $Ly6C^–$, or Nur77-GFP^{HI} $Ly6C^–$ populations have a higher propensity for Foxp3 expression under induced Treg differentiation conditions (73, 94, 115). This functional heterogeneity may reflect mechanisms to attenuate highly self-reactive cells or divert them from an inflammatory effector state. However, in a lymphopenic environment, strong tonic signal strength correlates with increased autoreactive potential, as $Ly6C^–$ naive $CD4^+$ cells induce more severe disease in an adoptive transfer model of colitis compared to $Ly6C^+$ cells (94). A correlation between basal TCR signaling and immunopathology can also be observed in mice that harbor

mutations in the TCR signaling pathway (116-118). The ZAP-70 mutation in SKG mice renders ZAP-70 hyporesponsive and thus allows positive thymic selection of T cell clones that otherwise would have undergone negative selection, resulting in an arthritis-like disease (119). In the SKG mouse model of rheumatoid arthritis, Nur77-GFP^{HI} naive CD4^{+} cells have increased arthritogenic potential compared to Nur77-GFP^{LO} cells (116). Likewise, T cells expressing a point mutation in LAT Tyrosine 136 experience weaker tonic signaling but paradoxically induce a Th2 lymphoproliferative disorder (117). More specifically, weaker tonic signaling reduces the constitutive nuclear export of histone deacetylase 7, a transcriptional repressor of *Nr4a1* and *Irf4* (120). Furthermore, a point-mutation in Rasgrp1 increases tonic mTORC1 signaling, which skews CD4^{+} T cells toward Th2 differentiation and instigates immunopathology in mice (118). Together, these studies underscore that (i) TCR signaling can influence T helper effector function and cell fate decisions and (ii) strong tonic TCR signals correlate with increased autoimmune pathology if tolerance is compromised.

Potential mechanisms of negative regulation

An elegant study by Trefzer et al. investigated the effects of chronic antigen stimulation on CD4^{+} T cells in the absence of infection by utilizing a TCR transgenic mouse model in which cognate antigen expression is inducible (121). In contrast to acute cognate antigen exposure, chronic exposure impaired cytokine production and induced gene expression signatures that bear similarities with gene expression patterns in anergic and exhausted T cells. Although constitutive cognate antigen stimulation differs from the constitutive low-level TCR stimulation T cells experience from self-pMHC interactions, T cells may similarly adapt to strong self-pMHC signals.

CD5 expression positively correlates with higher expression of IκB (a negative regulator of NFκB) (122), suggesting that self-reactive naive T cells potentially counterbalance an increased capacity

of tonic signaling by expressing negative regulators of TCR signaling. A negative regulator of strong tonic signaling may also be CD5 itself. CD5 deficiency results in hyperresponsive TCR signaling in thymocytes, and mature $CD5^{HI}$ T cells exhibit a decreased TCR-induced calcium flux, consistent with CD5 as an inhibitor of TCR signaling (40, 55, 56). Recent analyses of the CD5 interactome by mass spectrometry have highlighted several potential binding partners in mouse $CD4^+$ T cells. One analysis identified negative regulators such as the E3 ubiquitin ligase Cbl-b and the phosphatase Ubash3a in the CD5 signalosome (123). E3 ligases are involved in ubiquitin-mediated endocytosis and degradation of proteins, and therefore, Cbl-b can promote negative regulation of TCR signaling proteins by promoting ubiquitination (124). However, Cbl-b can also mediate negative regulation of some TCR signaling substrates in a non-ubiquitin ligase-dependent manner (125). Ubash3a encodes the phosphatase Sts2 that can dephosphorylate protein tyrosine kinases in the TCR signaling cascade, such as ZAP-70, and can, therefore, prevent the activation of positive signaling mediators (126). An independent analysis identified a required role for Tyrosine 429 of CD5 in the recruitment of c-Cbl, Cin85, and CrkL, which assemble molecular complexes that included both negative regulators (phosphatases SHIP-1 and Ubash3a) and positive regulators (PI3K) (127). Moreover, CD5 also has a reported pro-survival role in mature T cells (128-130). Hence, CD5 may have both positive and negative regulatory roles in TCR signaling, although further research is necessary to define the underlying mechanisms.

Tolerized and anergic T cells express high levels of Nur77 (131-133), and Nur77-deficiency impairs the induction of tolerance and exhaustion (131, 132). Furthermore, Nur77 deficient $CD4^+$ T cells exhibit enhanced basal and maximal respiration and glycolytic capacity (134) in addition to enhanced IL-2 secretion upon stimulation (83), consistent with a role for Nur77 as a negative regulator of T cell activation. Moreover, extensive tonic signaling results in elevated levels of Cbl-

b and GRAIL, E3 ubiquitin ligases that negatively regulate TCR signal transduction and are associated with T cell anergy (73, 135, 136).

Increasing tonic signal strength attenuates metabolism

Ectopic expression of Scn5a, the pore-forming subunit of a voltage-gated sodium channel, enhances tonic TCR signal strength as reflected by elevated CD5 expression (110, 111). Increasing tonic signal strength by ectopic expression of Scn5a resulted in impaired cell expansion during a primary response to *L. monocytogenes* infection (110). Furthermore, Scn5a-expressing cells have a decreased basal and maximal respiration rate and glycolytic rate (44). These results suggest that strong tonic signaling limits the basal metabolism of naive T cells, perhaps to limit the autoimmune potential of self-reactive T cells.

Role of tonic signaling in CD8$^+$ T cells

High CD5 expression positively correlates with increased persistence of antigen-specific CD8$^+$ T cells during a primary response (137), suggesting a positive correlation between tonic signal strength and the magnitude of naive CD8$^+$ T cell responses to foreign/agonist pMHC. Furthermore, utilizing TCR transgenic cells expressing identical TCR clonotypes, a similar skewing toward CD5^{HI} over CD5^{LO} naive CD8$^+$ T cells could be observed in a viral infection model (104). Hence, the paradigm in the field has primarily been that naive CD8$^+$ T cells that experience stronger tonic TCR signaling from self-antigens are better poised to respond to foreign antigens. Cho and colleagues proposed a more refined model showing that naive CD8$^+$ CD5^{HI} cells exhibited attenuated proximal TCR signaling upon TCR ligation relative to CD5^{LO} cells (138). However, the inverse relationship was true after more extended periods of stimulation, where CD5^{HI} cells proliferated more extensively than CD5^{LO} cells (138).

Stephen Jameson's group compared $CD8^+$ cells specific to the self-antigen tyrosinase-related protein 2 (Trp2) harvested from WT and Trp2-deficient mice (139). Although the Trp2-specific T cells were phenotypically and transcriptionally similar, Trp2-specific T cells from Trp2-deficient mice induced greater pathology in an adoptive transfer model of vitiligo. Moreover, a positive correlation between the expression of CD5 and the protein tyrosine phosphatase non-receptor type 2 (PTPN2), a negative regulator of TCR-proximal signal transduction due to dephosphorylation of positive signaling mediators such as protein tyrosine kinases and therefore preventing their activation, was detected in naive $CD8^+$ T cells (140). These findings are consistent with the concept that negative feedback from strong self-pMHC interactions reduces the pathogenic potential of the most self-reactive naive $CD8^+$ T cells.

Strong tonic signaling is associated with antigen-inexperienced memory-like T cells

Strong tonic signaling in $CD8^+$ T cells positively correlates with the conversion of naive cells into antigen-inexperienced $CD44^{HI}$ memory phenotype cells (141), so-called antigen-inexperienced memory-like T cells (AIMT). Mouse models that enhance tonic signaling, such as Dock2 mutant mice and mice expressing a chimeric CD8 that couples with Lck at superphysiological stoichiometry, illustrate this correlation (142, 143). Furthermore, TCR sequencing of AIMT cells revealed enrichment of distinct clonotypes that, upon re-expression, possessed higher self-reactivity compared to TCRs isolated from the naive repertoire (144).

Tonic signaling in human T cells

Transcriptional analysis of human $CD5^{LO}$ vs. $CD5^{HI}$ naive $CD4^+$ T cells revealed gene expression differences but whether genes associated with TCR signaling are upregulated in $CD5^{HI}$ cells is less clear (145). The transcriptional profile of naive human $CD8^+$ $CXCR3^+$ cells was more similar to naive murine $CD5^{HI}$ than $CD5^{LO}$ $CD8^+$ T cells (146). Consistent with this finding, CXCR3

expression in the murine naive $CD8^+$ population is limited to the $CD5^{HI}$ compartment (137). Hence, these studies suggest that CXCR3 expression could potentially function as a correlate marker of tonic TCR signaling in naive human $CD8^+$ T cells, although more research are needed. Further studies are also necessary to build on our understanding of the functional implications of tonic signaling in naive human T cells. There appears to be some similarity in the functional capacities of human and mouse $CD5^{LO}$ and $CD5^{HI}$ $CD4^+$ cells. Re-stimulation of activated human naive $CD4^+$ T cells revealed differences in cytokine production; $CD5^{LO}$ cells produced higher levels of IFNγ under Th1 conditions (145), consistent with previous results in mice (113).

Tonic signaling strength and adoptive cell therapy

Chimeric antigen receptor (CAR) T cell therapy is an individualized treatment strategy that relies on harvesting a patient's T cells, expanding them in vitro, and transducing them with a synthetic T cell receptor that can recognize and eliminate tumor cells upon reinfusion into the patient (147). Some degree of tonic signaling mediated by the endogenous TCR seems beneficial for CAR T cell therapy since deletion of the TCR negatively affected CAR T cell persistence in vivo (148). However, too much basal signaling may be detrimental since tonic signals through the synthetic CAR T cell receptor are associated with T cell exhaustion (149, 150). Furthermore, TCRs that were engineered to have increased affinity for self-MHC resulted in diminished responsiveness upon stimulation (151). Minguet and colleagues recently demonstrated that mutating a previously unknown Lck binding motif in CD3ε impaired the recruitment of Lck to the TCR complex and attenuated T cell activation (152). CARs incorporating this mutated binding motif induced enhanced anti-tumor responses, possibly due to reduced CAR tonic signals (152). Hence, determining the "optimum" amount of tonic signaling for T cells used in immunotherapy may further improve the therapeutic efficacy of ACT.

Outstanding questions in the field

The view of naive T cells as a functionally homogenous group of cells is under revision as increasing evidence reveals further heterogeneity. How the effects of tonic TCR signal strength influence T cell responses in different contexts (i.e., autoimmunity, infection, cancer) remain incompletely understood. Further studies are also needed to identify the molecular mechanisms that regulate adaptations to varying strengths of tonic TCR signaling, including at the signaling, transcriptional, and epigenetic levels.

Purpose of the study

Utilizing the expression of the TCR signaling reporter Nur77-GFP as a correlate readout of tonic TCR signaling enables a broader range of TCR:self-pMHC signaling compared to other correlate markers of TCR signaling in naive $CD4^+$ T cells (73). Nur77-GFP expression is, therefore, a valuable tool for isolating the cells that encounter the most extensive basal TCR signaling. Whether naive $CD8^+$ T cells experience such extensive signaling from TCR:self-pMHC interactions that it may influence how the naive cells respond to agonist TCR stimulation remains incompletely described. Hence, unanswered questions remain, including (i) whether tonic TCR signaling and Nur77-GFP expression in naive $CD8^+$ T cells is heterogenous, (ii) what the functional implications of extensive tonic TCR signaling in naive $CD8^+$ T cells are, and (iii) what are the potential molecular mechanisms induced by tonic TCR signaling that regulate naive $CD8^+$ T cell responsiveness. A better understanding of how basal TCR signaling in naive T cells relates to the heterogeneity of the T cell response to foreign antigens has implications for adoptive cell therapies as it might allow us to better anticipate different T cell outcomes. Moreover, broadening our knowledge of the molecular changes induced by tonic TCR signaling that affect the responsiveness of naive $CD8^+$ T cells could stimulate further research into limiting autoreactive T cells from

causing pathology.

References

1. Miller JF. The golden anniversary of the thymus. Nat Rev Immunol. 2011;11(7):489-95.
2. Chinn IK, Shearer WT. Severe Combined Immunodeficiency Disorders. Immunol Allergy Clin North Am. 2015;35(4):671-94.
3. Okoye AA, Picker LJ. CD4(+) T-cell depletion in HIV infection: mechanisms of immunological failure. Immunol Rev. 2013;254(1):54-64.
4. Khan U, Ghazanfar H. T Lymphocytes and Autoimmunity. Int Rev Cell Mol Biol. 2018;341:125-68.
5. Itohara S, Nakanishi N, Kanagawa O, Kubo R, Tonegawa S. Monoclonal antibodies specific to native murine T-cell receptor gamma delta: analysis of gamma delta T cells during thymic ontogeny and in peripheral lymphoid organs. Proc Natl Acad Sci U S A. 1989;86(13):5094-8.
6. Vroom TM, Scholte G, Ossendorp F, Borst J. Tissue distribution of human gamma delta T cells: no evidence for general epithelial tropism. J Clin Pathol. 1991;44(12):1012-7.
7. Haskins K, Kubo R, White J, Pigeon M, Kappler J, Marrack P. The major histocompatibility complex-restricted antigen receptor on T cells. I. Isolation with a monoclonal antibody. J Exp Med. 1983;157(4):1149-69.
8. Reinherz EL, Meuer SC, Fitzgerald KA, Hussey RE, Hodgdon JC, Acuto O, et al. Comparison of T3-associated 49- and 43-kilodalton cell surface molecules on individual human T-cell clones: evidence for peptide variability in T-cell receptor structures. Proc Natl Acad Sci U S A. 1983;80(13):4104-8.
9. Samelson LE, Harford JB, Klausner RD. Identification of the components of the murine T

cell antigen receptor complex. Cell. 1985;43(1):223-31.

10. Borst J, Alexander S, Elder J, Terhorst C. The T3 complex on human T lymphocytes involves four structurally distinct glycoproteins. J Biol Chem. 1983;258(8):5135-41.

11. Romeo C, Seed B. Cellular immunity to HIV activated by CD4 fused to T cell or Fc receptor polypeptides. Cell. 1991;64(5):1037-46.

12. Irving BA, Weiss A. The cytoplasmic domain of the T cell receptor zeta chain is sufficient to couple to receptor-associated signal transduction pathways. Cell. 1991;64(5):891-901.

13. Wegener AM, Letourneur F, Hoeveler A, Brocker T, Luton F, Malissen B. The T cell receptor/CD3 complex is composed of at least two autonomous transduction modules. Cell. 1992;68(1):83-95.

14. Bjorkman PJ, Saper MA, Samraoui B, Bennett WS, Strominger JL, Wiley DC. The foreign antigen binding site and T cell recognition regions of class I histocompatibility antigens. Nature. 1987;329(6139):512-8.

15. Garboczi DN, Ghosh P, Utz U, Fan QR, Biddison WE, Wiley DC. Structure of the complex between human T-cell receptor, viral peptide and HLA-A2. Nature. 1996;384(6605):134-41.

16. Garcia KC, Degano M, Stanfield RL, Brunmark A, Jackson MR, Peterson PA, et al. An alphabeta T cell receptor structure at 2.5 A and its orientation in the TCR-MHC complex. Science. 1996;274(5285):209-19.

17. Garcia KC, Degano M, Pease LR, Huang M, Peterson PA, Teyton L, et al. Structural basis of plasticity in T cell receptor recognition of a self peptide-MHC antigen. Science. 1998;279(5354):1166-72.

18. Kisielow P, Hirst JA, Shiku H, Beverley PC, Hoffman MK, Boyse EA, et al. Ly antigens

as markers for functionally distinct subpopulations of thymus-derived lymphocytes of the mouse. Nature. 1975;253(5488):219-20.

19. Cantor H, Boyse EA. Functional subclasses of T-lymphocytes bearing different Ly antigens. I. The generation of functionally distinct T-cell subclasses is a differentiative process independent of antigen. J Exp Med. 1975;141(6):1376-89.

20. Cantor H, Boyse EA. Functional subclasses of T lymphocytes bearing different Ly antigens. II. Cooperation between subclasses of Ly+ cells in the generation of killer activity. J Exp Med. 1975;141(6):1390-9.

21. Swain SL. Significance of Lyt phenotypes: Lyt2 antibodies block activities of T cells that recognize class 1 major histocompatibility complex antigens regardless of their function. Proc Natl Acad Sci U S A. 1981;78(11):7101-5.

22. Meuer SC, Schlossman SF, Reinherz EL. Clonal analysis of human cytotoxic T lymphocytes: T4+ and T8+ effector T cells recognize products of different major histocompatibility complex regions. Proc Natl Acad Sci U S A. 1982;79(14):4395-9.

23. Spits H, Borst J, Terhorst C, de Vries JE. The role of T cell differentiation markers in antigen-specific and lectin-dependent cellular cytotoxicity mediated by T8+ and T4+ human cytotoxic T cell clones directed at class I and class II MHC antigens. J Immunol. 1982;129(4):1563-9.

24. Wilde DB, Marrack P, Kappler J, Dialynas DP, Fitch FW. Evidence implicating L3T4 in class II MHC antigen reactivity; monoclonal antibody GK1.5 (anti-L3T4a) blocks class II MHC antigen-specific proliferation, release of lymphokines, and binding by cloned murine helper T lymphocyte lines. J Immunol. 1983;131(5):2178-83.

25. Teh HS, Kisielow P, Scott B, Kishi H, Uematsu Y, Bluthmann H, et al. Thymic major

histocompatibility complex antigens and the alpha beta T-cell receptor determine the CD4/CD8 phenotype of T cells. Nature. 1988;335(6187):229-33.

26. Kisielow P, Teh HS, Bluthmann H, von Boehmer H. Positive selection of antigen-specific T cells in thymus by restricting MHC molecules. Nature. 1988;335(6192):730-3.

27. Hogquist KA, Jameson SC, Heath WR, Howard JL, Bevan MJ, Carbone FR. T cell receptor antagonist peptides induce positive selection. Cell. 1994;76(1):17-27.

28. Ashton-Rickardt PG, Bandeira A, Delaney JR, Van Kaer L, Pircher HP, Zinkernagel RM, et al. Evidence for a differential avidity model of T cell selection in the thymus. Cell. 1994;76(4):651-63.

29. Myers DR, Zikherman J, Roose JP. Tonic Signals: Why Do Lymphocytes Bother? Trends Immunol. 2017;38(11):844-57.

30. Paprckova D, Stepanek O. Narcissistic T cells: reactivity to self makes a difference. FEBS J. 2020.

31. van Oers NS, Tao W, Watts JD, Johnson P, Aebersold R, Teh HS. Constitutive tyrosine phosphorylation of the T-cell receptor (TCR) zeta subunit: regulation of TCR-associated protein tyrosine kinase activity by TCR zeta. Mol Cell Biol. 1993;13(9):5771-80.

32. van Oers NS, Killeen N, Weiss A. ZAP-70 is constitutively associated with tyrosine-phosphorylated TCR zeta in murine thymocytes and lymph node T cells. Immunity. 1994;1(8):675-85.

33. Stefanova I, Dorfman JR, Germain RN. Self-recognition promotes the foreign antigen sensitivity of naive T lymphocytes. Nature. 2002;420(6914):429-34.

34. Hochweller K, Wabnitz GH, Samstag Y, Suffner J, Hammerling GJ, Garbi N. Dendritic cells control T cell tonic signaling required for responsiveness to foreign antigen. Proc Natl

Acad Sci U S A. 2010;107(13):5931-6.

35. Mandl JN, Monteiro JP, Vrisekoop N, Germain RN. T cell-positive selection uses self-ligand binding strength to optimize repertoire recognition of foreign antigens. Immunity. 2013;38(2):263-74.

36. Chan AC, Iwashima M, Turck CW, Weiss A. ZAP-70: a 70 kd protein-tyrosine kinase that associates with the TCR zeta chain. Cell. 1992;71(4):649-62.

37. Iwashima M, Irving BA, van Oers NS, Chan AC, Weiss A. Sequential interactions of the TCR with two distinct cytoplasmic tyrosine kinases. Science. 1994;263(5150):1136-9.

38. Madrenas J, Wange RL, Wang JL, Isakov N, Samelson LE, Germain RN. Zeta phosphorylation without ZAP-70 activation induced by TCR antagonists or partial agonists. Science. 1995;267(5197):515-8.

39. Takada K, Jameson SC. Self-class I MHC molecules support survival of naive CD8 T cells, but depress their functional sensitivity through regulation of CD8 expression levels. J Exp Med. 2009;206(10):2253-69.

40. Smith K, Seddon B, Purbhoo MA, Zamoyska R, Fisher AG, Merkenschlager M. Sensory adaptation in naive peripheral CD4 T cells. J Exp Med. 2001;194(9):1253-61.

41. Bhandoola A, Tai X, Eckhaus M, Auchincloss H, Mason K, Rubin SA, et al. Peripheral expression of self-MHC-II influences the reactivity and self-tolerance of mature CD4(+) T cells: evidence from a lymphopenic T cell model. Immunity. 2002;17(4):425-36.

42. Fischer UB, Jacovetty EL, Medeiros RB, Goudy BD, Zell T, Swanson JB, et al. MHC class II deprivation impairs CD4 T cell motility and responsiveness to antigen-bearing dendritic cells in vivo. Proc Natl Acad Sci U S A. 2007;104(17):7181-6.

43. This S, Rogers D, Mallet Gauthier E, Mandl JN, Melichar HJ. What's self got to do with

it: Sources of heterogeneity among naive T cells. Semin Immunol. 2022;65:101702.

44. Milam AAV, Bartleson JM, Buck MD, Chang CH, Sergushichev A, Donermeyer DL, et al. Tonic TCR Signaling Inversely Regulates the Basal Metabolism of CD4(+) T Cells. Immunohorizons. 2020;4(8):485-97.

45. Burgueno-Bucio E, Mier-Aguilar CA, Soldevila G. The multiple faces of CD5. J Leukoc Biol. 2019;105(5):891-904.

46. Van de Velde H, von Hoegen I, Luo W, Parnes JR, Thielemans K. The B-cell surface protein CD72/Lyb-2 is the ligand for CD5. Nature. 1991;351(6328):662-5.

47. Pospisil R, Fitts MG, Mage RG. CD5 is a potential selecting ligand for B cell surface immunoglobulin framework region sequences. J Exp Med. 1996;184(4):1279-84.

48. Vera J, Fenutria R, Canadas O, Figueras M, Mota R, Sarrias MR, et al. The CD5 ectodomain interacts with conserved fungal cell wall components and protects from zymosan-induced septic shock-like syndrome. Proc Natl Acad Sci U S A. 2009;106(5):1506-11.

49. Brown MH, Lacey E. A ligand for CD5 is CD5. J Immunol. 2010;185(10):6068-74.

50. Voisinne G, Gonzalez de Peredo A, Roncagalli R. CD5, an Undercover Regulator of TCR Signaling. Front Immunol. 2018;9:2900.

51. Davies AA, Ley SC, Crumpton MJ. CD5 is phosphorylated on tyrosine after stimulation of the T-cell antigen receptor complex. Proc Natl Acad Sci U S A. 1992;89(14):6368-72.

52. Brossard C, Semichon M, Trautmann A, Bismuth G. CD5 inhibits signaling at the immunological synapse without impairing its formation. J Immunol. 2003;170(9):4623-9.

53. Ledbetter JA, Martin PJ, Spooner CE, Wofsy D, Tsu TT, Beatty PG, et al. Antibodies to Tp67 and Tp44 augment and sustain proliferative responses of activated T cells. J

Immunol. 1985;135(4):2331-6.

54. Ceuppens JL, Baroja ML. Monoclonal antibodies to the CD5 antigen can provide the necessary second signal for activation of isolated resting T cells by solid-phase-bound OKT3. J Immunol. 1986;137(6):1816-21.

55. Tarakhovsky A, Kanner SB, Hombach J, Ledbetter JA, Muller W, Killeen N, et al. A role for CD5 in TCR-mediated signal transduction and thymocyte selection. Science. 1995;269(5223):535-7.

56. Pena-Rossi C, Zuckerman LA, Strong J, Kwan J, Ferris W, Chan S, et al. Negative regulation of CD4 lineage development and responses by CD5. J Immunol. 1999;163(12):6494-501.

57. Azzam HS, DeJarnette JB, Huang K, Emmons R, Park CS, Sommers CL, et al. Fine tuning of TCR signaling by CD5. J Immunol. 2001;166(9):5464-72.

58. Dennehy KM, Broszeit R, Ferris WF, Beyers AD. Thymocyte activation induces the association of the proto-oncoprotein c-cbl and ras GTPase-activating protein with CD5. Eur J Immunol. 1998;28(5):1617-25.

59. Voisinne G, Garcia-Blesa A, Chaoui K, Fiore F, Bergot E, Girard L, et al. Co-recruitment analysis of the CBL and CBLB signalosomes in primary T cells identifies CD5 as a key regulator of TCR-induced ubiquitylation. Mol Syst Biol. 2016;12(7):876.

60. Bachmaier K, Krawczyk C, Kozieradzki I, Kong YY, Sasaki T, Oliveira-dos-Santos A, et al. Negative regulation of lymphocyte activation and autoimmunity by the molecular adaptor Cbl-b. Nature. 2000;403(6766):211-6.

61. Chiang YJ, Kole HK, Brown K, Naramura M, Fukuhara S, Hu RJ, et al. Cbl-b regulates the CD28 dependence of T-cell activation. Nature. 2000;403(6766):216-20.

62. Naramura M, Jang IK, Kole H, Huang F, Haines D, Gu H. c-Cbl and Cbl-b regulate T cell responsiveness by promoting ligand-induced TCR down-modulation. Nat Immunol. 2002;3(12):1192-9.

63. Azzam HS, Grinberg A, Lui K, Shen H, Shores EW, Love PE. CD5 expression is developmentally regulated by T cell receptor (TCR) signals and TCR avidity. J Exp Med. 1998;188(12):2301-11.

64. Wong P, Barton GM, Forbush KA, Rudensky AY. Dynamic tuning of T cell reactivity by self-peptide-major histocompatibility complex ligands. J Exp Med. 2001;193(10):1179-87.

65. Weber KS, Li QJ, Persaud SP, Campbell JD, Davis MM, Allen PM. Distinct CD4+ helper T cells involved in primary and secondary responses to infection. Proc Natl Acad Sci U S A. 2012;109(24):9511-6.

66. Persaud SP, Parker CR, Lo WL, Weber KS, Allen PM. Intrinsic CD4+ T cell sensitivity and response to a pathogen are set and sustained by avidity for thymic and peripheral complexes of self peptide and MHC. Nat Immunol. 2014;15(3):266-74.

67. Odagiu L, May J, Boulet S, Baldwin TA, Labrecque N. Role of the Orphan Nuclear Receptor NR4A Family in T-Cell Biology. Front Endocrinol (Lausanne). 2020;11:624122.

68. Cheng LE, Chan FK, Cado D, Winoto A. Functional redundancy of the Nur77 and Nor-1 orphan steroid receptors in T-cell apoptosis. EMBO J. 1997;16(8):1865-75.

69. Philips A, Lesage S, Gingras R, Maira MH, Gauthier Y, Hugo P, et al. Novel dimeric Nur77 signaling mechanism in endocrine and lymphoid cells. Mol Cell Biol. 1997;17(10):5946-51.

70. Winoto A, Littman DR. Nuclear hormone receptors in T lymphocytes. Cell. 2002;109 Suppl:S57-66.

71. Moran AE, Holzapfel KL, Xing Y, Cunningham NR, Maltzman JS, Punt J, et al. T cell receptor signal strength in Treg and iNKT cell development demonstrated by a novel fluorescent reporter mouse. J Exp Med. 2011;208(6):1279-89.

72. Zikherman J, Parameswaran R, Weiss A. Endogenous antigen tunes the responsiveness of naive B cells but not T cells. Nature. 2012;489(7414):160-4.

73. Zinzow-Kramer WM, Weiss A, Au-Yeung BB. Adaptation by naive CD4(+) T cells to self-antigen-dependent TCR signaling induces functional heterogeneity and tolerance. Proc Natl Acad Sci U S A. 2019;116(30):15160-9.

74. Au-Yeung BB, Zikherman J, Mueller JL, Ashouri JF, Matloubian M, Cheng DA, et al. A sharp T-cell antigen receptor signaling threshold for T-cell proliferation. Proc Natl Acad Sci U S A. 2014;111(35):E3679-88.

75. Jennings E, Elliot TAE, Thawait N, Kanabar S, Yam-Puc JC, Ono M, et al. Nr4a1 and Nr4a3 Reporter Mice Are Differentially Sensitive to T Cell Receptor Signal Strength and Duration. Cell Rep. 2020;33(5):108328.

76. Li H, Kolluri SK, Gu J, Dawson MI, Cao X, Hobbs PD, et al. Cytochrome c release and apoptosis induced by mitochondrial targeting of nuclear orphan receptor TR3. Science. 2000;289(5482):1159-64.

77. Lin B, Kolluri SK, Lin F, Liu W, Han YH, Cao X, et al. Conversion of Bcl-2 from protector to killer by interaction with nuclear orphan receptor Nur77/TR3. Cell. 2004;116(4):527-40.

78. Thompson J, Winoto A. During negative selection, Nur77 family proteins translocate to mitochondria where they associate with Bcl-2 and expose its proapoptotic BH3 domain. J Exp Med. 2008;205(5):1029-36.

79. Banta KL, Wang X, Das P, Winoto A. B cell lymphoma 2 (Bcl-2) residues essential for Bcl-2's apoptosis-inducing interaction with Nur77/Nor-1 orphan steroid receptors. J Biol Chem. 2018;293(13):4724-34.

80. Calnan BJ, Szychowski S, Chan FK, Cado D, Winoto A. A role for the orphan steroid receptor Nur77 in apoptosis accompanying antigen-induced negative selection. Immunity. 1995;3(3):273-82.

81. Woronicz JD, Calnan B, Ngo V, Winoto A. Requirement for the orphan steroid receptor Nur77 in apoptosis of T-cell hybridomas. Nature. 1994;367(6460):277-81.

82. Zhou T, Cheng J, Yang P, Wang Z, Liu C, Su X, et al. Inhibition of Nur77/Nurr1 leads to inefficient clonal deletion of self-reactive T cells. J Exp Med. 1996;183(4):1879-92.

83. Hiwa R, Nielsen HV, Mueller JL, Mandla R, Zikherman J. NR4A family members regulate T cell tolerance to preserve immune homeostasis and suppress autoimmunity. JCI Insight. 2021.

84. Lee PP, Fitzpatrick DR, Beard C, Jessup HK, Lehar S, Makar KW, et al. A critical role for Dnmt1 and DNA methylation in T cell development, function, and survival. Immunity. 2001;15(5):763-74.

85. Ellmeier W, Sunshine MJ, Losos K, Hatam F, Littman DR. An enhancer that directs lineage-specific expression of CD8 in positively selected thymocytes and mature T cells. Immunity. 1997;7(4):537-47.

86. Sekiya T, Kashiwagi I, Yoshida R, Fukaya T, Morita R, Kimura A, et al. Nr4a receptors are essential for thymic regulatory T cell development and immune homeostasis. Nat Immunol. 2013;14(3):230-7.

87. Fassett MS, Jiang W, D'Alise AM, Mathis D, Benoist C. Nuclear receptor Nr4a1 modulates

both regulatory T-cell (Treg) differentiation and clonal deletion. Proc Natl Acad Sci U S A. 2012;109(10):3891-6.

88. Sekiya T, Hibino S, Saeki K, Kanamori M, Takaki S, Yoshimura A. Nr4a Receptors Regulate Development and Death of Labile Treg Precursors to Prevent Generation of Pathogenic Self-Reactive Cells. Cell Rep. 2018;24(6):1627-38 e6.

89. Bautista JL, Lio CW, Lathrop SK, Forbush K, Liang Y, Luo J, et al. Intraclonal competition limits the fate determination of regulatory T cells in the thymus. Nat Immunol. 2009;10(6):610-7.

90. Sekiya T, Kondo T, Shichita T, Morita R, Ichinose H, Yoshimura A. Suppression of Th2 and Tfh immune reactions by Nr4a receptors in mature T reg cells. J Exp Med. 2015;212(10):1623-40.

91. Lee PY, Wang JX, Parisini E, Dascher CC, Nigrovic PA. Ly6 family proteins in neutrophil biology. J Leukoc Biol. 2013;94(4):585-94.

92. Heng TS, Painter MW, Immunological Genome Project C. The Immunological Genome Project: networks of gene expression in immune cells. Nat Immunol. 2008;9(10):1091-4.

93. Morimoto J, Nishikawa Y, Kakimoto T, Furutani K, Kihara N, Matsumoto M, et al. Aire Controls in Trans the Production of Medullary Thymic Epithelial Cells Expressing Ly-6C/Ly-6G. J Immunol. 2018;201(11):3244-57.

94. Martin B, Auffray C, Delpoux A, Pommier A, Durand A, Charvet C, et al. Highly self-reactive naive CD4 T cells are prone to differentiate into regulatory T cells. Nat Commun. 2013;4:2209.

95. Guichard V, Bonilla N, Durand A, Audemard-Verger A, Guilbert T, Martin B, et al. Calcium-mediated shaping of naive CD4 T-cell phenotype and function. Elife. 2017;6.

96. Delpoux A, Yakonowsky P, Durand A, Charvet C, Valente M, Pommier A, et al. TCR signaling events are required for maintaining CD4 regulatory T cell numbers and suppressive capacities in the periphery. J Immunol. 2014;193(12):5914-23.

97. Lee JY, Kim J, Yi J, Kim D, Kim HO, Han D, et al. Phenotypic and Functional Changes of Peripheral Ly6C(+) T Regulatory Cells Driven by Conventional Effector T Cells. Front Immunol. 2018;9:437.

98. Marshall HD, Chandele A, Jung YW, Meng H, Poholek AC, Parish IA, et al. Differential expression of Ly6C and T-bet distinguish effector and memory Th1 CD4(+) cell properties during viral infection. Immunity. 2011;35(4):633-46.

99. Hale JS, Youngblood B, Latner DR, Mohammed AU, Ye L, Akondy RS, et al. Distinct memory CD4+ T cells with commitment to T follicular helper- and T helper 1-cell lineages are generated after acute viral infection. Immunity. 2013;38(4):805-17.

100. Iyer SS, Latner DR, Zilliox MJ, McCausland M, Akondy RS, Penaloza-Macmaster P, et al. Identification of novel markers for mouse CD4(+) T follicular helper cells. Eur J Immunol. 2013;43(12):3219-32.

101. Hu Z, Blackman MA, Kaye KM, Usherwood EJ. Functional heterogeneity in the CD4+ T cell response to murine gamma-herpesvirus 68. J Immunol. 2015;194(6):2746-56.

102. Kunzli M, Schreiner D, Pereboom TC, Swarnalekha N, Litzler LC, Lotscher J, et al. Long-lived T follicular helper cells retain plasticity and help sustain humoral immunity. Sci Immunol. 2020;5(45).

103. Osum KC, Jenkins MK. Toward a general model of CD4(+) T cell subset specification and memory cell formation. Immunity. 2023;56(3):475-84.

104. Ju YJ, Lee SW, Kye YC, Lee GW, Kim HO, Yun CH, et al. Self-reactivity controls

functional diversity of naive CD8(+) T cells by co-opting tonic type I interferon. Nat Commun. 2021;12(1):6059.

105. Jergovic M, Coplen CP, Uhrlaub JL, Besselsen DG, Cheng S, Smithey MJ, et al. Infection-induced type I interferons critically modulate the homeostasis and function of CD8(+) naive T cells. Nat Commun. 2021;12(1):5303.

106. DeLong JH, Hall AO, Konradt C, Coppock GM, Park J, Harms Pritchard G, et al. Cytokine- and TCR-Mediated Regulation of T Cell Expression of Ly6C and Sca-1. J Immunol. 2018;200(5):1761-70.

107. Morimoto J, Matsumoto M, Miyazawa R, Oya T, Tsuneyama K, Matsumoto M. No Major Impact of Two Homologous Proteins Ly6C1 and Ly6C2 on Immune Homeostasis. Immunohorizons. 2022;6(3):202-10.

108. Milam AV, Allen PM. Functional Heterogeneity in CD4(+) T Cell Responses Against a Bacterial Pathogen. Front Immunol. 2015;6:621.

109. Grossman Z. Immunological Paradigms, Mechanisms, and Models: Conceptual Understanding Is a Prerequisite to Effective Modeling. Front Immunol. 2019;10:2522.

110. Milam AAV, Bartleson JM, Donermeyer DL, Horvath S, Durai V, Raju S, et al. Tuning T Cell Signaling Sensitivity Alters the Behavior of CD4(+) T Cells during an Immune Response. J Immunol. 2018;200(10):3429-37.

111. Lo WL, Donermeyer DL, Allen PM. A voltage-gated sodium channel is essential for the positive selection of CD4(+) T cells. Nat Immunol. 2012;13(9):880-7.

112. Miller ML, Mashayekhi M, Chen L, Zhou P, Liu X, Michelotti M, et al. Basal NF-kappaB controls IL-7 responsiveness of quiescent naive T cells. Proc Natl Acad Sci U S A. 2014;111(20):7397-402.

113. Sood A, Lebel ME, Fournier M, Rogers D, Mandl JN, Melichar HJ. Differential interferon-gamma production potential among naive CD4(+) T cells exists prior to antigen encounter. Immunol Cell Biol. 2019;97(10):931-40.

114. Bartleson JM, Viehmann Milam AA, Donermeyer DL, Horvath S, Xia Y, Egawa T, et al. Strength of tonic T cell receptor signaling instructs T follicular helper cell-fate decisions. Nat Immunol. 2020.

115. Henderson JG, Opejin A, Jones A, Gross C, Hawiger D. CD5 instructs extrathymic regulatory T cell development in response to self and tolerizing antigens. Immunity. 2015;42(3):471-83.

116. Ashouri JF, Hsu LY, Yu S, Rychkov D, Chen Y, Cheng DA, et al. Reporters of TCR signaling identify arthritogenic T cells in murine and human autoimmune arthritis. Proc Natl Acad Sci U S A. 2019;116(37):18517-27.

117. Roncagalli R, Mingueneau M, Gregoire C, Malissen M, Malissen B. LAT signaling pathology: an "autoimmune" condition without T cell self-reactivity. Trends Immunol. 2010;31(7):253-9.

118. Myers DR, Norlin E, Vercoulen Y, Roose JP. Active Tonic mTORC1 Signals Shape Baseline Translation in Naive T Cells. Cell Rep. 2019;27(6):1858-74 e6.

119. Sakaguchi N, Takahashi T, Hata H, Nomura T, Tagami T, Yamazaki S, et al. Altered thymic T-cell selection due to a mutation of the ZAP-70 gene causes autoimmune arthritis in mice. Nature. 2003;426(6965):454-60.

120. Myers DR, Lau T, Markegard E, Lim HW, Kasler H, Zhu M, et al. Tonic LAT-HDAC7 Signals Sustain Nur77 and Irf4 Expression to Tune Naive CD4 T Cells. Cell Rep. 2017;19(8):1558-71.

121. Trefzer A, Kadam P, Wang SH, Pennavaria S, Lober B, Akcabozan B, et al. Dynamic adoption of anergy by antigen-exhausted CD4(+) T cells. Cell Rep. 2021;34(6):108748.

122. Matson CA, Choi S, Livak F, Zhao B, Mitra A, Love PE, et al. CD5 dynamically calibrates basal NF-kappaB signaling in T cells during thymic development and peripheral activation. Proc Natl Acad Sci U S A. 2020;117(25):14342-53.

123. Mori D, Gregoire C, Voisinne G, Celis-Gutierrez J, Aussel R, Girard L, et al. The T cell CD6 receptor operates a multitask signalosome with opposite functions in T cell activation. J Exp Med. 2021;218(2).

124. Tang R, Langdon WY, Zhang J. Regulation of immune responses by E3 ubiquitin ligase Cbl-b. Cell Immunol. 2019;340:103878.

125. Qiao G, Li Z, Molinero L, Alegre ML, Ying H, Sun Z, et al. T-cell receptor-induced NF-kappaB activation is negatively regulated by E3 ubiquitin ligase Cbl-b. Mol Cell Biol. 2008;28(7):2470-80.

126. San Luis B, Sondgeroth B, Nassar N, Carpino N. Sts-2 is a phosphatase that negatively regulates zeta-associated protein (ZAP)-70 and T cell receptor signaling pathways. J Biol Chem. 2011;286(18):15943-54.

127. Blaize G, Daniels-Treffandier H, Aloulou M, Rouquie N, Yang C, Marcellin M, et al. CD5 signalosome coordinates antagonist TCR signals to control the generation of Treg cells induced by foreign antigens. Proc Natl Acad Sci U S A. 2020;117(23):12969-79.

128. Axtell RC, Webb MS, Barnum SR, Raman C. Cutting edge: critical role for CD5 in experimental autoimmune encephalomyelitis: inhibition of engagement reverses disease in mice. J Immunol. 2004;173(5):2928-32.

129. Ryan KR, McCue D, Anderton SM. Fas-mediated death and sensory adaptation limit the

pathogenic potential of autoreactive T cells after strong antigenic stimulation. J Leukoc Biol. 2005;78(1):43-50.

130. Friedlein G, El Hage F, Vergnon I, Richon C, Saulnier P, Lecluse Y, et al. Human CD5 protects circulating tumor antigen-specific CTL from tumor-mediated activation-induced cell death. J Immunol. 2007;178(11):6821-7.

131. Liu X, Wang Y, Lu H, Li J, Yan X, Xiao M, et al. Genome-wide analysis identifies NR4A1 as a key mediator of T cell dysfunction. Nature. 2019;567(7749):525-9.

132. Chen J, Lopez-Moyado IF, Seo H, Lio CJ, Hempleman LJ, Sekiya T, et al. NR4A transcription factors limit CAR T cell function in solid tumours. Nature. 2019;567(7749):530-4.

133. Tuncel J, Benoist C, Mathis D. T cell anergy in perinatal mice is promoted by T reg cells and prevented by IL-33. J Exp Med. 2019;216(6):1328-44.

134. Liebmann M, Hucke S, Koch K, Eschborn M, Ghelman J, Chasan AI, et al. Nur77 serves as a molecular brake of the metabolic switch during T cell activation to restrict autoimmunity. Proc Natl Acad Sci U S A. 2018;115(34):E8017-E26.

135. Mueller DL. E3 ubiquitin ligases as T cell anergy factors. Nat Immunol. 2004;5(9):883-90.

136. Nguyen TTT, Wang ZE, Shen L, Schroeder A, Eckalbar W, Weiss A. Cbl-b deficiency prevents functional but not phenotypic T cell anergy. J Exp Med. 2021;218(7).

137. Fulton RB, Hamilton SE, Xing Y, Best JA, Goldrath AW, Hogquist KA, et al. The TCR's sensitivity to self peptide-MHC dictates the ability of naive CD8(+) T cells to respond to foreign antigens. Nat Immunol. 2015;16(1):107-17.

138. Cho JH, Kim HO, Ju YJ, Kye YC, Lee GW, Lee SW, et al. CD45-mediated control of TCR

tuning in naive and memory CD8(+) T cells. Nat Commun. 2016;7:13373.

139. Truckenbrod EN, Burrack KS, Knutson TP, Borges da Silva H, Block KE, O'Flanagan SD, et al. CD8(+) T cell self-tolerance permits responsiveness but limits tissue damage. Elife. 2021;10.

140. Wiede F, La Gruta NL, Tiganis T. PTPN2 attenuates T-cell lymphopenia-induced proliferation. Nat Commun. 2014;5:3073.

141. White JT, Cross EW, Burchill MA, Danhorn T, McCarter MD, Rosen HR, et al. Virtual memory T cells develop and mediate bystander protective immunity in an IL-15-dependent manner. Nat Commun. 2016;7:11291.

142. Mahajan VS, Demissie E, Alsufyani F, Kumari S, Yuen GJ, Viswanadham V, et al. DOCK2 Sets the Threshold for Entry into the Virtual Memory CD8(+) T Cell Compartment by Negatively Regulating Tonic TCR Triggering. J Immunol. 2020;204(1):49-57.

143. Drobek A, Moudra A, Mueller D, Huranova M, Horkova V, Pribikova M, et al. Strong homeostatic TCR signals induce formation of self-tolerant virtual memory CD8 T cells. EMBO J. 2018;37(14).

144. Miller CH, Klawon DEJ, Zeng S, Lee V, Socci ND, Savage PA. Eomes identifies thymic precursors of self-specific memory-phenotype CD8(+) T cells. Nat Immunol. 2020;21(5):567-77.

145. Sood A, Lebel ME, Dong M, Fournier M, Vobecky SJ, Haddad E, et al. CD5 levels define functionally heterogeneous populations of naive human CD4(+) T cells. Eur J Immunol. 2021;51(6):1365-76.

146. De Simone G, Mazza EMC, Cassotta A, Davydov AN, Kuka M, Zanon V, et al. CXCR3

Identifies Human Naive CD8(+) T Cells with Enhanced Effector Differentiation Potential. J Immunol. 2019;203(12):3179-89.

147. Guedan S, Ruella M, June CH. Emerging Cellular Therapies for Cancer. Annu Rev Immunol. 2019;37:145-71.

148. Stenger D, Stief TA, Kauferle T, Willier S, Rataj F, Schober K, et al. Endogenous TCR promotes in vivo persistence of CD19-CAR-T cells compared to a CRISPR/Cas9-mediated TCR knockout CAR. Blood. 2020.

149. Long AH, Haso WM, Shern JF, Wanhainen KM, Murgai M, Ingaramo M, et al. 4-1BB costimulation ameliorates T cell exhaustion induced by tonic signaling of chimeric antigen receptors. Nat Med. 2015;21(6):581-90.

150. Lynn RC, Weber EW, Sotillo E, Gennert D, Xu P, Good Z, et al. c-Jun overexpression in CAR T cells induces exhaustion resistance. Nature. 2019;576(7786):293-300.

151. Duong MN, Erdes E, Hebeisen M, Rufer N. Chronic TCR-MHC (self)-interactions limit the functional potential of TCR affinity-increased CD8 T lymphocytes. J Immunother Cancer. 2019;7(1):284.

152. Hartl FA, Beck-Garcia E, Woessner NM, Flachsmann LJ, Cardenas RMV, Brandl SM, et al. Noncanonical binding of Lck to CD3epsilon promotes TCR signaling and CAR function. Nat Immunol. 2020;21(8):902-13.

Chapter 2: Cbl-b mitigates the responsiveness of naive CD8$^+$ T cells that experience extensive tonic T cell receptor signaling

Authors: Joel Eggert[1], Wendy M. Zinzow-Kramer[1], Yuesong Hu[2], Elizabeth M. Kolawole[3], Yuan-Li Tsai[4], Arthur Weiss[4], Brian D. Evavold[3], Khalid Salaita[2], Christopher D. Scharer[5], and Byron B. Au-Yeung[1]*

Affiliations:

[1]Division of Immunology, Lowance Center for Human Immunology, Department of Medicine, Emory University; Atlanta, USA.

[2]Department of Chemistry, Emory University; Atlanta, USA.

[3]Department of Pathology, University of Utah School of Medicine, Salt Lake City, USA.

[4]Rosalind Russell and Ephraim P. Engleman Rheumatology Research Center, Departments of Medicine and of Microbiology and Immunology, University of California, San Francisco; San Francisco, USA.

[5]Department of Microbiology and Immunology, Emory University; Atlanta, USA.

*Corresponding author. Email: byron.au-yeung@emory.edu

This version of the manuscript was provisionally accepted in Science Signaling.

Abstract

Naive T cells experience tonic TCR signaling in response to self-antigens in the steady state. However, how these signals influence the responsiveness of naive $CD8^+$ T cells to subsequent agonist TCR stimulation remains incompletely understood. We investigated how relatively low or high levels of tonic TCR signaling influence naive $CD8^+$ T cell responses to stimulation with foreign antigens. A transcriptional reporter of Nr4a1 (Nur77-GFP) is heterogeneously expressed by naive $CD8^+$ T cells in the steady state, suggesting that individual naive T cells experience variable intensities or durations of tonic TCR signaling. Nur77-GFP^{HI} cells exhibited diminished activation marker expression and secretion of IFNγ and IL-2 relative to Nur77-GFP^{LO} cells in response to agonist TCR stimulation. Differential gene expression analyses revealed upregulation of genes associated with acutely stimulated T cells in Nur77-GFP^{HI} cells. Furthermore, Nur77-GFP^{HI} cells expressed higher protein levels of the ubiquitin ligase Cbl-b, a negative regulator of TCR signaling. Cbl-b deficiency partially restored the responsiveness of Nur77-GFP^{HI} cells. Our data suggest that the cumulative effects of experiencing extensive tonic TCR signaling under steady-state conditions induce a recalibration of naive $CD8^+$ T cell responsiveness. These changes include gene expression changes and negative regulation, dependent partly on Cbl-b. This cell-intrinsic negative feedback loop may allow the immune system to restrain naive $CD8^+$ T cells with higher self-reactivity.

One Sentence Summary: Naive $CD8^+$ T cells adapt to extensive tonic TCR signaling by inducing a negative feedback loop dependent in part on Cbl-b.

Introduction

The activation of T cell-mediated immune responses is associated with sustained, robust signal transduction triggered by the T cell antigen receptor (TCR) (1). Activating TCR signals induces changes in T cell metabolism, cytoskeleton arrangements, and gene expression (1). Transcription of immediate-early genes occurs rapidly in response to robust TCR stimuli and includes transcription factors of the Jun/Fos family and Nur77, an orphan nuclear receptor encoded by *Nr4a1 (2)*. However, T cells also experience weaker, non-activating TCR:self-pMHC signals in secondary lymphoid organs (SLOs) under steady-state conditions (3). These tonic or basal TCR signals induce constitutive tyrosine phosphorylation of the TCR complex and association of the tyrosine kinase ZAP-70 with the CD3 ζ-chain even in naive T cells (4, 5). TCR:self-pMHC signals do not typically produce a cellular phenotype associated with an effector T cell (3). However, tonic TCR signals can alter chromatin accessibility and influence the expression of several genes at the transcriptional or protein level in T cells (6-9). This feature of tonic TCR signaling also raises the possibility that variable gene expression patterns in response to tonic TCR signaling result in functional heterogeneity within the naive T cell population (10, 11). How the intensity of tonic TCR signals helps shape the responsiveness of naive T cells to subsequent foreign antigen stimulation remains unresolved (3).

The immediate downstream effects of strong tonic TCR signals, such as CD3 ζ-chain phosphorylation and ZAP-70 recruitment to the TCR complex, are transient events (4). For example, the loss of ζ-chain phosphorylation and the dissociation of ZAP-70 from the TCR complex is evident in peripheral blood T cells compared to cells harvested from SLOs (4). Hence, the expression of proteins induced by TCR signaling, such as Nur77 and CD5, function as surrogate markers of tonic TCR signaling (3). Transgenic reporters of *Nr4a* family genes,

including *Nr4a1* and *Nr4a3*, can provide fluorescence-based readouts of TCR signaling (12). The Nur77-GFP reporter transgene consists of enhanced green fluorescent protein (GFP) driven by the promoter and enhancer elements of the *Nr4a1* gene (13, 14). *Nr4a1* gene transcription and Nur77-GFP reporter expression are induced in relative proportion to TCR signal strength. For example, the mean fluorescence intensity of Nur77-GFP expressed by acutely stimulated T cells decreases with diminishing pMHC affinity (13, 15). Furthermore, Nur77-GFP expression is relatively insensitive to constitutively active STAT5 or inflammatory signals, suggesting that reporter transgene expression is activated selectively by TCR stimulation in T cells (13). TCR-induced Nur77-GFP expression is also sensitive to inhibitors of TCR signaling proteins, including the tyrosine kinase ZAP-70. Previous work showed that stimulation with a single concentration of TCR stimulus in the presence of graded concentrations of a pharmacologic inhibitor of ZAP-70 catalytic activity resulted in dose-dependent decreases in Nur77-GFP fluorescence intensity (16).

Naive T cells express a wide range of steady-state Nur77-GFP in response to tonic or basal TCR signals from self-pMHC interactions in SLOs (13, 17, 18). In this study, we investigated the functional responsiveness of naive $CD8^+$ T cells that express varying levels of Nur77-GFP. Naive $CD8^+$ T cells expressing the highest levels of Nur77-GFP exhibit relative hyporesponsiveness to stimulation with agonist TCR ligands and differential gene expression, including genes potentially inhibiting T cell activation. We found that Nur77-GFP^{HI} cells from mice lacking Cbl-b exhibit partially rescued responsiveness to TCR stimulation. Together, these findings suggest a model whereby naive $CD8^+$ T cells adapt to high levels of tonic TCR signaling through negative regulation that limits T cell responsiveness.

Results

Naive $CD8^+$ T cells experience variable strengths of tonic TCR signaling

We first sought to investigate the diversity of Nur77-GFP expression in the $CD8^+$ T cell population. TCR polyclonal naive $CD8^+$ and $CD4^+$ T cells, as defined by their $CD44^{LO}$ $CD62L^{HI}$ cell surface phenotype, express Nur77-GFP at steady-state, with a range spanning over three orders of magnitude (**Fig. 2.S1 A**). The GFP intensities of naive $CD4^+$ and $CD8^+$ T cells are notably higher than non-transgenic T cells but decreased compared to $CD4^+$ $Foxp3^+$ regulatory T cells (**Fig. 2.S1 A**), a T cell population with highly self-reactive TCRs (19-21). The 10% of naive $CD8^+$ T cells expressing the highest levels of GFP exhibited largely overlapping or slightly reduced levels of surface TCRβ and CD8α than the 10% lowest GFP-expressing cells (**Fig. 2.1 A**). We also did not detect differences in surface plus intracellular TCRβ staining intensity between naive polyclonal GFP^{LO} and GFP^{HI} cells (**Fig. 2.S1 B** and **C**), suggesting that Nur77-GFP is uncorrelated with total TCR levels. The surface expression of CD5 correlates with TCR reactivity to self-pMHC (22-26). CD5 staining intensity is increased in naive, polyclonal GFP^{HI} $CD8^+$ T cells, in agreement with previous results and consistent with the concept that the intensity of CD5 and Nur77-GFP expression can reflect the strength of tonic TCR signaling (**Fig. 2.S1 D**, (27)). Naive GFP^{HI} $CD8^+$ T cells are $CD44^{LO}$ $CD62L^{HI}$, consistent with a naive surface marker phenotype. However, within the naive $CD8^+$ population, GFP^{HI} cells exhibit increased CD44 staining intensity relative to GFP^{LO} cells (**Fig. 2.S1 E**). This result is consistent with previous studies showing that $CD5^{HI}$ naive $CD8^+$ T cells express higher levels of CD44 than $CD5^{LO}$ cells (27).

We hypothesized that restricting the repertoire to a single TCR specificity would decrease the heterogeneity of GFP expression in a TCR transgenic population. To test the influence of TCR specificity on the distribution of GFP expression, we compared the intensity and distribution of GFP between naive polyclonal, OT-I, and P14 TCR transgenic populations. The geometric mean fluorescence intensity (gMFI) of GFP expressed by naive $CD44^{LO}$ $CD62L^{HI}$ OT-I cells was higher

than the GFP gMFI for polyclonal naive $CD8^+$ cells, whereas P14 cells had a similar gMFI compared to polyclonal cells (**Fig. 2.1 B**; and **Fig. 2.S1 F**). These results suggest that TCR specificity can influence the intensity of TCR signaling experienced by individual T cells. We also confirmed that the Nur77-GFP distribution is similar between *Trac*$^{-/-}$ and *Trac*$^{+/-}$ P14 cells, suggesting that endogenous recombination of the TCR α-chain in TCR transgenic cells does not dramatically shift the level of experienced tonic TCR signaling in the periphery (**Fig. 2.S1 G**).

Increases in steady-state Nur77-GFP expression could reflect more intense or frequent tonic TCR signals. We hypothesized that GFP expression in naive OT-I cells would correlate with the relative TCR:pMHC 2D affinity. To test this hypothesis, we used a 2-dimensional micropipette adhesion frequency (2D-MP) assay (28). This assay measures the relative affinity of OT-I TCRs for pMHC in the context of 2-dimensional membrane environments. We compared naive GFP^{LO} and GFP^{HI} cells that expressed the OT-I TCR and were deficient for the endogenous TCR α-chain to prevent endogenous TCR recombination. Furthermore, we excluded $Qa2^{LO}$ recent thymic emigrants (RTEs), which were more abundant in 6-13 week-old OT-I or P14 TCR transgenic mice but present at low frequencies in WT mice (**Fig. 2.S1 H** and **I**). RTEs continue to undergo maturation and exhibit diminished functional responses compared to mature T cells (29).

Sorted naive GFP^{LO} and GFP^{HI} OT-I cells were brought into contact with human red blood cells (RBCs) coated with the cognate SIINFEKL (N4) peptide or the weaker affinity SIIVFEKL (V4) peptide presented by $H2K^b$ for the detection of RBC elongation as a measure of an adhesion event (30). By calculating the adhesion frequency from a set of different T cell: RBC interaction times, the generated binding curve is used to calculate the 2D affinity (31). GFP^{HI} naive OT-I cells exhibited an increase in relative TCR:pMHC 2-D affinity for both N4 and V4 antigens compared

to GFP^{LO} cells (**Fig. 2.1 C**). These data suggest that higher relative 2D affinity interactions with N4, V4, and possibly to self-pMHC correlate with increased steady-state Nur77-GFP expression. This result is consistent with a previous study from our lab that revealed a positive correlation between Nur77-GFP expression in naive $CD4^+$ OT-II cells and the relative 2D affinity to OVA peptide/MHC (7).

We hypothesized that GFP expression in naive $CD8^+$ T cells depends on exposure to pMHC. To test this hypothesis, we adoptively transferred naive polyclonal $CD8^+$ T cells into *B2m*$^{-/-}$ or *B2m*$^{+/+}$ recipients for ten days (**Fig. 2.1 D**). The $CD8^+$ T cells transferred into *B2m*$^{-/-}$ recipients exhibited a reduction of GFP fluorescence intensity and CD5 staining intensity (**Fig. 2.1 D**). These results suggest that steady-state Nur77-GFP expression in naive $CD8^+$ T cells depends on the continuous exposure to and the abundance of pMHC. Likewise, previous studies have shown that steady-state Nur77-GFP expression in $CD4^+$ T cells also requires perpetual exposure to pMHC (13, 18). Hence, Nur77-GFP expression in naive T cells in the steady state reflects the frequency and intensity of relatively recently experienced tonic TCR signaling.

We adoptively transferred the 20% lowest and highest GFP-expressing naive OT-I cells into congenic lymphoreplete recipients to determine whether the bias in GFP expression is sustained beyond several half-lives of GFP protein in a TCR transgenic population (**Fig. 2.1 E**). Four weeks post-transfer, the distribution of Nur77-GFP fluorescence overlapped completely (**Fig. 2.1 E**). These results suggest that GFP biases in a naive TCR transgenic population shift over extended periods.

We next investigated how Nur77-GFP expression changes in naive polyclonal $CD8^+$ T cells over several days by adoptively transferring the 10% lowest and highest GFP-expressing naive

polyclonal $CD8^+$ T cells into congenic lymphoreplete recipients for one week (**Fig. 2.1 F**). Donor GFP^{LO} cells tended to sustain low GFP intensity, even though weak affinity antigens can induce OT-I cells to upregulate Nur77-GFP in less than eight hours (13). These results suggested that polyclonal GFP^{LO} cells tend to experience weak tonic TCR signals over a time scale of one week (**Fig 2.1. F**). TCR stimulation by GFP^{HI} naive donor T cells also sustained relatively high GFP expression (**Fig. 2.1 F**), although part of this phenotype could be due to the reported half-life of GFP lasting 26-54 hours (32, 33). These results are consistent with previous work, which showed that sorted TCR polyclonal $CD5^{LO}$ and $CD5^{HI}$ naive $CD4^+$ and $CD8^+$ T cells maintained skewed CD5 expression more than four weeks post-adoptive transfer into lymphoreplete recipients (22, 27). Hence, differences in TCR specificities may enable Nur77-GFP biases in naive polyclonal T cells for more extended periods.

We next asked whether GFP expression by naive $CD8^+$ T cells varied between cells harvested from different anatomical locations. Hence, we analyzed naive $CD8^+$ T cells from different SLOs, such as the spleen, mesenteric lymph nodes, and Peyer's patches, and compared the expression of GFP between these populations. However, we did not detect differences in the intensity or distribution of GFP expression (**Fig. 2.S1 J**). Subsequently, we queried whether the location within the spleen could still contribute to heterogenous Nur77-GFP expression in naive $CD8^+$ T cells. To compare the GFP distribution of T cells located in the more vascularized red pulp versus the white pulp of the spleen, we performed intravascular labeling with fluorescently labeled anti-CD45 antibodies 3 minutes before euthanasia. We detected largely overlapping GFP intensities for naive polyclonal $CD8^+$ T cells labeled with anti-CD45 and cells not labeled with anti-CD45, interpreted to represent cells located in the red and white pulp, respectively (**Fig. 2.S1 K)**. These results suggest that GFP^{LO} and GFP^{HI} cells are not skewed in their distribution at steady-state between the

red or white pulp in the spleen or the SLOs we analyzed.

Taken together, we interpret steady-state levels of GFP to function as a readout of relatively recently experienced TCR signals. TCR specificity, relative 2-D affinity, and frequency and duration of TCR stimulations can influence the intensity of steady-state GFP expression.

Naive $CD8^+$ T cells that experience extensive tonic TCR signaling are hyporesponsive to TCR stimulation

To analyze the functional responsiveness of GFP^{LO} and GFP^{HI} naive T cells, we isolated three populations across the GFP distribution (GFP^{LO}, GFP^{MED}, and GFP^{HI}) from naive, polyclonal $CD8^+$ T cells (**Fig. 2.2 A**; and **Fig. 2.S2 A**). After 24 hours of stimulation with soluble anti-CD3 antibodies and splenocyte APCs, we labeled cells with an IFNγ catch-reagent consisting of an anti-CD45 antibody conjugated with an anti-IFNγ antibody (34, 35). After a 45-minute secretion period at 37°C, we labeled the cells with a second anti-IFNγ antibody for detection purposes to visualize the secreted and "captured" IFNγ (35). Approximately 25% of GFP^{LO} cells secreted IFNγ, whereas two-fold fewer GFP^{MED} and less than 1% of GFP^{HI} cells secreted IFNγ (**Fig. 2.2 B** and **C**). Hence, there was an apparent inverse correlation between the intensity of steady-state GFP expression and the magnitude of anti-CD3-induced IFNγ-secretion. Although cytokine production increases after T cells have undergone cell division, naive T cells have the capacity to produce effector cytokines within 24 hours of stimulation and before cell division (23, 36-43). We also detected a similar inverse correlation between Nur77-GFP expression and IFNγ-secretion in naive P14 TCR transgenic cells specific for the lymphocytic choriomeningitis virus (LCMV) epitope GP33 upon cognate antigen stimulation (**Fig. 2.S2 B** and **C**) (44).

To determine whether GFP^{LO}, GFP^{MED}, and GFP^{HI} cells similarly upregulated markers associated

with acute T cell activation, we analyzed their expression of the activation markers CD25, CD69, and transferrin receptor (CD71), in addition to the Nur77-GFP reporter. All three populations upregulated Nur77-GFP and CD69 above baseline levels (**Fig. 2.2 D**; and **Fig. 2.S2 D**). However, on average, GFP^{LO} cells expressed higher levels of CD69 than GFP^{MED} and GFP^{HI} cells (**Fig. 2.2 D**). Similarly, higher frequencies of the GFP^{LO} population fully upregulated CD25 and CD71 (**Fig. 2.2 D**). Following stimulation, the sorted GFP^{LO}, GFP^{MED}, and GFP^{HI} populations each expressed similar levels of Nur77-GFP at the 24-hour endpoint.

To test whether GFP^{LO} and GFP^{HI} cells exhibit differences in survival after stimulation, we quantified the proportion of viable $CD8^+$ T cells after the 24-hour stimulation period. GFP^{HI} cells had a 1.5-fold reduction in the percentage of viable cells compared with GFP^{LO} cells (**Fig. 2.S2 E**). Hence, GFP^{HI} cells experience a decrease in cell survival following TCR stimulation.

We next asked whether GFP^{LO} and GFP^{HI} cells exhibit differences in cell division. We hypothesized that more extensive tonic TCR signaling would result in delayed or reduced cell division upon stimulation of naive $CD8^+$ T cells. We thus labeled $CD8^+$ T cells with a cell proliferation dye and sorted naive GFP^{LO} and GFP^{HI} polyclonal T cells for *in vitro* stimulation with anti-CD3 antibodies and APCs (**Fig. 2.S2 F**). Three days post-stimulation, the proliferation index (the average number of divisions of cells that divided at least once) of GFP^{LO} cells was greater than that of GFP^{HI} cells (**Fig. 2.S2 G**). This result suggests that extensive tonic TCR signaling negatively impacts the proliferative responses of naive $CD8^+$ T cells under the conditions tested.

We further hypothesized that naive GFP^{LO} cells might have a competitive advantage during the early phase of an immune response in vivo relative to GFP^{HI} cells. To investigate this hypothesis,

we sorted the 10% highest and lowest GFP-expressing P14 cells with a $CD44^{LO}$ $CD62L^{HI}$ $Qa2^{HI}$ $V\alpha2^{HI}$ phenotype to isolate mature, naive P14 cells (**Fig. 2.S2 H**). In a competitive-transfer experiment, we co-transferred 3000 congenically distinct donor cells each, from GFP^{LO} and GFP^{HI} populations into WT recipients to analyze the ratiometric difference between the two populations in an acute infection model (**Fig. 2.S2 I**). Five days post LCMV infection, the ratio between GFP^{LO} and GFP^{HI} cells in the spleen significantly skewed toward GFP^{LO} cells (**Fig. 2.S2 I**). Hence, GFP^{LO} cells, relative to GFP^{HI} cells, have a slight competitive advantage in the early phase of an immune response that persists through multiple rounds of cell division.

We next asked how the cellular responses of GFP^{LO} and GFP^{HI} naive $CD8^{+}$ OT-I TCR transgenic cells compared in response to titrated doses of peptide and with altered peptides that vary in affinity for the OT-I TCR. We postulated that GFP^{HI} T cells exhibited decreased responsiveness for pMHC at low concentrations or weak affinity pMHC ligands. We sorted naive T cells with a $CD8^{+}$ $CD44^{LO}$ $CD62L^{HI}$ $Qa2^{HI}$ phenotype from OT-I $TCR\alpha^{-/-}$ TCR transgenic mice to compare mature T cell populations differing only in basal GFP expression. From this naive T cell population, we isolated the 10% lowest and highest GFP-expressing cells (**Fig. 2.3 A**). We assessed the upregulation of CD25 and CD69 after stimulating GFP^{LO} and GFP^{HI} OT-I cells for 16 hours with APCs and the cognate N4 peptide. The dose-response curve of GFP^{HI} cells was shifted further to the right compared to GFP^{LO} cells, indicating a reduction in CD25 and CD69 upregulation. The calculated Log_{10} EC_{50} value for GFP^{LO} cells was -11.36 compared to -11.23 for GFP^{HI} cells (**Fig. 2.3 B**; and **Fig. 2.S3 A and B**). These results suggest that GFP^{HI} cells exhibit reduced responsiveness to a high-affinity antigen under non-saturating antigen doses.

To test whether extensive tonic TCR signaling affected the responsiveness to antigen affinity, we

also stimulated OT-I cells with the SIIQFERL (Q4R7) altered peptide, which has reduced affinity for the OT-I TCR relative to the N4 peptide (45). The dose-response curve of GFP^{HI} compared to GFP^{LO} cells was increasingly shifted to the right when stimulated with Q4R7 relative to N4. The calculated Log_{10} EC_{50} value for GFP^{LO} cells was -9.657 compared to -9.190 for GFP^{HI} cells (**Fig. 2.3 B**; and **Fig. 2.S3 B**). Upon stimulation with the weak agonist peptide SIIGFEKL (G4), the dose-response curve also shifted to the right for GFP^{HI} cells. The calculated Log_{10} EC_{50} value for GFP^{LO} cells was -6.907 compared to -6.155 for GFP^{HI} cells (**Fig. 2.3 B**; and **Fig. 2.S3 B**). These results indicate that higher levels of accumulated TCR signaling from self-pMHC in naive $CD8^+$ T cells result in hyporesponsiveness to subsequent stimulation.

We next asked whether GFP^{LO} and GFP^{HI} OT-I cells exhibit differences in TCR-induced cytokine secretion. We hypothesized that GFP^{HI} cells would exhibit decreased IL-2 and IFNγ secretion relative to GFP^{MED} and GFP^{LO} cells. After sorting GFP^{LO}, GFP^{MED}, and GFP^{HI} OT-I cells and stimulating them for 16 hours with a concentration ($1x10^{-11}$ M) of N4 peptide that was on the linear range of the curve for CD25- and CD69-upregulation, we performed IL-2- and IFNγ-capture assays (**Fig. 2.3 C** and **D**; and **Fig. 2.S3 C** and **D**). GFP^{LO} OT-I cells generated the highest percentage of IFNγ-secreting cells (approximately 25%) (**Fig. 2.3 C** and **D**). There was a trend toward reduced IFNγ-secreting cells in the GFP^{MED} population (about 15%) and a significant reduction in the GFP^{HI} population (about 6%) (**Fig. 2.3 C** and **D**). The frequency of IL-2-secreting cells was below 5% for all populations at a dose of $1x10^{-11}$ M N4 peptide (**Fig. 2.3 C** and **D**).

To induce more robust IL-2 secretion, we stimulated the three populations with a ten-fold higher dose of N4 peptide ($1x10^{-10}$ M). At this dose, there was comparable IFNγ secretion (**Fig. 2.3 C** and **D**). However, approximately 25% of GFP^{LO} cells secreted IL-2, whereas about 6% of GFP^{HI} cells

secreted IL-2 (**Fig. 2.3 C** and **D**). Similarly, the frequency of cells that secreted both IL-2 and IFNγ was significantly higher in GFP^{LO} cells (about 5%) than in GFP^{MED} (approximately 2.5%) or GFP^{HI} cells (about 1%) (**Fig. 2.3 C** and **D**). Hence, a dose-dependent, inverse correlation exists between GFP expression in naive $CD8^+$ T cells and cytokine secretion in response to subsequent foreign antigen stimulation.

$CD8^+$ GFP^{HI} cells exhibit attenuated calcium flux responses and exert reduced mechanical forces

We next wanted to investigate whether GFP^{HI} cells exhibited an attenuated response at more proximal events of T cell activation upon stimulation with cognate peptide. Among the early T cell responses to pMHC stimulation is the exertion of mechanical forces through the TCR (46). Previous work found a positive correlation between increases in the exertion of mechanical tension by T cells and increases in the intensity of ZAP-70 phosphorylation, suggesting a positive regulatory role for mechanical forces in early T cell activation (47). We hypothesized that GFP^{LO} and GFP^{HI} cells would exhibit differences in tension exerted on pMHC ligands. To test this hypothesis, we utilized DNA hairpin-based "tension" probes linked to pMHC. The tension probe consists of a DNA hairpin conjugated to fluorophore (Atto647N) and quencher (BHQ2) molecules positioned to quench fluorescence by fluorescence resonance energy transfer (FRET) when the DNA hairpin is in its closed configuration (**Fig. 2.4 A**) (48). When a T cell, through its TCR, applies forces to a pMHC molecule with a magnitude exceeding 4.7 piconewtons (pN), the DNA hairpin unfolds, separating the FRET pair and causing dequenching of the dye. A "locking" DNA strand is then introduced to selectively hybridize to the mechanically unfolded DNA hairpin and prevent refolding to capture the tension signal. After isolating the 10% lowest and highest GFP-expressing OT-I cells, we cultured them on substrates coated with tension probes conjugated to $H2\text{-}K^b$ loaded with OVA N4 peptide (**Fig. 2.S4 A** and **B**). GFP^{LO} cells induced, on average, a 20%

higher fluorescence signal from the tension probes than GFP^{HI} cells (**Fig. 2.4 B** and **C**). These results indicate that GFP^{LO} cells were more likely to exert the 4.7 pN tension force required to unfold the DNA hairpins than GFP^{HI} cells in response to pMHC stimulation.

We next sought to determine whether GFP^{LO} and GFP^{HI} naive $CD8^+$ T cells exhibited differences in proximal TCR signaling. We hypothesized that naive GFP^{HI} OT-I T cells would exhibit decreased cytosolic Ca^{2+} concentrations relative to GFP^{LO} cells upon stimulation with cognate N4 peptide antigen. Hence, we co-incubated OT-I cells labeled with the Indo-1 ratiometric indicator dye with N4 peptide-pulsed APCs and analyzed the fluorescent signal of the calcium indicator dye in T cells by flow cytometry. Compared to the peak free Ca^{2+} concentration signal generated by GFP^{LO} cells, the peak signal generated by GFP^{HI} cells was reduced by 20% (**Fig. 2.4 D**). Together, these data suggest that GFP^{HI} naive $CD8^+$ T cells, which previously experienced more TCR signaling in the basal state, trigger downstream signals with weaker intensity in response to subsequent TCR stimulation. These results are consistent with a previous study using CD5 as a surrogate marker of self-pMHC reactivity, which showed an inverse correlation between the intensity of CD5 expression and the magnitude of anti-CD3-induced Ca^{2+} increases in naive $CD8^+$ T cells (23).

We further hypothesized that naive GFP^{HI} OT-I cells would exhibit attenuated integrated TCR signaling in response to antigen stimulation. Upregulation of the transcription factor IFN regulatory factor 4 (IRF4) occurs within hours in response to TCR stimulation and is sensitive to both antigen affinity and antigen dose in $CD8^+$ T cells (49, 50). Hence, we sorted naive GFP^{LO} and GFP^{HI} OT-I cells to investigate the induced IRF4 expression five hours post-stimulation with the weak agonist peptide G4. The gMFI of IRF4 staining intensity in GFP^{LO} cells was, on average, 1.6-fold higher than in GFP^{HI} cells (**Fig. 2.4 E**). Thus, naive GFP^{HI} cells exhibit a reduced intensity

of integrated TCR signaling within hours of stimulation compared to GFP^{LO} cells.

Extensive tonic TCR signaling in naive $CD8^+$ T cells correlates with differences in gene expression

To identify gene expression patterns associated with increased tonic TCR signaling in naive $CD8^+$ T cells, we performed RNA-sequencing of naive $CD8^+$ $CD44^{LO}$ $CD62L^{HI}$ $Qa2^{HI}$ OT-I cells isolated based on the 10% highest versus 10% lowest GFP fluorescence intensities. We detected a total of 601 differentially expressed genes (DEGs) at a false discovery rate (FDR) < 0.05 (**Fig. 2.5 A**). Considering the correlation between Nur77-GFP expression and TCR signal strength, we hypothesized that GFP^{HI} cells would exhibit a gene expression profile with more similarities to acutely stimulated cells than GFP^{LO} cells. To test this hypothesis, we performed Gene Set Enrichment Analysis (GSEA) to compare our dataset of GFP^{LO} and GFP^{HI} naive $CD8^+$ T cells with DEGs upregulated in viral infection-induced effector OT-I cells compared to naive cells (51). Consistent with this hypothesis, GFP^{HI} cells showed enrichment of genes upregulated in effector $CD8^+$ T cells (**Fig. 2.5 B**).

Additionally, we compared the degree of overlap between DEGs in naive GFP^{HI} versus GFP^{LO} cells and DEGs in *Listeria* infection-induced OT-I effector cells versus naive OT-I cells (52) (**Fig. 2.S5 A**). Linear regression analysis indicated a significant correlation between genes enriched in GFP^{HI} cells and acutely stimulated OT-I cells (**Fig. 2.S5 B**). These results suggest that the effects of extensive tonic TCR signaling share similarities with the gene expression changes associated with acutely stimulated and effector $CD8^+$ T cells. However, GFP^{HI} cells also showed enrichment of genes upregulated in effector compared to resting memory OT-I cells (**Fig. 2.5 B**). We did not detect a statistically significant enrichment of genes associated with T cell exhaustion, senescence, or deletional tolerance in GFP^{HI} cells (**Fig. 2.5 B**).

We next sought to explore the sets of DEGs in GFP^{HI} naive $CD4^+$ and $CD8^+$ T cells. Therefore, we compared the DEGs between GFP^{LO} and GFP^{HI} naive $CD8^+$ T cells and the DEGs upregulated in naive GFP^{HI} $Ly6C^-$ $CD4^+$ T cells (7) (**Fig. 2.S5 C**). Among the overlapping DEGs from both analyses ($CD8^+$ and $CD4^+$ cells), linear regression analysis suggested a significant correlation (**Fig. 2.S5 D**). Hence, extensive tonic TCR signals during steady-state conditions induce similar transcriptional changes in naive $CD4^+$ and $CD8^+$ T cells.

In addition, we detected increased transcripts of genes involved in cell division in GFP^{HI} relative to GFP^{LO} cells, consistent with a gene signature indicative of acutely activated T cells (**Fig. 2.5 C**). In agreement, naive $CD8^+$ T cells that experience stronger tonic TCR signals and express higher levels of CD5 likewise show enrichment for cell cycle-associated genes (53). GFP^{HI} cells also expressed higher levels of transcription factors associated with T cell differentiation, such as *Bcl6* and *Ikzf2* (Helios), and TCR stimulation, such as *Tox* and *Irf8* (**Fig. 2.5 C**) (54-56). Consistent with a gene signature of T cell activation, GFP^{HI} cells upregulated immunomodulatory molecules such as *Tnfrsf9* (4-1bb), *Tnfsf11* (Rankl), and *Cd200* (**Fig. 2.5 C**) (57-60). GFP^{HI} cells expressed lower levels of *Il7r* (CD127) in addition to other common γ-chain cytokine receptors such as *Il4ra*, *Il6ra* (CD126), and *Il15ra* (**Fig. 2.5 C**). Among genes involved in signal transduction, GFP^{HI} cells had lower expression levels of kinases such as Pim1 and Pdk1. In contrast, GFP^{HI} cells expressed higher levels of the phosphatases *Ubash3b* (Sts1), *Dusp22* (Jkap), and *Ptpn14* (**Fig. 2.5 C**). Taken together, gene expression patterns associated with higher levels of tonic TCR signaling bear similarities to gene expression patterns induced by acute TCR stimulation. This gene signature includes higher expression levels of immunomodulatory receptors and ligands, including negative regulators of TCR signaling.

We next performed flow cytometry analyses to determine whether differential gene expression

patterns correlated with differential protein expression. We analyzed the 10% highest vs. lowest GFP-expressing naive, polyclonal $CD8^+$ T cells to compare the protein levels of several DEGs, including *Bcl6*, *Ikzf2* (Helios), *Izumo1r* (Folate receptor 4), *Il6ra* (CD126), *Il7ra* (CD127), and *Cd200* (**Fig. 2.5 D**; and **Fig. 2.S5 E**). For four of the six selected DEGs, protein staining was increased in GFP^{HI} relative to GFP^{LO} cells and thus correlated with the RNA-sequencing data. GFP^{HI} cells expressed lower surface levels of CD126 and CD127, consistent with the RNA-seq analysis. Flow cytometry analysis of naive $CD8^+$ T cells showed a spectrum of CD127 and CD200 expression (**Fig. 2.5 E**). Within the naive $CD8^+$ population, the $CD127^{HI}$ $CD200^{LO}$ cell subset enriched for Nur77-GFP^{LO} cells, and in contrast, the $CD127^{LO}$ $CD200^{HI}$ population enriched for GFP^{HI} cells (**Fig. 2.5 E**). These results indicate that Nur77-GFP^{LO} and GFP^{HI} cells exhibit differential expression of several genes at the protein level.

We hypothesized that $CD127^{LO}$ $CD200^{HI}$ cells would exhibit an attenuated responsiveness similar to GFP^{HI} cells. To test this hypothesis, we sorted $CD127^{HI}$ $CD200^{LO}$ (GFP^{LO}-like) and $CD127^{LO}$ $CD200^{HI}$ (GFP^{HI}-like) naive $CD8^+$ T cells from WT mice and stimulated these populations with APCs and anti-CD3 antibodies (**Fig. 2.5 F**). After 24 hours of stimulation, we performed an IFNγ secretion assay. The frequency of IFNγ-secreting $CD127^{LO}$ $CD200^{HI}$ (GFP^{HI}-like) cells was, on average, more than four-fold lower than the frequency of IFNγ-secreting $CD127^{HI}$ $CD200^{LO}$ (GFP^{LO}-like) cells (**Fig. 2.5 F**). These results suggest that GFP^{HI}-like naive $CD8^+$ T cells from WT mice exhibit attenuated early responsiveness and a similar functional phenotype as Nur77-GFP^{HI} naive $CD8^+$ T cells.

Cbl-b deficiency partially rescues the responsiveness of GFP^{HI} naive $CD8^+$ T cells

We hypothesized that increased steady-state expression of negative regulators mitigates the

activation of GFP^{HI} cells. Previous studies in our lab revealed that naive GFP^{HI} Ly6C^{-} CD4^{+} T cells express higher steady-state protein levels of the E3 ubiquitin ligase Cbl-b, a negative regulator of TCR signaling (18, 61). We hypothesized that CD8^{+} GFP^{HI} cells, similarly to their CD4^{+} counterparts, would express higher levels of Cbl-b. Our RNA-seq analyses did not detect a significant difference in *Cblb* mRNA levels between GFP^{LO} and GFP^{HI} naive CD8^{+} T cells. We next compared Cbl-b protein expression by GFP^{LO} and GFP^{HI} cells by intracellular staining analysis. Both cell populations stained positive for Cbl-b; however, the gMFI of Cbl-b staining intensity in GFP^{HI} cells was almost 1.5-fold higher than in GFP^{LO} cells (**Fig. 2.6 A**). Hence, extensive tonic TCR signaling is associated with an upregulation of Cbl-b protein levels in naive CD8^{+} T cells.

Considering the inhibitory function of Cbl-b in the TCR signal transduction pathway and its increased expression in GFP^{HI} cells, we hypothesized that Cbl-b deficiency would rescue the attenuated responsiveness of GFP^{HI} cells. We first generated *Cblb*$^{-/-}$ Nur77-GFP mice to test this hypothesis. *Cblb*$^{+/+}$ and *Cblb*$^{-/-}$ naive CD8^{+} cells express a similar range of Nur77-GFP at steady-state, although the gMFI of GFP was higher in *Cblb*$^{-/-}$ cells (**Fig. 2.6 B**). To determine whether Cbl-b deficiency rescues the responsiveness of GFP^{HI} cells, we isolated the 10% lowest and highest GFP-expressing cells (**Fig 2.6 C**). After stimulation for 24 hours with APCs and anti-CD3 antibodies, *Cblb*$^{+/+}$ and *Cblb*$^{-/-}$ cells upregulated GFP to comparable levels (**Fig. 2.6 D**). The frequency of GFP^{HI} cells that upregulated CD25 and CD69 after 24 hours of stimulation was approximately two-fold higher in *Cblb*$^{-/-}$ compared to *Cblb*$^{+/+}$ cells (**Fig. 2.6 E**). The frequencies of CD25^{HI}CD69^{HI} cells were higher in GFP^{LO} cells and not significantly different between *Cblb*$^{+/+}$ and *Cblb*$^{-/-}$ cells (**Fig. 2.6 E**). In a complementary approach, we analyzed Cbl-b-deficient naive CD8^{+} T cells using the CD127^{HI} CD200^{LO} (GFP^{LO}-like) and CD127^{LO} CD200^{HI} (GFP^{HI}-like)

gating strategy (**Fig. 2.S6A** and **B**). While only 5% of *Cblb*$^{+/+}$ GFP^{HI}-like cells fully upregulated CD25 and CD69, the frequency was more than ten-fold higher in *Cblb*$^{-/-}$ GFP^{HI}-like cells (**Fig. 2.S6 C**). The frequency of CD25^{HI}CD69^{HI} cells was 1.5-fold higher in *Cblb*$^{-/-}$ compared to *Cblb*$^{+/+}$ GFP^{LO}-like cells (**Fig. 2.S6 C**).

We next quantified the increases in CD25 gMFI from *Cblb*$^{+/+}$ to *Cblb*$^{-/-}$ populations. The CD25 gMFI increased for both GFP^{LO} and GFP^{HI} populations; however, the fold increase in CD25 gMFI was significantly higher for GFP^{HI} than GFP^{LO} cells (**Fig 2.6 F**). We next compared the CD25 gMFI between *Cblb*$^{-/-}$ and *Cblb*$^{+/+}$ GFP^{LO}-like and GFP^{HI}-like cells. The CD25 gMFI increased in *Cblb*$^{-/-}$ cells for both populations (**Fig. 2.S6 D**). There was also a trend of a higher fold increase for GFP^{LO}-like cells, but that did not reach statistical significance (**Fig. 2.S6 D**). These data suggest that the CD25 upregulation of GFP^{HI} cells was rescued to a greater extent by Cbl-b deficiency than in GFP^{LO} cells.

We next asked how Cbl-b deficiency affected the secretion of IFNγ in GFP^{LO} and GFP^{HI} cells. After 24 hours of stimulation with anti-CD3-mediated TCR-crosslinking, we performed an IFNγ-capture assay. The percentage of *Cblb*$^{+/+}$ GFP^{HI} cells that secreted IFNγ was on average 6% +/- 3.4%, whereas the percentage of *Cblb*$^{-/-}$ GFP^{HI} cells that secreted IFNγ was on average 28% +/- 4.7% (**Fig. 2.6 F**). Among GFP^{LO} cells, Cbl-b-deficiency increased the frequency of IFNγ-secreting cells almost two-fold (**Fig. 2.6 F**). We next asked whether Cbl-b deficiency could also rescue the secretion of IFNγ in GFP^{HI}-like cells. Approximately 20% of GFP^{HI}-like *Cblb*$^{-/-}$ T cells secreted IFNγ, while the frequency of IFNγ-secreting cells was less than 1% in the GFP^{HI}-like *Cblb*$^{+/+}$ population (**Fig. 2.S6 E**). IFNγ secretion in GFP^{LO}-like Cbl-b-deficient T cells was about four-fold more prevalent compared to GFP^{LO}-like *Cblb*$^{+/+}$ cells (**Fig. 2.S6 E**). Together, these

results indicate that naive GFP^{LO} and GFP^{HI} $CD8^+$ T cells differentially express Cbl-b at the protein level and are more responsive to TCR stimulation in the absence of Cbl-b. However, some GFP^{HI} responses, such as CD25 upregulation, appear to be rescued more profoundly by Cbl-b deficiency. These data support a model where extensive tonic TCR signals induce negative regulation, partly mediated by increased Cbl-b expression.

Discussion

In this study, we found that naive $CD8^+$ T cell responsiveness correlates inversely with steady-state Nur77-GFP expression. Hence, we propose a model where extensive tonic TCR signaling induces negative feedback mechanisms that limit the responsiveness to subsequent TCR stimulations.

Steady-state Nur77-GFP expression in naive T cells is heterogeneous, and the strength, frequency, and recency of tonic TCR signals may all influence Nur77-GFP expression levels in naive $CD8^+$ T cells. Our findings showed that steady-state Nur77-GFP expression depended on continuous exposure to MHC I, indicating that recurrent TCR signals continuously drive Nur77-GFP expression. These results are consistent with previous studies that showed that naive T cells engage in multiple transient interactions with APCs that, on average, last for less than five minutes per interaction (62). These findings suggest that naive T cells experience discontinuous tonic TCR signaling during these short-lived interactions with APCs. The GFP proteins expressed as a result of TCR stimulation persist in T cells with a half-life of 26-54 hours, longer than most T cell:APC interactions (32, 33). In light of these results, we conclude that steady-state GFP expression can reflect cumulative tonic TCR signals experienced by T cells as they scan APCs in SLOs. On the other hand, it is formally possible that high basal Nur77-GFP expression reflects very recent acute TCR stimulation. However, studies of the reporter transgene Nur77-Tempo suggest this may not

be the case. In Nur77-Tempo transgenic mice, the *Nr4a1* promoter drives the expression of a Fluorescent Timer (FT) protein (63). The FT protein shifts its fluorescence emission spectrum with a half-life of around four hours in T cells (64). Analysis of the FT fluorescence in $CD69^{-}$ $CD8^{+}$ T cells in the spleen showed non-detectable levels of the less mature form of FT, indicating that the contribution of very recent tonic TCR signals to steady-state FT expression was minimal. These results are consistent with the model that fluorescent reporters can reflect the accumulated output of multiple discontinuous tonic TCR signals experienced by naive T cells at steady-state. Considering these findings and the decay of Nur77-GFP in naive $CD8^{+}$ T cells seen after ten days in $B2m^{-/-}$ mice, we interpret steady-state Nur77-GFP expression in naive T cells to reflect the accumulation of TCR signaling events occurring within days.

The influence of discrete, recurrent TCR signaling events on T cell biology is also apparent during development. For example, $CD4^{+}$ $CD8^{+}$ double positive (DP) thymocytes experience multiple transient TCR stimulations over hours to days during thymic positive selection, as observed by transitory calcium increases (65). Inhibition of ZAP-70 kinase activity decreased the intensity and frequency of these discontinuous signaling events and correlated with an impairment in positive selection (66).

Our gene expression analyses revealed that high GFP expression in naive T cells correlates with upregulation of a gene expression profile associated with T cell activation and negative regulators of TCR signaling. This finding is reminiscent of recent studies showing that constitutive agonist TCR stimulation in mice unperturbed by infection or inflammatory mediators is associated with tolerogenic responses in $CD4^{+}$ T cells (67). In this system, constitutive expression of even low doses of cognate antigen over an extended period induces the upregulation of genes associated with anergy (67). Furthermore, we previously found that naturally occurring naive Nur77-GFP^{HI}

$CD4^+$ T cells exhibit a gene expression profile associated with T cell activation and negative regulation (7). Moreover, naive $CD4^+$ T cells expressing a hyperactive ZAP-70 mutant experience increased tonic TCR signaling but exhibit reduced responsiveness to agonist TCR stimulation (68). However, Cbl-b-deficiency restored the responsiveness of those T cells, highlighting the role of Cbl-b in $CD4^+$ T cell anergy (68). These studies suggest that extensive TCR signals can induce negative feedback mechanisms.

Here, we propose that the attenuated responsiveness of the most self-reactive naive $CD8^+$ T cells due to induced negative regulation is dependent, at least in part, on the ubiquitin ligase Cbl-b. Nur77-GFP expression in naive $CD8^+$ T cells positively correlates with increased protein levels of the ubiquitin ligase Cbl-b. The signalosome of Cbl-b in $CD4^+$ T cells consists of nearly 100 interacting partners, including Sts1, Sts2, CD5, CSK, and LAT (69). Studies of Cbl-b deficiency in T cells have established Cbl-b as a negative regulator of T cell activation (61). Cbl-b deficient T cells exhibit many altered signal transduction pathways in response to TCR signaling, such as increased NF-κB activation and Vav1 phosphorylation (70, 71).

Recent studies also suggest that Nr4a transcription factors restrain peripheral T cell responses (72). Consistent with this concept, in vivo-tolerized murine T cells express high levels of *Nr4a1*, and *Nr4a1* overexpression results in the upregulation of anergy-associated genes, including Cbl-b (73). *Nr4a1* deficiency results in resistance to anergy induction and exacerbates autoimmune disease severity (73-75). Moreover, $Nr4a1^{-/-}$ $Nr4a2^{-/-}$ $Nr4a3^{-/-}$ CAR T cells had an enhanced antitumor response in a solid tumor mouse model (76). These studies suggest that *Nr4a1* and the other *Nr4a* family genes can act as negative regulators (77). We propose that the transcriptional upregulation of *Nr4a1* in Nur77-GFP^{HI} naive $CD8^+$ cells is part of a negative feedback mechanism also associated with tonic TCR stimulation.

Our differential gene expression analyses suggested that strong tonic TCR signaling induced upregulation of genes associated with acute TCR stimulation, as well as the phosphatases *Ubash3b* (encoding Sts1), *Dusp22* (encoding Jkap), and *Ptpn14,* which have the potential to function as negative regulators of intracellular signaling in naive OT-I GFP^{HI} cells. *Ubash3b*$^{-/-}$ and *Ubash3b*$^{-/-}$ *Ubash3a*$^{-/-}$ T cells are hyperresponsive to TCR stimulation (78, 79). Sts1's role in negatively regulating T cell responsiveness may involve the inhibition of ZAP-70 through the dephosphorylation of regulatory tyrosine residues (79). The phosphatase Jkap can dephosphorylate kinases of the proximal TCR signaling cascade, while Ptpn14 has unclear functions in T cells (80, 81). The higher gene expression of these phosphatases in GFP^{HI} cells is coherent with the higher expression of the phosphatase Ptpn2 in CD5^{HI} over CD5^{LO} naive CD8^{+} T cells (82). Furthermore, T cells deficient in *Ptpn2* tend to undergo more extensive lymphopenia-induced proliferation, suggesting Ptpn2 negatively regulates TCR:self-pMHC signaling (82).

CD5-deficient T cells are hyperresponsive to TCR stimulation, suggesting that CD5 can act as a negative regulator of TCR signaling (83, 84). CD5 and Nur77-GFP are both surrogate markers of tonic TCR signaling (3). However, although a positive correlation exists between CD5 staining intensity and Nur77-GFP expression in naive CD8^{+} T cells, we show in this study that the 10% lowest and highest GFP-expressing cells still have overlapping CD5 staining intensity. Likewise, previous studies showed that the 20% top and bottom CD5-expressing naive CD8^{+} T cells have overlapping Nur77-GFP expression (27). Hence, CD5^{HI} and Nur77-GFP^{HI} expression phenotypes mark different cell populations. Similarly, CD5^{LO} and Nur77-GFP^{LO} expression phenotypes label diverging cell populations. We propose that the differences in cellular compositions of CD5^{LO} and GFP^{LO} (or CD5^{HI} and GFP^{HI}) cell populations can lead to different functional phenotypes. For example, previous studies suggested that CD5^{HI} naive CD8^{+} T cells have a competitive advantage

over $CD5^{LO}$ cells in response to foreign antigen stimulation (27, 85). In contrast, our results suggest that GFP^{LO} cells have a competitive advantage over GFP^{HI} cells. Understanding the differences between CD5 and *Nr4a1*-reporter expression as markers of tonic TCR signaling would require additional studies.

The upregulation of negative regulators in naive T cells in response to tonic TCR signaling is consistent with models proposing that T cell responsiveness depends on previously experienced TCR signals (9, 86). A negative feedback loop is one way in which relatively strong basal TCR signaling could effectively result in T cell desensitization and hyporesponsiveness to subsequent TCR stimulations. "Adaptive tuning" in this context could attenuate the responsiveness of the naive T cells that respond most intensely to self-pMHC (87). Strong TCR stimulation of naive T cells can re-calibrate the activation thresholds of recently stimulated T cells through upregulation of checkpoint receptor expression (88).

Variable levels of Nur77-GFP expression appear to correlate with functional heterogeneity within the naive $CD8^+$ T cell population. Tonic TCR signal strength may influence such variations at the single-cell level. Lineage-tracing studies have previously identified diversity in the expansion and differentiation of single TCR transgenic T cells through primary and recall responses (89). Cellular heterogeneity may also contribute to the dynamic nature of adaptive immune responses to respond to a breadth of antigens (11, 90).

In conclusion, we observed reduced responsiveness in GFP^{HI} naive $CD8^+$ T cells that have experienced extensive tonic TCR stimulation in the steady state. We speculate that such negative feedback mechanisms may constitute a form of cell-intrinsic tolerance in naive T cells.

Materials and Methods

Mice

Nur77-GFP (Tg(Nr4a1-EGFP)GY139Gsat) transgenic mice, ZAP-70 deficient mice lacking mature T cells (Zap70tm1Weis), and Foxp3-RFP mice (C57BL/6-Foxp3tm1Flv/J) have been previously described (14, 91, 92). C57BL/6J mice (WT mice in the text), CD45.1 mice (B6.SJL-Ptprca Pepcb/BoyJ), and *B2m*$^{-/-}$ mice (B6.129P2-B2mtm1Unc/DcrJ) were purchased from the Jackson Laboratory (93). When noted, the Nur77-GFP strain was interbred with the CD45.1 strain. A Nur77-GFP strain that is interbred with the OT-I (C57BL/6-Tg(TcraTcrb)1100Mjb/J) TCR transgenic strain was described previously (15). This OT-I-Nur77-GFP strain was interbred with a *Trac*$^{-/-}$ strain (B6.129S2-Tcratm1Mom/J) purchased from the Jackson Laboratory. A Nur77-GFP strain interbred with the Foxp3-RFP strain has previously been described (18). P14 mice have been described before and were generously provided by Rafi Ahmed at Emory University (94). P14 mice on the C57BL/6J background were interbred with the Nur77-GFP and the CD45.1 strains. All mice were housed under specific pathogen-free conditions in the Division of Animal Resources at Emory University. The *Cblb*$^{-/-}$ strain was previously described and was interbred with the Nur77-GFP strain (95). These two strains were maintained in the Laboratory Animal Resource Center at the University of California, San Francisco. Both female and male mice were used throughout the study. All animal experiments were conducted in compliance with the Institutional Animal Care and Use Committees at Emory University (PROTO201700761) and the University of California, San Francisco (AN184320-02D).

Antibodies and reagents

The antibodies and reagents used in this study are listed in table S1. For the negative enrichment of CD8^{+} T cells, the following biotinylated anti-mouse or anti-mouse/human antibodies were used: CD4 (clone RM4-5), CD19 (6D5), B220 (RA3-6B2), CD11b (M1/70), CD11c (N418), CD49b

(DX5), and Erythroid cells (TER119), for the negative selection of APCs, biotinylated anti-CD4 (RM4-5), anti-CD8α (53-6.7), and anti-Erythroid cells (TER119) were used.

Lymphocyte isolation and flow cytometry

Single-cell suspensions of lymphoid organs were generated by mashing organs through a 70 μm cell strainer or using a Dounce homogenizer. For phenotypic analysis of T cells by flow cytometry, red blood cells (RBCs) were lysed using RBC Lysis Buffer (Tonbo Biosciences) prior to Fc-block incubation (anti-mouse CD16/CD32, clone 2.4G2). $CD8^+$ T cells were purified by negative selection using biotinylated antibodies and magnetic beads, as previously described (96). Splenocytes were used as APCs, isolated from *Zap70*$^{-/-}$ or *Trac*$^{-/-}$ mice after RBC lysis or by negative selection using biotinylated antibodies and magnetic beads on single-cell suspensions from C57BL/6 mice. Single-cell suspensions were stained in PBS and washed with FACS buffer (PBS with 0.5% BSA and 2 mM EDTA) for surface stains. For intracellular Bcl6, Helios, and IRF4 staining, samples were fixed and permeabilized with the Foxp3/Transcription Factor Staining kit (Thermo Fisher Scientific) according to the manufacturer's instructions. For intracellular staining of TCR-β and Cbl-b, samples were fixed with 4% paraformaldehyde in PBS and permeabilized with Perm/Wash buffer (BD Biosciences) according to the manufacturer's instructions. All intracellular stainings were performed at room temperature. Cbl-b were stained with a primary Rabbit anti-Mouse antibodies and a secondary stain with a Donkey anti-Rabbit IgG FAB fragment (Jackson ImmunoResearch). For in vitro proliferation analysis, T cells were labeled with CellTrace Violet (ThermoFisher Scientific) according to the manufacturer's instructions. Samples were analyzed using FACSymphony A5 (BD Biosciences), FACSymphony A3 (BD Biosciences), LSRFortessa (BD Biosciences), or Cytek Aurora instruments. Flow cytometry data were analyzed using FlowJo v.10.8.1 software (BD Biosciences).

Intravascular labeling

Intravascular labeling was performed as previously described (97). Briefly, 3 µg anti-CD45.2-APC antibody was injected in 200 µl PBS intravenously 3 min before euthanasia. Cells from the spleen were analyzed by flow cytometry. Lymph nodes and peripheral blood were harvested as negative and positive controls, respectively. Positive staining with anti-CD45 antibodies was interpreted to indicate cells located within the red pulp; the absence of staining with anti-CD45 was interpreted to indicate cells located within the white pulp.

Cell sorting

Naive $CD8^+$ GFP^{LO} and GFP^{HI} T cells were sorted from bulk $CD8^+$ T cells using a FACS Aria II SORP cell sorter (BD Bioscience). From viable polyclonal $CD8^+$ $CD44^{LO}$ $CD62L^{HI}$ cells, the 10% of cells with the highest and the 10% of cells with the lowest GFP fluorescence intensity were sorted. For OT-I cells, samples were sorted on GFP expression (top and bottom 10%) from viable $CD8^+$ $CD44^{LO}$ $CD62L^{HI}$ $Qa2^{HI}$ cells. For the DNA hairpin tension probe experiment, bulk $CD8^+$ T cells were sorted based on a viable $CD4^-$ $CD19^-$ phenotype, then GFP^{LO} and GFP^{HI} cells were isolated from the 10% of cells with the highest and lowest GFP fluorescence intensity. The purity of $CD8^+$ T cells post-enrichment was >96%.

Adoptive transfer and infections

For the polyclonal Nur77-GFP stability experiment, 5×10^5 sorted $CD44^{LO}$ $CD62L^{HI}$ polyclonal GFP^{LO} or GFP^{HI} (top and bottom 10%) $CD8^+$ T cells were injected intravenously into congenic WT recipients in 200 µl PBS. For the OT-I Nur77-GFP stability experiment, $1.3\text{-}1.8\times10^6$ sorted $CD44^{LO}$ $CD62L^{HI}$ $Qa2^{HI}$ OT-I GFP^{LO} or GFP^{HI} (top and bottom 20%) $CD8^+$ T cells were injected intravenously into congenic WT recipients in 200 µl PBS. Flow cytometry analysis was conducted

seven days (polyclonal experiment) or four weeks (OT-I experiment) later on $CD8^+$ T cells enriched from the spleen and lymph nodes. For the parking experiment of Nur77-GFP naive $CD8^+$ T cells in *B2m*$^{-/-}$ vs. *B2m*$^{+/+}$ recipients, 2.2-2.5×10^6 sorted $CD44^{LO}$ $CD62L^{HI}$ polyclonal $CD8^+$ T cells crossed to the CD45.1 strain, were injected intravenously in 200 µl PBS. Flow cytometry analysis was conducted ten days later on $CD8^+$ T cells enriched from the spleen and lymph nodes.

For the co-transfer experiment of P14 cells, GFP^{LO} and GFP^{HI} (top and bottom 10%) P14 cells were sorted from $Va2^+$ $CD44^{LO}$ $CD62L^{HI}$ $Qa2^{HI}$ $CD8^+$ T cells. Three thousand cells of each population were co-injected intravenously in 200 µl PBS into $CD45.1^+$ WT recipients (donor cells were either $CD45.1^+$ $CD45.2^+$ or $CD45.2^+$.). Recipients were infected with 2×10^5 PFU LCMV Armstrong i.p. the following day, and flow cytometry analysis was conducted five days later on splenic cells.

T cell stimulation

For in vitro stimulation of T cells, 5 × 10^4 sorted $CD8^+$ T cells were cultured with 2.5 × 10^5 APCs (T cell-depleted splenocytes) per well in a 96-well U-bottom plate. Polyclonal $CD8^+$ T cells were incubated with 0.25 µg/ml anti-CD3ε antibodies (clone 145-2C11), whereas OT-I cells were incubated with SIINFEKL (N4) or SIIQFERL (Q4R7) or SIIGFEKL (G4) peptides (GenScript) at indicated concentrations. As a positive control of TCR internalization, splenocytes were incubated with 10 µg/ml anti-CD3ε antibodies and 2 µg/ml anti-CD28 antibodies (clone E18) for 90 minutes at 37°C prior to staining. Cells were cultured in RPMI 1640 (Thermo Fisher Scientific) supplemented with 10% FBS, 1% Penicillin-Streptomycin-Glutamine, 1% non-essential Amino Acids, 10 mM HEPES, 1 mM Sodium Pyruvate, and 50 µM 2-mer-capto-ethanol at 37°C with 5% CO^2.

Cytokine secretion assay

To detect IFNγ secretion by stimulated polyclonal $CD8^+$ T cells, we used the IFNγ Secretion Assay Kit (Miltenyi Biotech, catalog #130-090-984) after 24 hours of stimulation with APCs and peptide. This assay enabled sensitive detection of cytokine secretion with low numbers of sorted cells compared to fixation, permeabilization, and intracellular staining. IFNγ- and IL-2-secreting OT-I cells were co-labeled using the IFNγ Secretion Assay Kit (Miltenyi Biotech, catalog #130-090-516) and the IL-2 Secretion Assay Kit (Miltenyi Biotech, catalog #130-090-987) after 16 hours of stimulation. Briefly, 1-1.5 $\times 10^5$ T cells, including co-cultured T cell-depleted splenocytes, were labeled with the bispecific catch reagent and incubated in 50 ml of pre-warmed RPMI supplemented with 10% FBS for 45 min at 37°C. 50 ml conical tubes were inverted every 5 minutes several times during incubation. After washing, cells were stained with the cytokine detection antibody/antibodies in addition to surface antibodies.

Calcium analysis

OT-I cells were labeled with 1.5 μM Indo-1 AM dye (ThermoFisher Scientific) according to the manufacturer's instructions. APCs (T cell-depleted splenocytes) were pulsed for 30 minutes at 37°C with 1 μM SIINFEKL peptide and washed. All cells were incubated at 37°C during the acquisition and for 5 min before the start of the experiment. After the baseline calcium levels of 4 $\times 10^6$ OT-I cells were recorded for 30 seconds, cells were pipetted to an Eppendorf tube containing 8×10^6 peptide-pulsed APCs and spun down for 5 seconds in a microcentrifuge. The acquisition was resumed after the cell pellet was resuspended. The ratio of bound dye (Indo-violet) to unbound dye (Indo-blue) was analyzed for the 10% top and bottom GFP-expressing cells gated on viable $CD8^+$ $CD44^{LO}$ cells.

Preparation of tension probe surfaces

No. 1.5H glass coverslips (Ibidi) were placed in a rack and sequentially sonicated in Milli-Q water (18.2 megohms cm−1) and ethanol for 10 minutes. The glass slides were then rinsed with Milli-Q water and immersed in freshly prepared piranha solution (3:1 sulfuric acid:H_2O_2) for 30 minutes. The cleaned substrates were rinsed with Milli-Q water at least six times in a 200-mL beaker and washed with ethanol thrice. Slides were then incubated with 3% 3-aminopropyltriethoxysilane (APTES) in 200 mL ethanol for 1 hour, after which the surfaces were washed with ethanol three times and baked in an oven at 100°C for 30 minutes. The slides were then mounted onto a six-channel microfluidic cell (Sticky-Slide VI 0.4, Ibidi). To each channel, ~50 mL of NHS-PEG4-azide (10 mg/ml) in 0.1 M $NaHCO_3$ (pH 9) was added and incubated for 1 hour. Afterward, the channels were washed with 1 mL Milli-Q water three times, and the remaining water in the channel was removed by pipetting. The surfaces were then blocked with 0.1% BSA for 30 minutes and washed with PBS three times. Subsequently, the hairpin tension probes were assembled in 1 M NaCl by mixing the Atto647N-biotin labeled ligand strand (220 nM), the DBCO-BHQ2 labeled quencher strand (220 nM), and the hairpin strand (200 nM) in the ratio of 1.1:1.1:1. The mixture was heat-annealed at 95°C for 5 minutes and cooled down to 25°C over a 30-minute time window. The assembled probe (~50 mL) was added to the channels (Final concentration = 100 nM) and incubated overnight at room temperature. This strategy allows for covalent immobilization of the tension probes on azide-modified substrates via strain-promoted cycloaddition reaction. Unbound DNA probes were washed away by PBS the next day. Then, streptavidin (10 mg/ml) was added to the channels and incubated for 45 minutes, followed by washes with PBS. Next, a biotinylated pMHC (OVA N4-H2K^b) ligand (10 mg/ml) was added to the surfaces, incubated for 45 minutes, and washed with PBS. Surfaces were buffer exchanged with Hanks' balanced salt solution before

imaging.

Imaging TCR tension with DNA hairpin tension probes

TCR:pMHC interactions exert force and mechanically unfold the DNA hairpin, leading to the dye's (Atto647N-BHQ2) dequenching. T-cells were added to the tension probe surface and incubated for 20 minutes at room temperature. 200 nM of locking strand was then added to the surface for 10 minutes to capture the tension signal.

Relative 2D affinity assay

Negative enrichment of $CD8^+$ T cells from OT-I-Nur77-GFP-*Trac*$^{-/-}$ spleens was performed using the $CD8\alpha^+$ T Cell Isolation Kit (Miltenyi Biotec) according to the manufacturer's instructions. Naive OT-I cells were sorted on Nur77-GFP expression (top and bottom 10%) from viable $CD44^{LO}$ $CD62L^{HI}$ $Qa2^{HI}$ cells. To prevent CD8 co-receptor binding to MHC, monomers with an $H\text{-}2K^b$ a3 domain with a human HLA-A2 a3 domain were generated. The 2D-MP assay was performed as previously described (28, 98, 99). Briefly, human RBCs coated with various concentrations of Biotin-LC-NHS (BioVision) were coated with 0.5 mg/ml of streptavidin (Thermo Fisher Scientific), followed by 1 μg of SIINFEKL (N4) or SIIVFEKL (V4) monomer generated by the National Institutes of Health Tetramer Core Facility. Surface pMHC and TCR densities were determined by flow cytometry using anti-TCR-β PE antibody (BD Biosciences) and anti-mouse β2-microglobulin PE antibody (BioLegend) with BD QuantiBRITE PE beads for standardization (BD Biosciences). TCR:pMHC affinity calculations were determined as previously described (28, 98).

RNA-Sequencing

1×10^5 $CD8^+$ $CD44^{LO}$ $CD62L^{HI}$ $Qa2^{HI}$ OT-I GFP^{LO} and GFP^{HI} cells from three biological

replicates were sorted into RLT Lysis Buffer (Qiagen) containing 1% 2-mercaptoethanol. RNA was isolated using the Zymo Quick-RNA MicroPrep kit (Zymo Research), cDNA was prepared from 1000 cell equivalent of RNA using the SMART-Seq v4 Ultra Low Input RNA Kit for Sequencing (Takara Bio), and next-generation sequencing libraries were generated using the Nextera XT DNA Library Preparation kit (Illumina). The library size patterning from a 2100 Bioanalyzer (Agilent) and the DNA concentration were used as quality control metrics of the generated libraries. Samples were sequenced at the Emory Nonhuman Primate Genomics Core on a NovaSeq6000 (Illumina) using PE100. FastQC (https://www.bioinformatics.babraham.ac.uk/projects/fastqc/) was used to validate the quality of sequencing reads. Adapter sequences were trimmed using Skewer, and reads were mapped to the mm10 genome using STAR (100, 101). Duplicate reads were identified using PICARD (http://broadinstitute.github.io/picard/) and were removed from the following analyses. Reads mapping to exons were counted using the R package GenomicRanges (102). Genes were considered expressed if three reads per million were detected in all samples of at least one experimental group.

Analysis of differentially expressed genes was conducted in R v.4.1.1 using the edgeR package v.3.36.0 (103). Genes were considered differentially expressed at a Benjamini-Hochberg FDR-corrected p-value < 0.05. Heatmaps were generated using the ComplexHeatmap v.2.10.0 R package (104). Venn diagrams were generated using the ggvenn package (https://CRAN.R-project.org/package=ggvenn). Preranked GSEA was conducted using the GSEA tool v.4.2.3 (105). The ranked list of all detected transcripts was generated by multiplying the sign of the fold change by the $-\log_{10}$ of the p-value. All other RNA sequencing plots were generated using the ggplot2 v.3.3.5 R package (106).

Statistical analysis

All statistical analyses were performed in Prism v.9.4.1 (GraphPad) or R v.4.1.1. A p-value < 0.05 was considered significant. Details about the statistical tests used are available in each figure legend. The sample sizes of experiments were determined based on preliminary or prior experiments with $CD4^+$ T cells that yielded significant results. No power analyses to calculate sample sizes were performed.

Data and materials availability

RNA sequencing data are available under accession number GSE223457 in the Gene Expression Omnibus (https://www.ncbi.nlm.nih.gov/geo/query/acc.cgi?acc= GSE223457).

Acknowledgments

We thank Simon Grassmann and Wan-Lin Lo for critical reading of the manuscript. We also thank the Pediatric/Winship Flow Cytometry Core for cell sorting, the Emory Integrated Genomics Core (EIGC) for RNA-sequencing, and the NIH Tetramer Core Facility for providing pMHC tetramers. We would like to thank Rafi Ahmed for kindly providing LCMV Armstrong virus and Daniel McManus for assistance with LCMV experiments.

Author contributions

J.E. and B.B.A.-Y. conceptualized the study. J.E., W.M.Z.-K., B.B.A.-Y., Y.H., and E.M.K performed experiments. J.E., W.M.Z.-K., and C.D.S. analyzed the RNA-sequencing data. K.S. and Y.H. designed and performed the tension probe experiments. E.M.K. and B.D.E. designed and performed the relative 2D affinity experiments. Y.-L.T. and A.W. contributed conceptual input and provided *Cblb*$^{-/-}$ and Nur77-GFP-*Cblb*$^{-/-}$ cells. J.E. and B.B.A.-Y. wrote the manuscript with input from all authors. B.B.A.-Y. supervised the study.

Figures

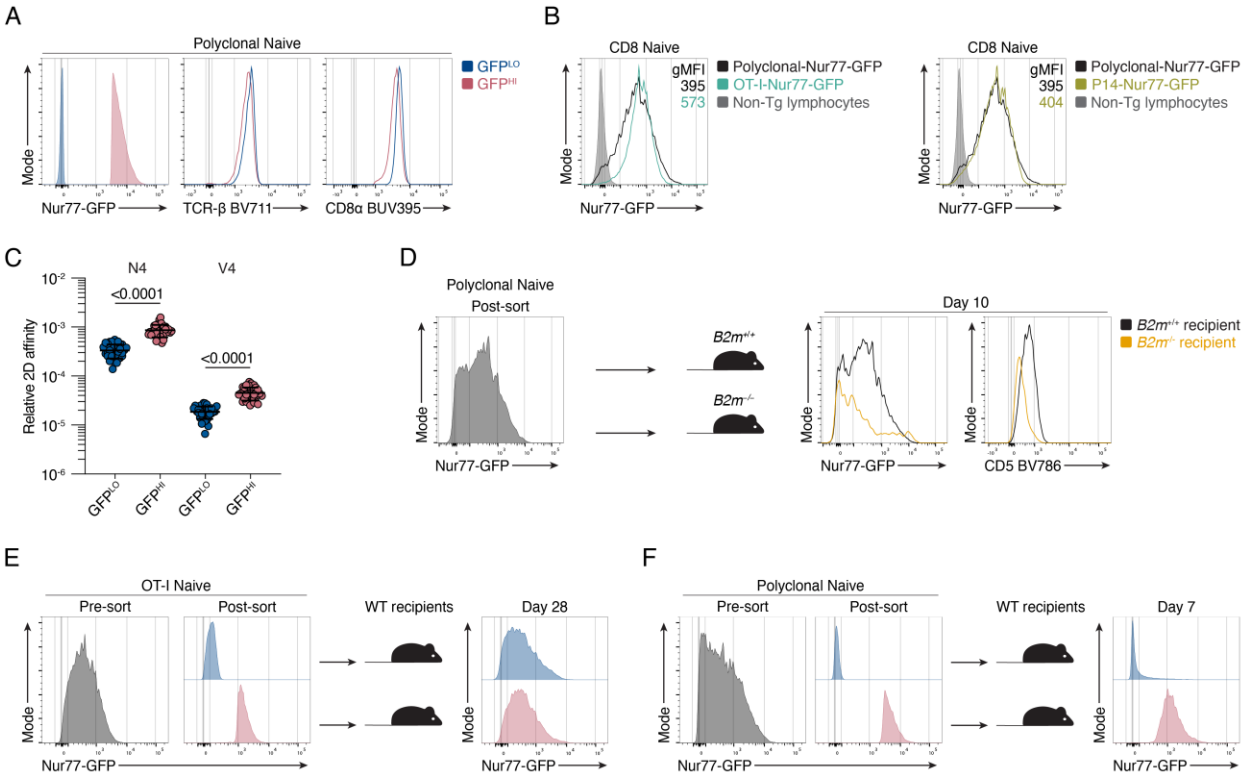

Fig. 2.1. The intensity of tonic TCR signaling in naive CD8$^+$ T cells is heterogeneous.

(**A**) Overlaid histogram (left) depicts GFP fluorescence for GFP^{LO} and GFP^{HI} cells in the spleen. GFP^{LO} cells are the 10% of cells with the lowest (blue) GFP fluorescence intensity, whereas GFP^{HI} cells are the 10% of cells with the highest (red) GFP fluorescence intensity. Histograms (middle/right) show expression of TCRβ and CD8α by polyclonal naive GFP^{LO} and GFP^{HI} CD8$^+$ T cells. (**B**) Representative flow cytometry plots of Nur77-GFP fluorescence of splenic naive polyclonal or TCR transgenic CD8$^+$ T cells. Polyclonal (black) and OT-I-*Trac*$^{-/-}$ (cyan) T cells were gated on CD44^{LO} CD62L^{HI} CD8$^+$ cells (left), and P14 T cells (green) were gated on CD44^{LO} CD62L^{HI} Vα2$^+$ CD8$^+$ cells (right). Grey histograms depict non-transgenic lymphocytes, and the numbers indicate the geometric mean fluorescence intensity (gMFI) calculated for the whole population. (**C**) Graph displays the relative two-dimensional affinity of naive GFP^{LO} and GFP^{HI}

OT-I cells to N4 or V4 peptide/H2K^{b} monomers. Each symbol represents one cell with a total of 33-34 cells from three independent experiments. Bars depict the mean, and error bars show ± s.d. Statistical testing was performed by unpaired two-tailed Student's t test. (**D**). Histogram (left) shows the GFP fluorescence intensity of FACS-sorted naive polyclonal CD8^{+} T cells. ~2.5×10^{6} naive polyclonal CD8^{+} T cells were adoptively transferred into *B2m*$^{+/+}$ or *B2m*$^{-/-}$ recipients. Histograms (middle/right) shows GFP fluorescence and CD5 staining intensity of transferred T cells ten days post-transfer into B2m$^{+/+}$ (black) vs. B2m$^{-/-}$ (orange) recipients. (**E**) Histograms show the GFP fluorescence intensity of total naive OT-I cells (left) or FACS-sorted GFP^{LO} and GFP^{HI} cells (middle). 1.3-1.8×10^{6} GFP^{LO} or GFP^{HI} (top and bottom 20%) OT-I cells were adoptively transferred into separate WT congenic recipients. Histogram (right) shows GFP fluorescence of transferred T cells four weeks post-transfer. (**F**) Histograms show the GFP fluorescence intensity of total CD8^{+} T cells (left) or FACS-sorted GFP^{LO} and GFP^{HI} cells (middle). A total of 5×10^{5} GFP^{LO} or GFP^{HI} (top and bottom 10%) polyclonal CD8^{+} T cells were adoptively transferred into separate WT congenic recipients. Histogram (right) shows GFP fluorescence of transferred T cells seven days post-transfer. For adoptive transfer experiments, donor cells were gated on naive CD8^{+} T cells, the congenic marker expression (E and F) and in addition, TCR-β^{+} cells (D). Data represent two independent experiments with n = 2 mice (B, D, and F) or three independent experiments with n = 3 mice (A, C, and E).

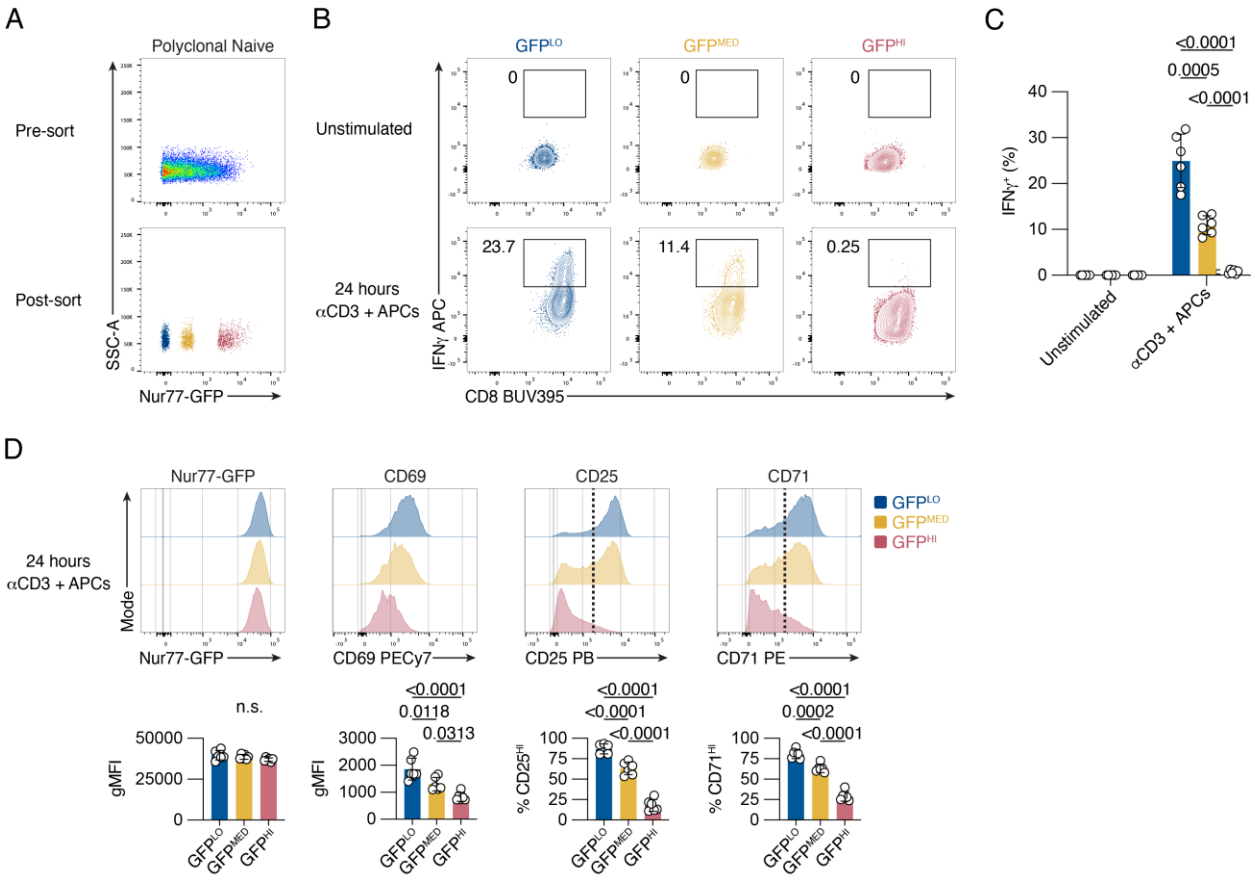

Fig. 2.2. Extensive tonic TCR signaling correlates negatively with naive polyclonal CD8 T cell responsiveness.

(**A**) Representative flow cytometry plots show GFP fluorescence of total $CD8^+$ cells (top) and sorted GFP^{LO}, GFP^{MED}, and GFP^{HI} naive, polyclonal CD8 T cell populations (bottom). (**B**) Contour plots depict CD8 and IFNγ expression by unstimulated and stimulated viable polyclonal $CD8^+$ T cells after a 45-minute IFNγ-secretion assay. Numbers indicate the percentage of cells within the indicated gates. (**C**) Bar graph displays the frequencies of GFP^{LO}, GFP^{MED}, and GFP^{HI} IFNγ-secreting cells. Cells were either unstimulated or stimulated for 24 hours with 0.25 µg/ml anti-CD3 and APCs before the secretion assay. (**D**) Histograms show expression of the indicated activation markers of cells stimulated for 24 hours with 0.25 µg/ml anti-CD3 and APCs. Cells were gated on viable $CD8^+$ T cells. Bar graphs display the gMFI for Nur77-GFP and CD69 or the

frequency of marker-positive cells for CD25 and CD71 (as indicated by the dotted line in the histogram). Data represent three independent experiments with $n = 6$ mice (A, B, C, and D). Bars in (C and D) depict the mean, error bars show ± s.d., and each symbol represents one mouse. Statistical testing in (C) was performed by one-way analysis of variance (ANOVA) ($p < 0.0001$) followed by Tukey's multiple comparisons test indicated in the graph. Statistical testing in (D) was performed by one-way ANOVA ($p < 0.0001$ for CD69, CD25, and CD71), followed by Tukey's multiple comparisons test. n.s., not significant.

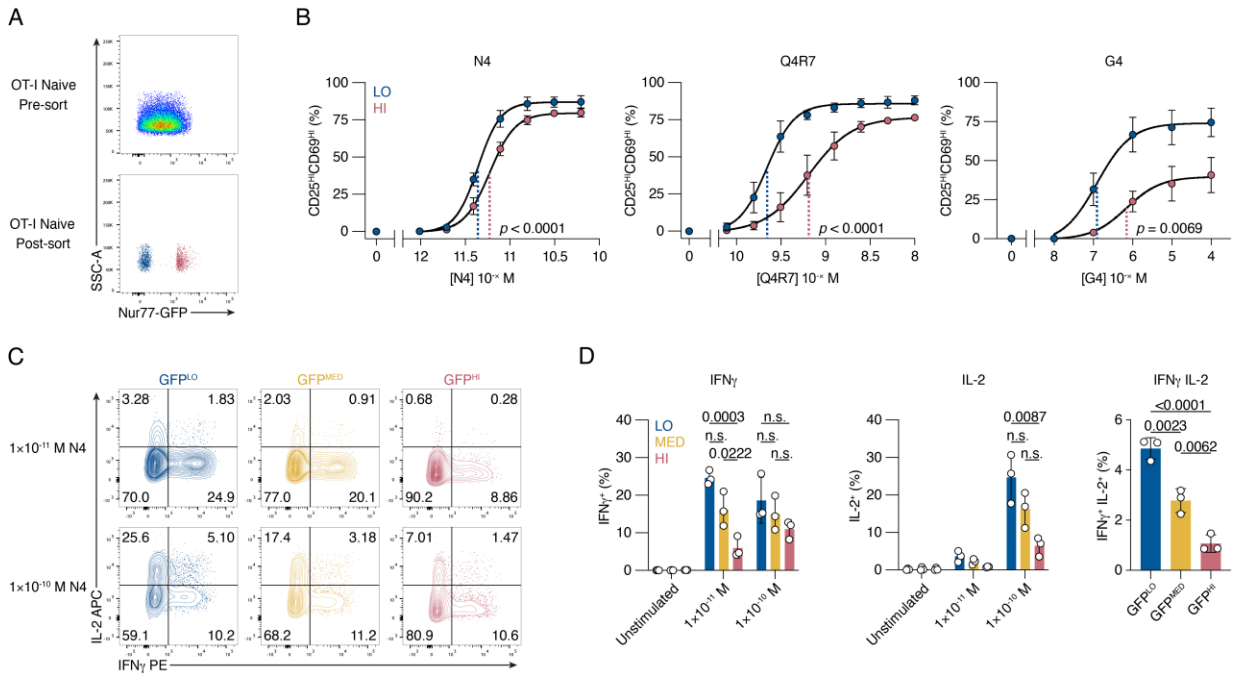

Fig. 2.3. Extensive tonic TCR signaling correlates negatively with naive OT-I cell responsiveness.

(**A**) Representative flow cytometry plots show GFP fluorescence of total cells (top) and sorted GFP^{LO} and GFP^{HI} naive CD8 T cell populations (bottom) from OT-I-Nur77-GFP-$TCR\alpha^{-/-}$ mice. (**B**) Graphs show the frequencies of $CD25^{HI}CD69^{HI}$ cells after 16 hours of stimulation with indicated peptide concentrations and APCs. Plotted are mean values fitted by non-linear regression curves. The dotted lines indicate the $Log_{10}EC_{50}$ for GFP^{LO} (blue) and GFP^{HI} (red) cells. The *p*-value indicates the *t* test for the $Log_{10}EC_{50}$ (the null hypothesis being that the $Log_{10}EC_{50}$ is the same for the two populations). (**C**) Contour plots depict viable $CD8^+$ T cells after a 45-minute assay of IFNγ- and IL-2-secretion of stimulated (16 hours) OT-I $CD8^+$ T cells. (**D**) Bar graphs show the frequencies of IFNγ, IL-2, or IFNγ and IL-2-secreting cells after 16 hours of stimulation with indicated N4 peptide concentrations and APCs or unstimulated control. Data represent three independent experiments with $n = 3$ biological replicates (A, B, C, and D). Bars in (B and D) depict the mean, error bars show ± s.d., and each symbol represents one biological replicate. Statistical

testing in (D) was performed by two-way analysis of variance (ANOVA) (p = 0.0004) (left), or one-way ANOVA (p = 0.0107) (middle), (p = 0.0001) (right), followed by Tukey's multiple comparisons test. n.s., not significant.

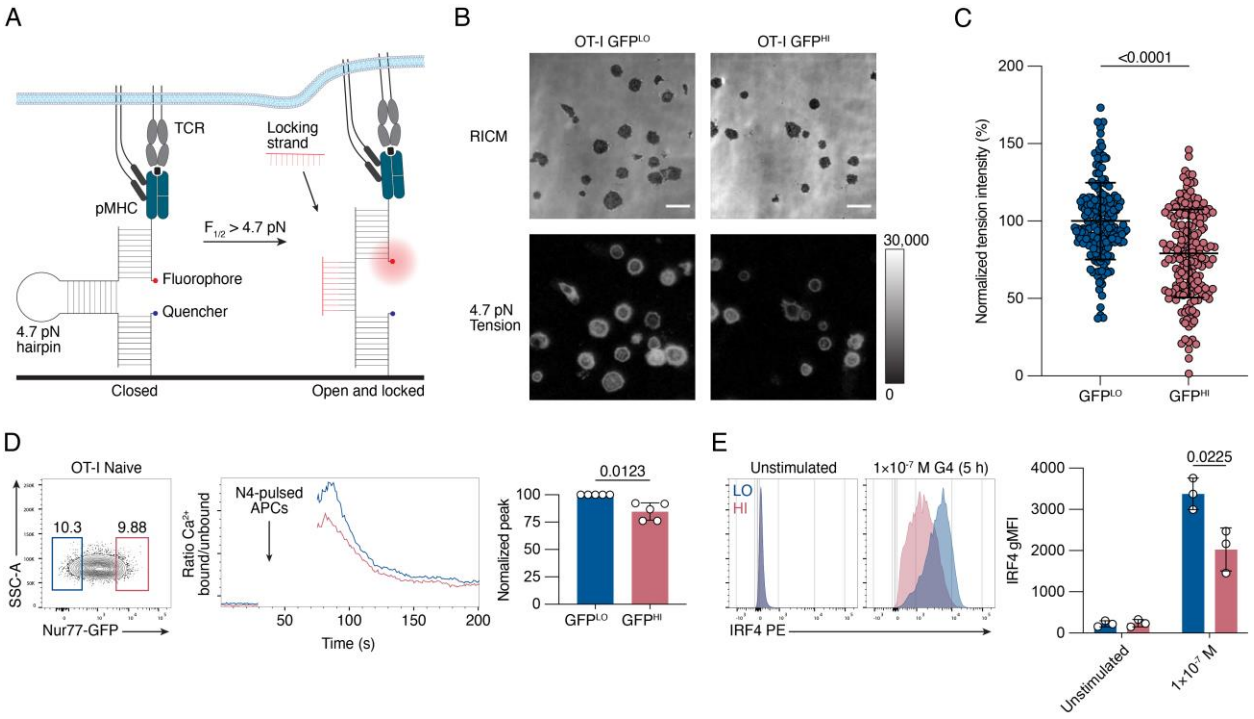

Fig. 2.4. Nur77-GFP^{HI} CD8^{+} T cells exert less TCR-mediated tension forces and exhibit attenuated proximal and integrated TCR signaling.

(**A**) Schematic outline of the DNA hairpin-based tension probe. In its closed conformation, the fluorescence of Atto647N is quenched. The DNA hairpin unfolds when TCR-mediated tension exceeds 4.7 piconewtons (pN). A "locking" DNA strand that hybridizes to the mechanically unfolded probe stabilizes the unfolded conformation of the DNA hairpin. (**B**) Representative Reflection Interference Contrast Microscopy (RICM) and fluorescence images showing GFP^{LO} and GFP^{HI} (top and bottom 10%) OT-I CD8^{+} T cells spread on DNA hairpin tension probe coated surfaces after 30 minutes. Scale bars, 10 µm. (**C**) Graph displays the normalized unquenched fluorescence intensities of the unfolded tension probes for 176-180 cells from three independent experiments (each symbol represents one cell). (**D**) Contour plot shows the distribution of Nur77-GFP fluorescence intensity for CD8^{+} CD44^{LO} OT-I T cells. Numbers indicate the percentages of cells within the indicated gates, representing GFP^{LO} and GFP^{HI} cells (left). Histogram shows the

relative concentration of free Ca^{2+} over time. Shown are the mean values for GFP^{LO} and GFP^{HI} naive OT-I $CD8^{+}$ T cells (middle). Baseline Ca^{2+} levels were recorded for 30 seconds, and the arrow indicates the time point when the T cells were mixed with N4-pulsed APCs, centrifuged, and resuspended before the continuation of data acquisition. The bar graph shows the normalized peak intracellular free Ca^{2+} values during ten seconds of GFP^{LO} and GFP^{HI} cells ~70 seconds after the initial acquisition (right). (**E**) Histograms depict the IRF4 staining intensity of FACS-sorted GFP^{LO} and GFP^{HI} (top and bottom 10%) OT-I cells that were either unstimulated (left) or stimulated for five hours with 1×10^{-7} M G4 peptide and APCs. Bar graph displays the IRF4 gMFI. Data represent three independent experiments with $n = 3$ mice or biological replicates (B, C, and E) or $n = 5$ mice (D). Bars in (C, D, and E) depict the mean, and error bars show ± s.d. Statistical testing was performed by unpaired two-tailed Student's t test (C and E) or unpaired two-tailed Student's t test with Welch's correction (D).

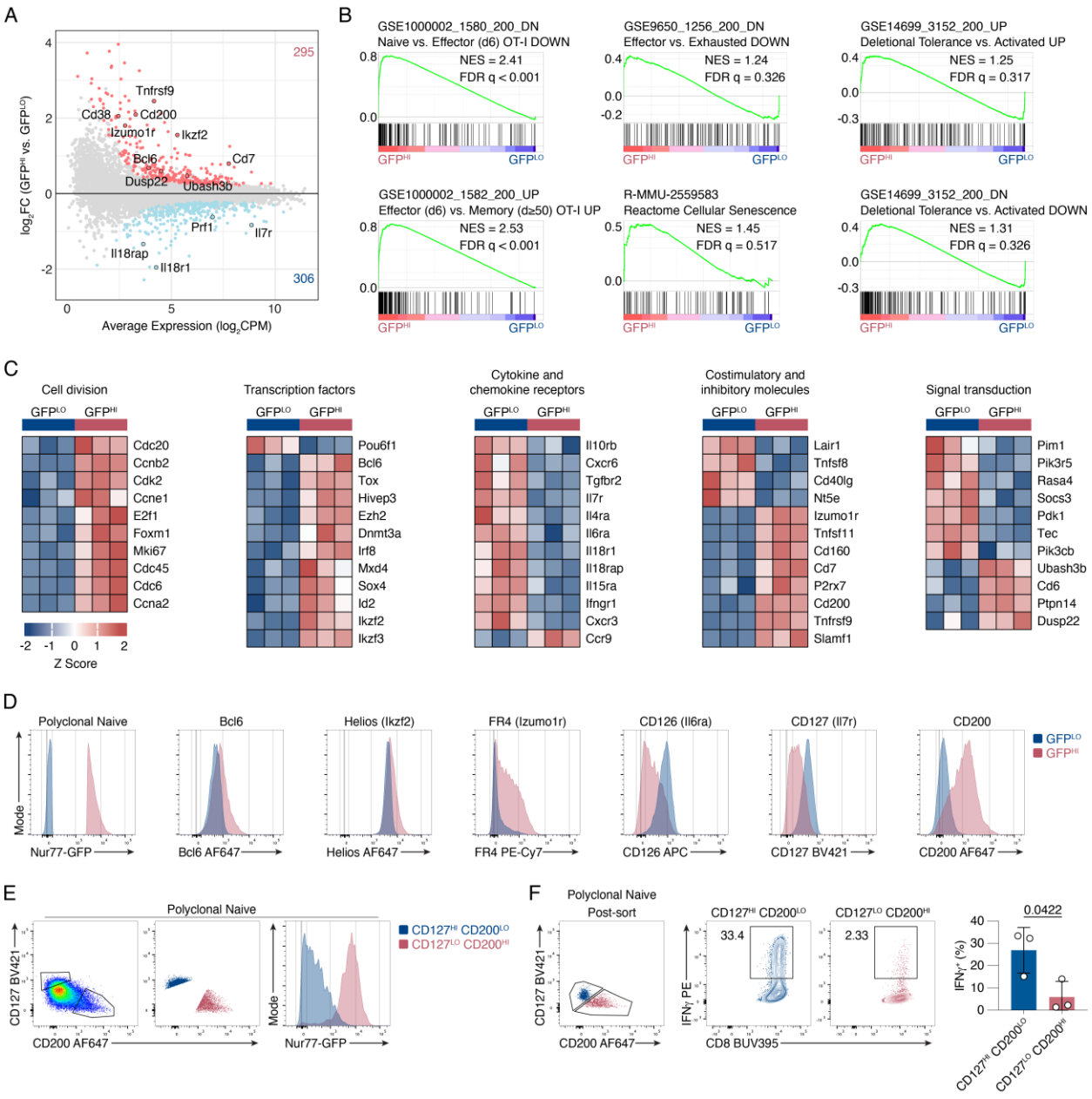

Fig. 2.5. Nur77-GFP expression in naive CD8$^+$ T cells during steady-state conditions correlates with gene expression changes.

(**A**) MA plot of DEGs between GFP^{LO} and GFP^{HI} naive OT-I CD8$^+$ T cells. DEGs were defined as genes with an FDR < 0.05. Selected genes have been highlighted. The number of upregulated and downregulated genes in GFP^{HI} relative to GFP^{LO} cells are indicated in red and blue, respectively. (**B**) GSEA of genes downregulated in naive compared to effector CD8$^+$ T cells (top

left panel) and genes upregulated in effector compared to resting memory $CD8^+$ T cells (bottom left panel) (51). GSEA of genes downregulated in effector compared to exhausted $CD8^+$ T cells (top middle panel) and genes associated with cellular senescence (bottom middle panel) (107). GSEA of genes upregulated (top right panel) or downregulated (bottom right panel) in cells subjected to deletional tolerance compared to activated $CD8^+$ T cells (108). FDR values were derived from running GSEA on the c7_Immunesigdb.v2022.1 database or the c2.cp.reactome.v2023.1 database. (**C**) Curated heatmaps of normalized expression of DEGs in indicated categories. (**D**) Histograms show the expression of the indicated markers by GFP^{LO} and GFP^{HI} cells. The cells were gated on naive, polyclonal $CD8^+$ T cells. Bar graphs depict gMFI of indicated proteins. (**E**) Flow cytometry plots (left, middle) show the gating scheme to identify $CD127^{HI}$ $CD200^{LO}$ and $CD127^{LO}$ $CD200^{HI}$ populations. Histogram (right) shows the GFP fluorescence intensity for $CD127^{HI}$ $CD200^{LO}$ and $CD127^{LO}$ $CD200^{HI}$ populations. Plots depict naive, polyclonal Nur77-GFP $CD8^+$ T cells. (F) Overlaid dot plot of sorted $CD127^{HI}$ $CD200^{LO}$ and $CD127^{LO}$ $CD200^{HI}$ naive polyclonal $CD8^+$ T cells (left). Contour plots (middle/right) depict CD8 and IFNγ expression by stimulated viable polyclonal $CD8^+$ T cells after a 45 min IFNγ-secretion assay. Numbers indicate the percentage of cells within the indicated gates. Bar graph displays the frequencies of $CD127^{HI}$ $CD200^{LO}$ and $CD127^{LO}$ $CD200^{HI}$ IFNγ-secreting cells. Cells were stimulated for 24 hours with 0.25 μg/ml anti-CD3 and APCs before the secretion assay. Bars depict the mean, error bars show ± s.d., and each symbol represents one mouse. Statistical testing was performed by unpaired two-tailed Student's t test. Data represent two to three independent experiments with n = 3-6 mice (D, E, and F). NES, normalized enrichment score.

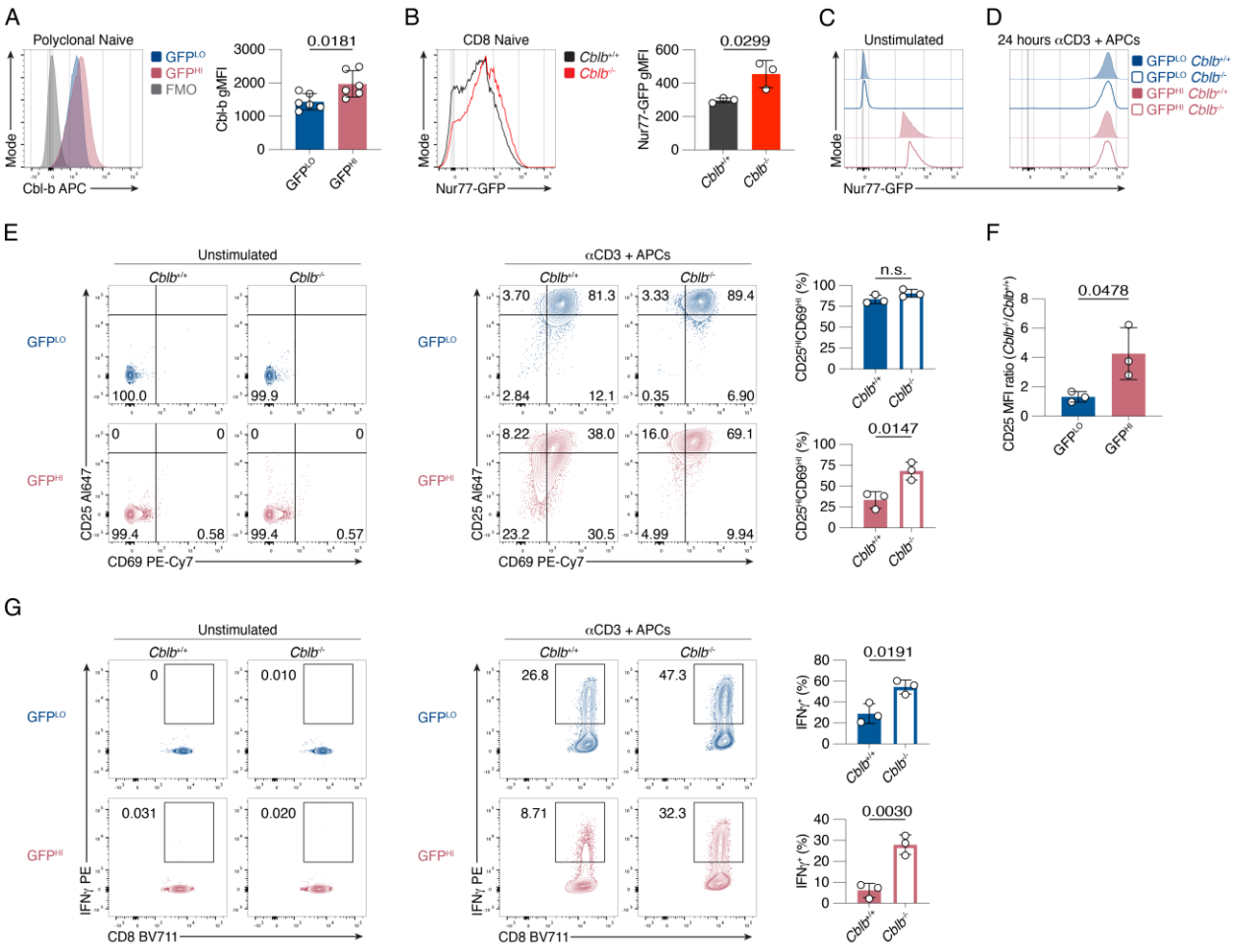

Fig. 2.6. Increased Cbl-b expression in naive GFP^{HI} cells contributes to the attenuation in responsiveness.

(**A**) Histogram depicts the staining intensity of Cbl-b in naive polyclonal GFP^{LO} and GFP^{HI} CD8^{+} T cells. Bar graph displays the Cbl-b gMFI from three independent experiments. (**B**) Histogram depicts the Nur77-GFP staining intensity of naive polyclonal CD8^{+} T cells from Cbl-b$^{+/+}$ (black) and Cbl-b$^{-/-}$ (red) mice. Bar graph shows the Nur77-GFP gMFI. (**C** and **D**) Histograms display Nur77-GFP expression in naive polyclonal GFP^{LO} (blue) and GFP^{HI} (red) cells from Cbl-b$^{+/+}$ (filled symbols or Cbl-b$^{-/-}$ (open symbols) mice. Cells were either unstimulated (left) or stimulated for 24 hours with 0.25 µg/ml anti-CD3 and APCs (right). (**E**) Contour plots depict CD25/CD69 expression in naive, polyclonal GFP^{LO} and GFP^{HI} CD8^{+} T cells that were either unstimulated (left)

or stimulated as in **D** (right). Numbers indicate the percentage of cells within the indicated gates. Bar graphs show the percentages of $CD25^{HI}$ $CD69^{HI}$ cells. (**F**) Bar graph depicts the ratio of the CD25 MFI of Cbl-$b^{-/-}$ to Cbl-$b^{+/+}$ mice. (**G**) Contour plots of IFNγ-secretion of $CD8^+$ T cells that were either unstimulated (left) or stimulated as in D, after a 45-minute IFNγ-secretion assay (right). Numbers indicate the percentage of cells within the indicated gates. Bar graphs show the percentages of $IFN\gamma^+$ cells. Data represent three independent experiments with $n = 6$ mice (A) or $n = 3$ mice or biological replicates (B, C, D, E, F, and G). Bars in (A, B, E, F, and G) depict the mean, error bars depict ± s.d., and each symbol represents one mouse or biological replicate. Statistical testing was performed by unpaired two-tailed Student's *t* test. n.s., not significant, FMO, Fluorescence Minus One control.

Supplemental Information

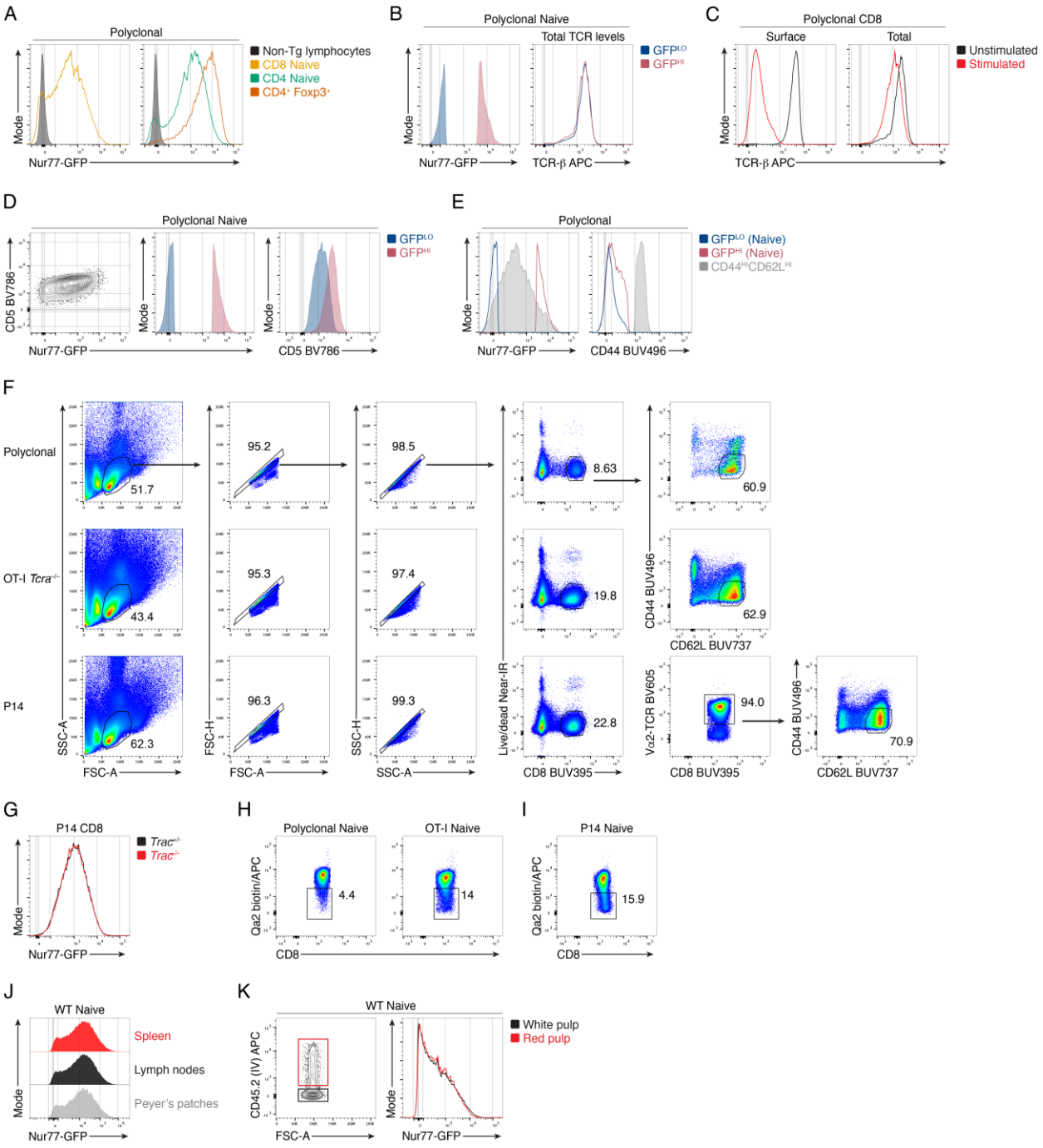

Fig. 2.S1. The intensity of tonic TCR signaling in naive CD8$^+$ T cells is heterogeneous, supporting data.

(**A**) Representative flow cytometry plots of Nur77-GFP fluorescence of naive, splenic, polyclonal

$CD44^{LO}$ $CD62L^{HI}$ $CD8^+$ (left) and $CD4^+$ cells (cyan) or $CD4^+$ Foxp3-IRES-RFP^+ (red) T cells (right). (**B**) Overlaid histogram (left) depicts GFP fluorescence for naive GFP^{LO} and GFP^{HI} cells in the spleen. Histogram (right) shows the expression of TCR-β in permeabilized, naive GFP^{LO} and GFP^{HI} $CD8^+$ T cells. (**C**) Histograms display the staining intensity of TCR-β at the surface (left) or total (right) level. Polyclonal $CD8^+$ T cells were either unstimulated (black) or stimulated for 90 minutes with 10 μg/ml anti-CD3 and 4 μg/ml anti-CD28 (red). (**D**) Contour plot (left) shows CD5 and Nur77-GFP expression by total naive polyclonal $CD8^+$ T cells. Overlaid histogram (center) depicts GFP fluorescence for GFP^{LO} and GFP^{HI} cells. Histogram (right) shows the CD5 expression for GFP^{LO} and GFP^{HI} populations. (**E**) Histograms depict Nur77-GFP expression (left) and CD44 staining intensity (right) of polyclonal naive GFP^{LO} and GFP^{HI} cells or $CD44^{HI}$ $CD62L^{HI}$ cells. (**F**) Representative gating of naive polyclonal, OT-I, and P14 $CD8^+$ T cells. Numbers indicate the percentage of cells within each gate. (**G**) Histogram show Nur77-GFP expression in *Trac*$^{+/-}$ (black) and *Trac*$^{-/-}$ (red) P14 $CD8^+$ T cells. (**H**) Representative dot plots depict Qa2 and CD8 expression in naive polyclonal or OT-I $CD8^+$ T cells in mice aged 6-9 weeks. Numbers indicate the percentage of cells within the indicated gates. (**I**) Representative dot plots depict Qa2 and CD8 expression in naive P14 $CD8^+$ T cells in mice aged 6-13 weeks. (**J**) Offset histograms show Nur77-GFP expression in naive polyclonal $CD8^+$ T cells harvested from the spleen, mesenteric lymph nodes, or Peyer's Patches. (**K**) Flow cytometry plots of naive polyclonal $CD8^+$ T cells after intravascular labeling of cells in the red pulp by intravenous injection of CD45.2-APC antibody intravenously prior to euthanasia. Data represent two (A, B, C, G, H, I, and J) to three (D, E, and K) independent experiments with n = 3-4 mice (B, C, H, I, J, and K) or n = 6-7 mice (A, D, E, and G).

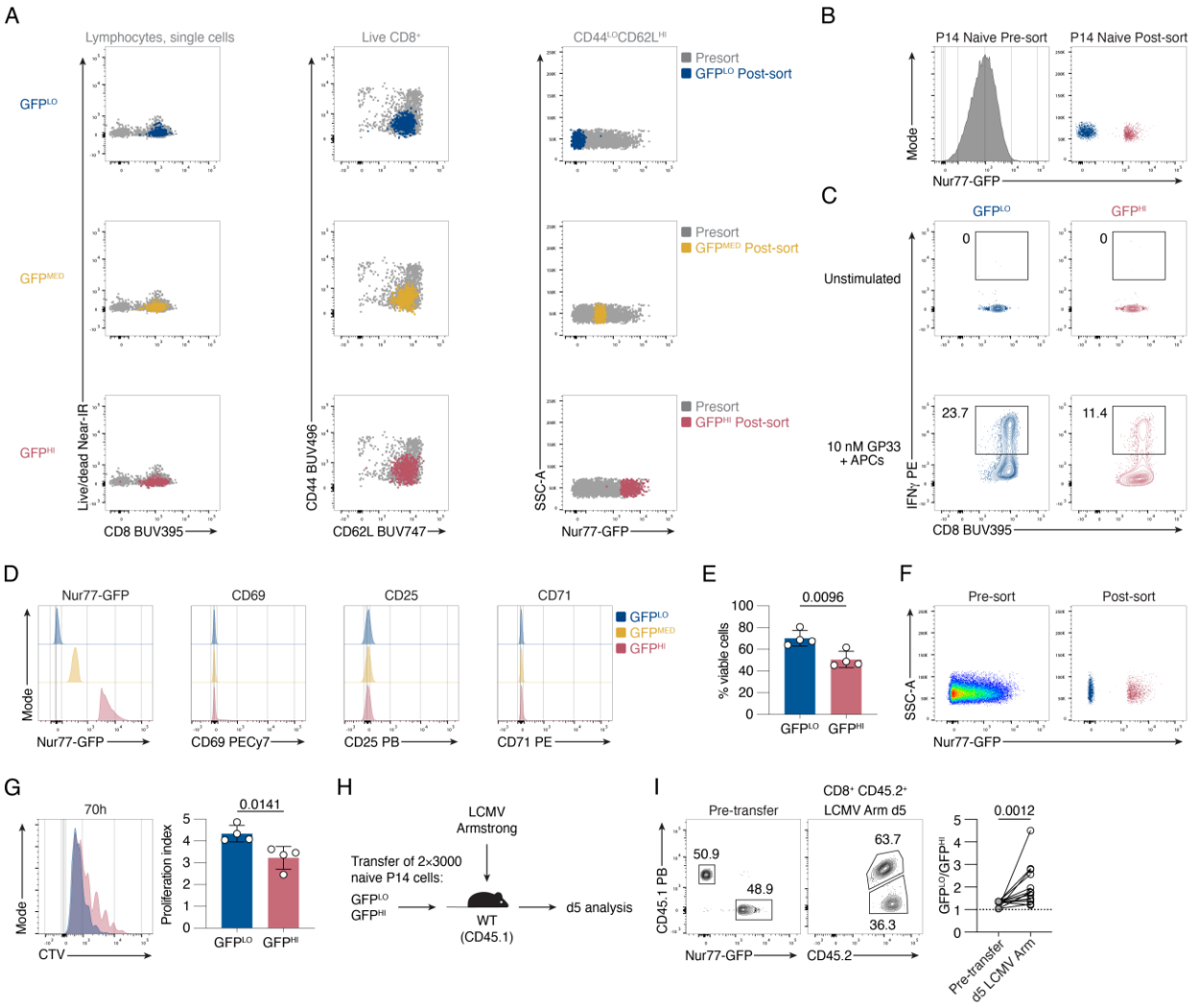

Fig. 2.S2. Extensive tonic TCR signaling correlates negatively with naive, polyclonal CD8 T cell responsiveness, supporting data.

(**A**) Representative backgating analysis of sorted naive polyclonal GFP^{LO}, GFP^{MED}, and GFP^{HI} cells. Sorted cells were gated on lymphocytes and single cells, and the pre-sort sample was gated as indicated in grey above the plots. (**B**) Representative histogram (left) and dot plot (right) depict Nur77-GFP expression in total and sorted GFP^{LO} versus GFP^{HI} naive P14 CD8^{+} T cells, respectively. (**C**) Representative contour plots depict CD8 and IFNγ expression by unstimulated and stimulated viable P14 CD8^{+} T cells after a 45 min IFNγ-secretion assay. Cells were stimulated for 16 hours with GP33 and APCs before the secretion assay. Numbers indicate the percentage of

cells within the indicated gates. (**D**) Histograms show the expression of the indicated activation markers of unstimulated control cells. (**E**) The frequency of viable $CD8^+$ T cells was determined after 24 hours of stimulation with 0.25 μg/ml anti-CD3 and APCs. (**F**) Representative flow cytometry plots of the pre-sort GFP distribution (left) and sorted GFP^{LO} and GFP^{HI} naive, polyclonal CD8 T cell populations (right). (**G**) CTV-labeled naive, polyclonal GFP^{LO} and GFP^{HI} $CD8^+$ T cells were incubated for 70 hours with 0.25 μg/ml anti-CD3 and APCs. The representative flow cytometry plot was gated on viable $CD8^+$ T cells. The graph depicts the proliferation index (the average number of divisions of cells that divided at least once). (**H**) Schematic overview of the competitive-transfer experiment. 3000 cells each of GFP^{LO} and GFP^{HI} naive P14 cells were co-transferred into WT recipients, followed by infection with LCMV Armstrong (2×10^5 PFU i.p.). (**I**) Contour plots (left) depict mixed GFP^{LO} and GFP^{HI} cells pre-transfer and (right) cells harvested from the spleen on day five post-infection gated on viable donor cells. Scatterplot displays the ratio of GFP^{LO} to GFP^{HI} P14 donor cells pooled from three independent experiments. Each symbol represents one mouse. Data represent two (B and C), three (D and I), or four (E, F, and G) independent experiments with $n = 4$ mice (E, F, and G), $n = 6$-7 mice (B, C, and D), or $n = 15$ mice (I). Bars in (E and G) depict the mean, error bars depict ± s.d., and each symbol represents one mouse. Statistical testing was performed by unpaired two-tailed Student's *t* test (B and D) or by two-tailed Wilcoxon matched-pairs signed-rank test (I).

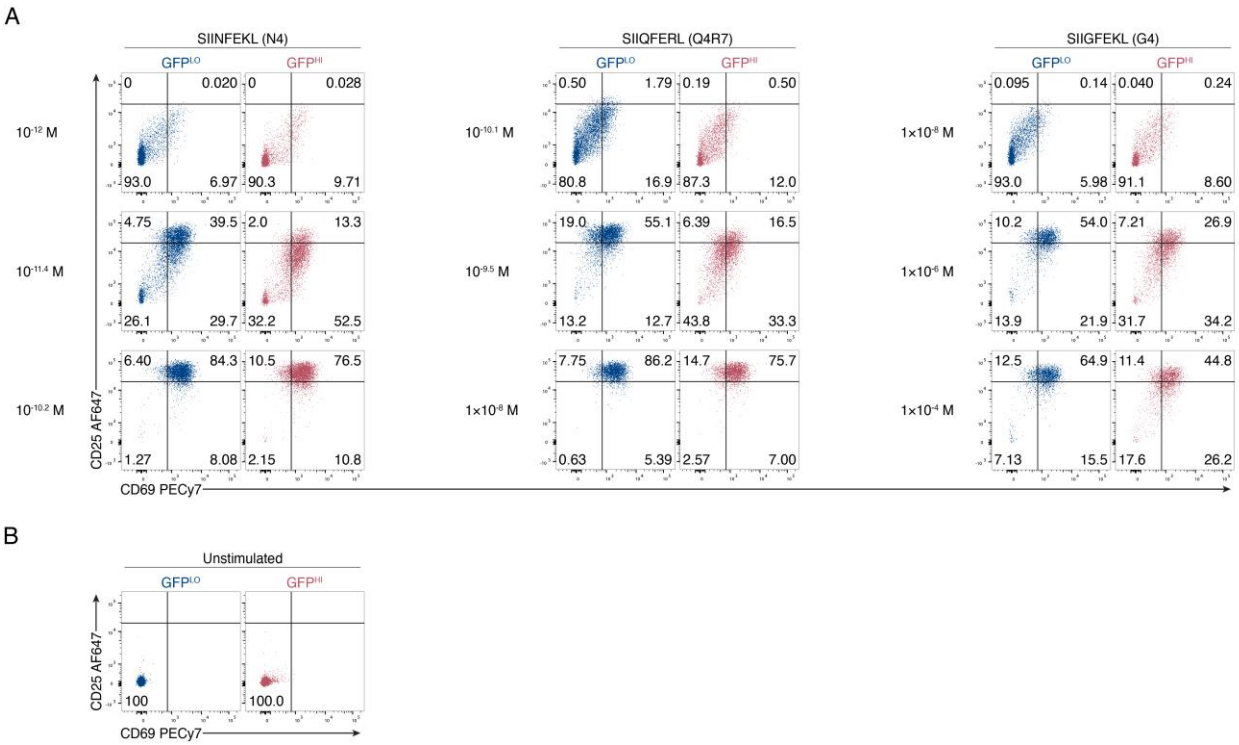

Fig. 2.S3. Extensive tonic TCR signaling correlates negatively with naive OT-I cell responsiveness, supporting data.

(**A**) Representative flow cytometry plots depicting CD25 and CD69 upregulation after 16 hours of stimulation with indicated peptide concentrations are shown from one experiment. Panels in the first row represent suboptimal peptide concentrations, the second row depicts peptide concentrations on the linear part of the dose-response curve, and the third-row show saturating peptide concentrations. Numbers indicate the percentage of cells within the indicated gates. (**B**) Unstimulated control of CD25 and CD69 upregulation in GFP^{LO} and GFP^{HI} naive OT-I cells. Data represent three (A and B) independent experiments with $n = 3$ biological replicates (A and B).

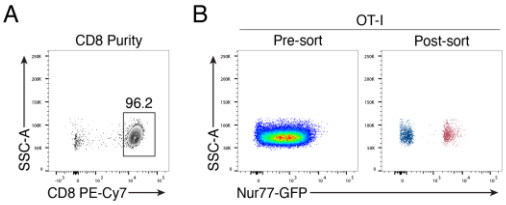

Fig. 2.S4. Nur77-GFP^{HI} CD8^{+} T cells exert less TCR-mediated tension forces and exhibit attenuated proximal and integrated TCR signaling, supporting data.

(**A**) CD8 staining of OT-I cells post-negative enrichment. The CD8 purity was >96% for all experiments. (**B**) Dot plots depict Nur77-GFP fluorescent intensity of total (left) and sorted OT-I cells based on GFP expression (top and bottom 10%) from viable, CD4^{-} CD19^{-} cells (right). CD8^{+} T cells were enriched by negative selection before sorting. Data represent three independent experiments with n = 3 mice (A and B).

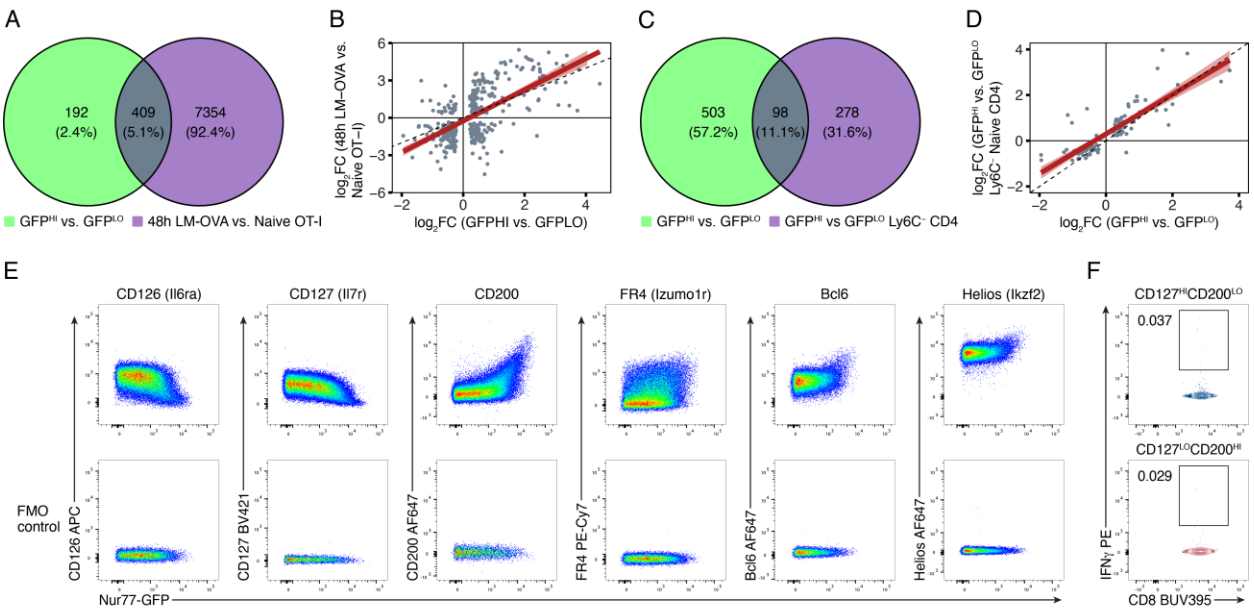

Fig. 2.S5. Nur77-GFP expression in naive CD8$^+$ T cells during steady-state conditions correlates with gene expression changes, supporting data.

(**A**) Venn diagram of DEGs defined as genes with an FDR < 0.05 present in the GFP^{HI} vs. GFP^{LO} naive OT-I dataset (green), the effector vs. naive dataset (purple), or in both datasets (grey). The number of DEGs and the percentage of the total DEGs is depicted within each condition. (**B**) Log_2 fold-change plot of genes upregulated in effector compared to naive OT-I CD8$^+$ T cells on the Y-axis (*52*) and genes upregulated in Nur77-GFP^{HI} compared to GFP^{LO} naive OT-I CD8$^+$ T cells on the X-axis. Each dot represents an overlapping DEG defined as in A. The red line depicts the correlation with a 95% confidence interval. The dotted black line depicts a 1:1 relationship between the two datasets. (**C**) Similar to A, the Venn Diagram depicts DEGs defined as genes with an FDR < 0.05 present in the GFP^{HI} vs. GFP^{LO} dataset (green), the GFP^{HI} vs. GFP^{LO} CD4$^+$ Ly6C$^-$ dataset (purple) or in both datasets (grey). The number of DEGs and the percentage of the total DEGs is depicted within each condition. (**D**) Similar to B, the plot depicts the Log_2 fold-change of genes upregulated in Nur77-GFP^{HI} compared to GFP^{LO} naive Ly6C$^-$ CD4$^+$ T cells on the Y-axis (*7*) and genes upregulated in GFP^{HI} compared to GFP^{LO} naive OT-I CD8$^+$ T cells on the X-axis.

(**E**) The top row depicts Nur77-GFP expression in relationship to indicated markers in naive, polyclonal $CD8^+$ T cells. The bottom row indicates the Fluorescence Minus One (FMO) control for the indicated markers. (**F**) Contour plots depict CD8 and IFNγ expression by unstimulated $CD127^{HI}$ $CD200^{LO}$ (top) and $CD127^{LO}$ $CD200^{HI}$ (bottom) polyclonal naive $CD8^+$ T cells after a 45 min IFNγ-secretion assay. Data represent represent two to three (E) or three (F) independent experiments from n = 3-6 (E) or n = 3 (F) mice. Statistical analysis in (B and D) was performed by a one-sample t test (the null hypothesis being that the slope was equal to zero).

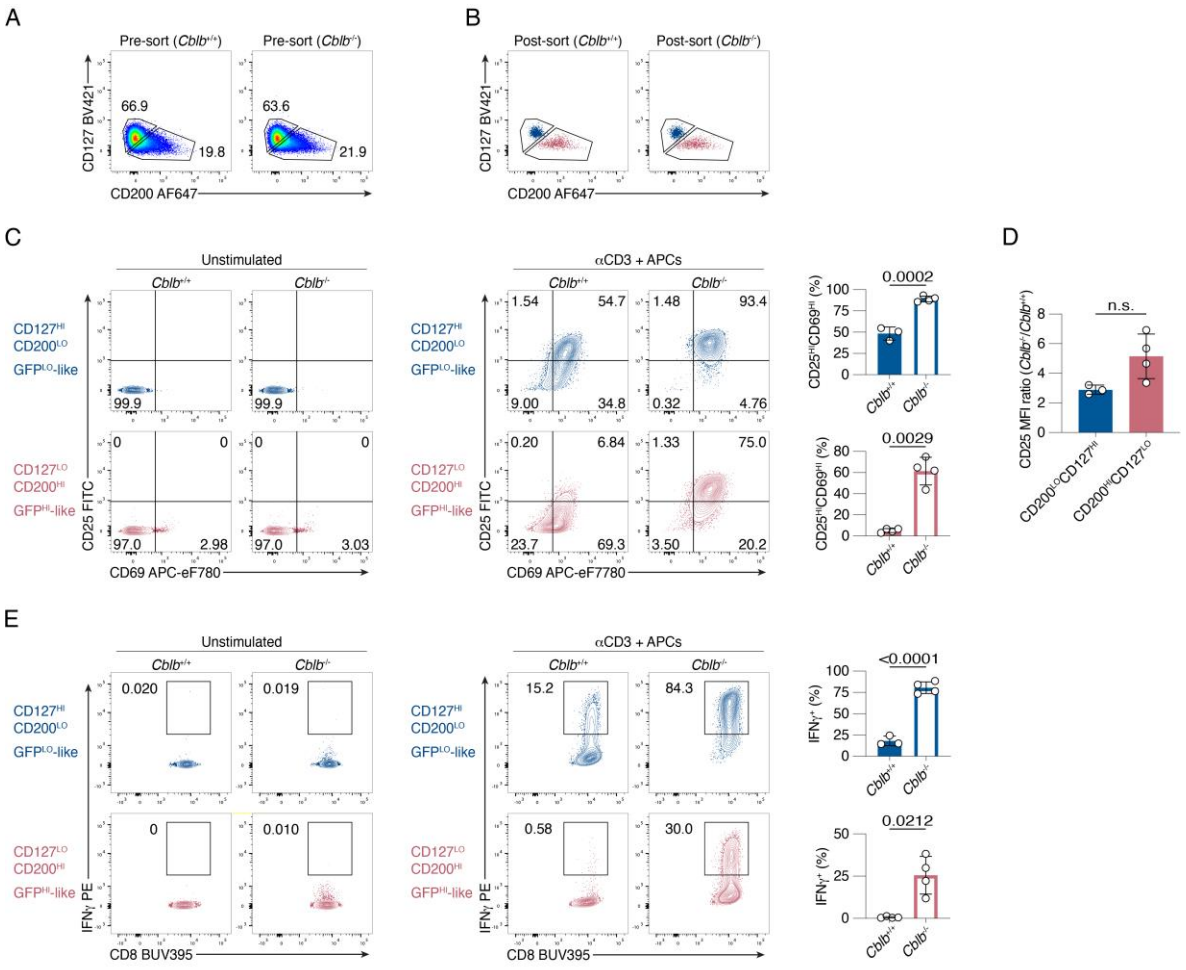

Fig. 2.S6. Increased Cbl-b expression in naive GFP^{HI} cells contributes to the attenuation in responsiveness, supporting data.

(**A**) Dot plots depict the expression of CD127 and CD200 in naive, polyclonal CD8$^+$ T cells from *Cblb*$^{+/+}$ and *Cblb*$^{-/-}$ mice. (**B**) Representative flow cytometry plots of sorted, naive GFP^{LO}-like (blue) and GFP^{HI}-like cells (red) CD8$^+$ T cells from *Cblb*$^{+/+}$ and *Cblb*$^{-/-}$ mice. (**C**) Contour plots depict CD25/CD69 expression in naive, polyclonal GFP^{LO} and GFP^{HI} CD8$^+$ T cells that were either unstimulated (left) or stimulated for 24 hours with 0.25 µg/ml anti-CD3 and APCs (right). Numbers indicate the percentage of cells within the indicated gates. Bar graphs show the percentages of CD25^{HI} CD69^{HI} cells. (**D**) Bar graph depicts the ratio of the CD25 MFI of Cblb$^{-/-}$ to Cblb$^{+/+}$ mice. (**E**) Contour plots of IFNγ-secretion of CD8$^+$ T cells that were either unstimulated

(left) or stimulated as in C, after a 45-minute IFNγ-secretion assay (right). Numbers indicate the percentage of cells within the indicated gates. Bar graphs show the percentages of $IFN\gamma^+$ cells. Bars (in C, D, and E) depict the mean, error bars depict ± s.d., and each symbol represents one biological replicate. Data represent three to four independent experiments with n = 3-4 biological replicates (A, B, C, D, and E). Statistical testing was performed by unpaired two-tailed Student's *t* test in (C and E (upper panels)). Statistical testing was performed by unpaired two-tailed Student's *t* test with Welch's correction in (C and E (lower panels), and D. n.s., not significant.

Table S1: Materials and Reagents

REAGENT or RESOURCE	SOURCE	IDENTIFIER
Antibodies		
Anti-mouse CD3ε (Clone 145-2C11	BioLegend	Cat#100331; RRID:AB_1877073
Anti-mouse CD4, biotin (Clone RM4-5)	BioLegend	Cat#100508; RRID:AB_312711
Anti-mouse CD4, Pacific Blue (Clone RM4-5)	BioLegend	Cat#100531; RRID:AB_493374
Anti-mouse CD4, APC (Clone RM4-5)	BioLegend	Cat#100516; RRID:AB_312719
Anti-mouse CD5, BV786 (Clone 53-7.3)	BD Biosciences	Cat#740842; RRID:AB_2740496
Anti-mouse CD8a, biotin (Clone 53-6.7)	BioLegend	Cat#100704; RRID:AB_312743
Anti-mouse CD8a, PerCP-Cy5.5 (Clone 53-6.7)	BioLegend	Cat#100734; RRID:AB_2075238
Anti-mouse CD8a, PE-Cy7 (Clone 53-6.7)	BioLegend	Cat#100722; RRID:AB_312761
Anti-mouse CD8a, Pacific Blue (Clone 53-6.7)	BioLegend	Cat#100725; RRID:AB_493425
Anti-mouse CD8a, BV711 (Clone 53-6.7)	BioLegend	Cat#100759; RRID:AB_2563510
Anti-mouse CD8a, BV605 (Clone 53-6.7)	BioLegend	Cat#100744; RRID:AB_2562609
Anti-mouse CD8a, BUV395 (Clone 53-6.7)	BD Biosciences	Cat#563786; RRID:AB_2732919
Anti-mouse CD11b, biotin (Clone M1/70)	BioLegend	Cat# 101204; RRID:AB_312787
Anti-mouse CD11c, biotin (Clone N418)	BioLegend	Cat#117304; RRID:AB_313773
Anti-mouse CD16/CD32 (Fc Block) (Clone 2.4G2)	Tonbo Biosciences	Cat#70-0161-U500; N/A
Anti-mouse CD19, biotin (Clone 6D5)	BioLegend	Cat#115504; RRID:AB_313639
Anti-mouse CD19, Pacific Blue (Clone 6D5)	BioLegend	Cat#115523; RRID:AB_439718
Anti-mouse CD25, Pacific Blue (Clone PC61)	BioLegend	Cat#102022; RRID:AB_493643
Anti-mouse CD25, FITC (Clone PC61)	BioLegend	Cat#102006; RRID:AB_312855
Anti-mouse CD25, Al647 (Clone PC61)	BioLegend	Cat#102020; RRID:AB_493458
Anti-Mouse CD28 (Clone 37.51)	BioLegend	Cat#102112; RRID:AB_312877
Anti-mouse CD44, PE-Cy7 (Clone IM7)	BioLegend	Cat#103030; RRID:AB_830787
Anti-mouse CD44, PE (Clone IM7)	BioLegend	Cat#103008; RRID:AB_312959
Anti-mouse CD44, Pacific Blue (Clone IM7)	BioLegend	Cat#103020; RRID:AB_493683
Anti-mouse CD44, Al488 (Clone IM7)	BioLegend	Cat#103016; RRID:AB_493679
Anti-mouse CD44, Al647 (Clone IM7)	BioLegend	Cat#103018; RRID:AB_493681
Anti-mouse CD44, BUV496 (Clone IM7)	BD Biosciences	Cat#741057; RRID:AB_2870671
Anti-mouse CD44, BUV737 (Clone IM7)	BD Biosciences	Cat#612799; RRID:AB_2870126
Anti-mouse CD45.1, Pacific Blue (Clone A20)	BioLegend	Cat#110722; RRID:AB_492866
Anti-mouse CD45.2, PE-Cy7 (Clone 104)	BioLegend	Cat#109830; RRID:AB_1186098
Anti-mouse CD45.2, APC (Clone 104)	BioLegend	Cat#109814; RRID:AB_389211
Anti-mouse CD45R/B220, biotin (Clone RA3-6B2)	BioLegend	Cat#103204; RRID:AB_312989
Anti-mouse CD49b, biotin (Clone DX5)	BioLegend	Cat#108904; RRID:AB_313411
Anti-mouse CD62L, PE (Clone MEL-14)	BioLegend	Cat#104408; RRID:AB_313095
Anti-mouse CD62L, APC (Clone MEL-14)	BioLegend	Cat#104412; RRID:AB_313099
Anti-mouse CD62L, BUV737 (Clone MEL-14)	BD Biosciences	Cat#612833; RRID:AB_2870155
Anti-mouse CD69, PE-Cy7 (Clone H1.2F3)	eBioscience	Cat#25-0691-82; RRID:AB_469637
Anti-mouse CD69, eF780 (Clone H1.2F3)	eBioscience	Cat#47-0691-82; RRID:AB_2573966
Anti-mouse CD71, PE (Clone C2)	BD Biosciences	Cat#553267; RRID:AB_394744
Anti-mouse CD126, APC (Clone D7715A7)	BioLegend	Cat#115811; RRID:AB_2127937
Anti-mouse CD127, BV421 (Clone SB/199)	BD Biosciences	Cat#562959; RRID: AB_2737917
Anti-mouse CD200, Al647 (Clone OX-90)	BD Biosciences	Cat#565544; RRID:AB_2739287
Anti-mouse β2-microglobulin, PE (Clone A16041A)	BioLegend	Cat#154504; RRID:AB_2721340
Anti-mouse Bcl-6, Al647 (Clone K112-91)	BD Biosciences	Cat#561525; RRID:AB_10898007
Anti-Cbl-b (Clone D3C12)	Cell Signaling	Cat#9498; RRID:AB_2797707

Continued

REAGENT or RESOURCE	SOURCE	IDENTIFIER
Anti-mouse Erythroid cells, biotin (Clone TER-119)	BioLegend	Cat#116204; RRID:AB_313705
Anti-mouse FR4, PE-Cy7 (Clone eBio12A5)	eBioscience	Cat#25-5445-80; RRID:AB_842812
Anti-mouse Helios, Al647 (Clone 22F6)	BD Biosciences	Cat#563951; RRID:AB_2738506
Anti-rabbit IgG AffiniPure Fab Fragment, APC	Jackson ImmunoResearch	Cat#711-136-152; RRID:AB_2340601
Anti-mouse IRF4, PE (Clone 3E4)	eBioscience	Cat#12-9858-80; RRID:AB_10853179
Anti-mouse TCRβ, APC (Clone H57-597)	BioLegend	Cat#109212; RRID:AB_313435
Anti-mouse TCRβ, BV711 (Clone H57-597)	BioLegend	Cat#109243; RRID:AB_2629564
Anti-mouse TCRβ, PE (Clone H57-597)	BD Biosciences	Cat#553172; RRID:AB_394684
Anti-mouse TCR Vα2, PE (Clone B20.1)	BioLegend	Cat#127808; RRID:AB_1134183
Anti-mouse TCR Vα2, BV605 (Clone B20.1)	BD Biosciences	Cat#747768; RRID:AB_2872232
Anti-mouse Qa-2, biotin (Clone 695H1-9-9)	BioLegend	Cat#121703; RRID:AB_572000
Virus strains		
LCMV Armstrongp	Dr. Rafi Ahmed (Ahmed et al., 1984) (109)	N/A
Chemicals and peptides		
OVA (257-264) (SIINFEKL)	GenScript	Cat#RP10611
OVA (257-264) (SIIQFERL)	GenScript	Custom
OVA (257-264) (SIIGFEKL)	GenScript	Custom
OVA (257-264) (SIIVFEKL)	In house (University of Utah)	N/A
GP33-41 (KAVYNFATC)	GenScript	Cat#RP20091
LIVE/DEAD Fixable Near-IR	Thermo Fisher Scientific	Cat#L34976
LIVE/DEAD Fixable Violet	Thermo Fisher Scientific	Cat#L34955
LIVE/DEAD Fixable Yellow	Thermo Fisher Scientific	Cat#L34967
Ghost Dye Red 780	Cytek Biosciences	Cat#13-0865-T100
CellTrace Violet	Thermo Fisher Scientific	Cat#C34557
Indo-1 AM	Thermo Fisher Scientific	Cat#I1223
Streptavidin (APC)	Thermo Fisher Scientific	Cat#SA1005
Streptavidin (eFlour 450)	eBioscience	Cat#48-4317-82
BD Perm/Wash buffer	BD Biosciences	Cat#554723
Foxp3 Staining buffer set	eBioscience	Cat#00-5523-00
RBC lysis buffer	Tonbo Biosciences	Cat#TNB-4300-L100
RPMI 1640	Thermo Fisher Scientific	Cat#11875-119
Fetal bovine serum	Omega Scientific	Cat#FB-21
HEPES	Thermo Fisher Scientific	Cat#15630-080
MEM Non-essential amino acid solution	Sigma-Aldrich	Cat#M7145-100ML
Penicillin-Streptomycin-Glutamine	Thermo Fisher Scientific	Cat#10378-016
Sodium pyruvate	Sigma-Aldrich	Cat#S8636-100ML
2-Mercaptoethanol	Thermo Fisher Scientific	Cat#31350-010
Critical commercial assays		
Mouse IFN-γ Secretion Assay – Detection Kit (PE)	Miltenyi Biotec	Cat#130-090-516
Mouse IFN-γ Secretion Assay – Detection Kit (APC)	Miltenyi Biotec	Cat#130-090-984
Mouse IL-2 Secretion Assay – Detection Kit (APC)	Miltenyi Biotec	Cat#130-090-987
EasySep Mouse Streptavidin RapidSpheres Isolation Kit	STEMCELL Technologies	Cat#19860A
Deposited data		
RNA-seq (raw data and count data)	This study	GEO: GSE223457

Continued

REAGENT or RESOURCE	SOURCE	IDENTIFIER
Experimental models: Organisms/strains		
C57BL/6J	Jackson Laboratory	Cat#000664; RRID:IMSR_JAX:000664
B6.SJL-Ptprca Pepcb/BoyJ	Jackson Laboratory	Cat#002014; RRID:IMSR_JAX:002014
B6.129P2-B2mtm1Unc/DcrJ	Jackson Laboratory	Cat#002087; RRID:IMSR_JAX:002087
Zap70tm1Weis	Kadlecek et al., 1998 (*91*)	N/A
Tg(Nr4a1-EGFP)GY139Gsat	Zikherman et al., 2013 (*14*)	N/A
Nur77-GFP-Foxp3-RFP	Zinzow-Kramer et al., 2019 (*18*)	N/A
OT-I-Nur77-GFP-*Trca*$^{-/-}$	This study	N/A
P14-Nur77-GFP	This study	N/A
Cbl-b$^{-/-}$	Chiang et al., 2000 (*95*)	N/A
Nur77-GFP-Cbl-b$^{-/-}$	This study	N/A
Oligonucleotides		
Atto647N-biotin labeled ligand strand: *Atto647N* - CGC ATC TGT GCG GTA TTT CAC TTT - *Biotin*	Ma et al., 2019 (*48*)	N/A
DBCO-BHQ2 labeled quencher strand: *DBCO* - TTT GCT GGG CTA CGT GGC GCT CTT - *BHQ2*	Ma et al., 2019 (*48*)	N/A
Hairpin strand: GTG AAA TAC CGC ACA GAT GCG TTT GTA TAA ATG TTT TTT TCA TTT ATA CTTTAA GAG CGC CAC GTA GCC CAG C	Ma et al., 2019 (*48*)	N/A
Software and algorithms		
FlowJo V10	BD Biosciences	https://www.flowjo.com
Gene Set Enrichment Analysis (GSEA)	Subramanian et al., 2005 (*105*)	https://www.gsea-msigdb.org/gsea
Prism 9	GraphPad Software	https://www.graphpad.com
R (version 4.1.1) and dependencies	The Comprehensive R Archive Network	https://cran.r-project.org/
Other		
BD Quantibrite PE beads	BD Biosciences	Cat#340495

References

1. Courtney AH, Lo WL, Weiss A. TCR Signaling: Mechanisms of Initiation and Propagation. Trends Biochem Sci. 2018;43(2):108-23.
2. Kelly K, Siebenlist U. Immediate-early genes induced by antigen receptor stimulation. Curr Opin Immunol. 1995;7(3):327-32.
3. Myers DR, Zikherman J, Roose JP. Tonic Signals: Why Do Lymphocytes Bother? Trends Immunol. 2017;38(11):844-57.
4. Stefanova I, Dorfman JR, Germain RN. Self-recognition promotes the foreign antigen sensitivity of naive T lymphocytes. Nature. 2002;420(6914):429-34.
5. van Oers NS, Killeen N, Weiss A. ZAP-70 is constitutively associated with tyrosine-phosphorylated TCR zeta in murine thymocytes and lymph node T cells. Immunity. 1994;1(8):675-85.
6. Rogers D, Sood A, Wang H, van Beek JJP, Rademaker TJ, Artusa P, et al. Pre-existing chromatin accessibility and gene expression differences among naive CD4(+) T cells influence effector potential. Cell Rep. 2021;37(9):110064.
7. Zinzow-Kramer WM, Kolawole EM, Eggert J, Evavold BD, Scharer CD, Au-Yeung BB. Strong Basal/Tonic TCR Signals Are Associated with Negative Regulation of Naive CD4(+) T Cells. Immunohorizons. 2022;6(9):671-83.
8. This S, Rogers D, Mallet Gauthier E, Mandl JN, Melichar HJ. What's self got to do with it: Sources of heterogeneity among naive T cells. Semin Immunol. 2022;65:101702.
9. Myers DR, Lau T, Markegard E, Lim HW, Kasler H, Zhu M, et al. Tonic LAT-HDAC7 Signals Sustain Nur77 and Irf4 Expression to Tune Naive CD4 T Cells. Cell Rep. 2017;19(8):1558-71.

10. Eggert J, Au-Yeung BB. Functional heterogeneity and adaptation of naive T cells in response to tonic TCR signals. Curr Opin Immunol. 2021;73:43-9.

11. Richard AC. Divide and Conquer: Phenotypic and Temporal Heterogeneity Within CD8(+) T Cell Responses. Front Immunol. 2022;13:949423.

12. Jennings E, Elliot TAE, Thawait N, Kanabar S, Yam-Puc JC, Ono M, et al. Nr4a1 and Nr4a3 Reporter Mice Are Differentially Sensitive to T Cell Receptor Signal Strength and Duration. Cell Rep. 2020;33(5):108328.

13. Moran AE, Holzapfel KL, Xing Y, Cunningham NR, Maltzman JS, Punt J, et al. T cell receptor signal strength in Treg and iNKT cell development demonstrated by a novel fluorescent reporter mouse. J Exp Med. 2011;208(6):1279-89.

14. Zikherman J, Parameswaran R, Weiss A. Endogenous antigen tunes the responsiveness of naive B cells but not T cells. Nature. 2012;489(7414):160-4.

15. Au-Yeung BB, Smith GA, Mueller JL, Heyn CS, Jaszczak RG, Weiss A, et al. IL-2 Modulates the TCR Signaling Threshold for CD8 but Not CD4 T Cell Proliferation on a Single-Cell Level. J Immunol. 2017;198(6):2445-56.

16. Au-Yeung BB, Zikherman J, Mueller JL, Ashouri JF, Matloubian M, Cheng DA, et al. A sharp T-cell antigen receptor signaling threshold for T-cell proliferation. Proc Natl Acad Sci U S A. 2014;111(35):E3679-88.

17. Dorfman JR, Stefanova I, Yasutomo K, Germain RN. CD4+ T cell survival is not directly linked to self-MHC-induced TCR signaling. Nat Immunol. 2000;1(4):329-35.

18. Zinzow-Kramer WM, Weiss A, Au-Yeung BB. Adaptation by naive CD4(+) T cells to self-antigen-dependent TCR signaling induces functional heterogeneity and tolerance. Proc Natl Acad Sci U S A. 2019;116(30):15160-9.

19. Lee HM, Bautista JL, Scott-Browne J, Mohan JF, Hsieh CS. A broad range of self-reactivity drives thymic regulatory T cell selection to limit responses to self. Immunity. 2012;37(3):475-86.

20. Hinterberger M, Aichinger M, Prazeres da Costa O, Voehringer D, Hoffmann R, Klein L. Autonomous role of medullary thymic epithelial cells in central CD4(+) T cell tolerance. Nat Immunol. 2010;11(6):512-9.

21. Jordan MS, Boesteanu A, Reed AJ, Petrone AL, Holenbeck AE, Lerman MA, et al. Thymic selection of CD4+CD25+ regulatory T cells induced by an agonist self-peptide. Nat Immunol. 2001;2(4):301-6.

22. Mandl JN, Monteiro JP, Vrisekoop N, Germain RN. T cell-positive selection uses self-ligand binding strength to optimize repertoire recognition of foreign antigens. Immunity. 2013;38(2):263-74.

23. Cho JH, Kim HO, Ju YJ, Kye YC, Lee GW, Lee SW, et al. CD45-mediated control of TCR tuning in naive and memory CD8(+) T cells. Nat Commun. 2016;7:13373.

24. Azzam HS, Grinberg A, Lui K, Shen H, Shores EW, Love PE. CD5 expression is developmentally regulated by T cell receptor (TCR) signals and TCR avidity. J Exp Med. 1998;188(12):2301-11.

25. Azzam HS, DeJarnette JB, Huang K, Emmons R, Park CS, Sommers CL, et al. Fine tuning of TCR signaling by CD5. J Immunol. 2001;166(9):5464-72.

26. Wong P, Barton GM, Forbush KA, Rudensky AY. Dynamic tuning of T cell reactivity by self-peptide-major histocompatibility complex ligands. J Exp Med. 2001;193(10):1179-87.

27. Fulton RB, Hamilton SE, Xing Y, Best JA, Goldrath AW, Hogquist KA, et al. The TCR's sensitivity to self peptide-MHC dictates the ability of naive CD8(+) T cells to respond to

foreign antigens. Nat Immunol. 2015;16(1):107-17.

28. Huang J, Zarnitsyna VI, Liu B, Edwards LJ, Jiang N, Evavold BD, et al. The kinetics of two-dimensional TCR and pMHC interactions determine T-cell responsiveness. Nature. 2010;464(7290):932-6.

29. Boursalian TE, Golob J, Soper DM, Cooper CJ, Fink PJ. Continued maturation of thymic emigrants in the periphery. Nat Immunol. 2004;5(4):418-25.

30. Kolawole EM, Lamb TJ, Evavold BD. Relationship of 2D Affinity to T Cell Functional Outcomes. Int J Mol Sci. 2020;21(21).

31. Zarnitsyna VI, Zhu C. Adhesion frequency assay for in situ kinetics analysis of cross-junctional molecular interactions at the cell-cell interface. J Vis Exp. 2011(57):e3519.

32. Corish P, Tyler-Smith C. Attenuation of green fluorescent protein half-life in mammalian cells. Protein Eng. 1999;12(12):1035-40.

33. Sacchetti A, El Sewedy T, Nasr AF, Alberti S. Efficient GFP mutations profoundly affect mRNA transcription and translation rates. FEBS Lett. 2001;492(1-2):151-5.

34. Manz R, Assenmacher M, Pfluger E, Miltenyi S, Radbruch A. Analysis and sorting of live cells according to secreted molecules, relocated to a cell-surface affinity matrix. Proc Natl Acad Sci U S A. 1995;92(6):1921-5.

35. Campbell JD. Detection and enrichment of antigen-specific CD4+ and CD8+ T cells based on cytokine secretion. Methods. 2003;31(2):150-9.

36. Bird JJ, Brown DR, Mullen AC, Moskowitz NH, Mahowald MA, Sider JR, et al. Helper T cell differentiation is controlled by the cell cycle. Immunity. 1998;9(2):229-37.

37. Gett AV, Hodgkin PD. Cell division regulates the T cell cytokine repertoire, revealing a mechanism underlying immune class regulation. Proc Natl Acad Sci U S A.

1998;95(16):9488-93.

38. Grogan JL, Mohrs M, Harmon B, Lacy DA, Sedat JW, Locksley RM. Early transcription and silencing of cytokine genes underlie polarization of T helper cell subsets. Immunity. 2001;14(3):205-15.

39. Laouar Y, Crispe IN. Functional flexibility in T cells: independent regulation of CD4+ T cell proliferation and effector function in vivo. Immunity. 2000;13(3):291-301.

40. Kersh EN, Fitzpatrick DR, Murali-Krishna K, Shires J, Speck SH, Boss JM, et al. Rapid demethylation of the IFN-gamma gene occurs in memory but not naive CD8 T cells. J Immunol. 2006;176(7):4083-93.

41. Auphan-Anezin N, Verdeil G, Schmitt-Verhulst AM. Distinct thresholds for CD8 T cell activation lead to functional heterogeneity: CD8 T cell priming can occur independently of cell division. J Immunol. 2003;170(5):2442-8.

42. Achar SR, Bourassa FXP, Rademaker TJ, Lee A, Kondo T, Salazar-Cavazos E, et al. Universal antigen encoding of T cell activation from high-dimensional cytokine dynamics. Science. 2022;376(6595):880-4.

43. Wolint P, Betts MR, Koup RA, Oxenius A. Immediate cytotoxicity but not degranulation distinguishes effector and memory subsets of CD8+ T cells. J Exp Med. 2004;199(7):925-36.

44. Pircher H, Moskophidis D, Rohrer U, Burki K, Hengartner H, Zinkernagel RM. Viral escape by selection of cytotoxic T cell-resistant virus variants in vivo. Nature. 1990;346(6285):629-33.

45. Daniels MA, Teixeiro E, Gill J, Hausmann B, Roubaty D, Holmberg K, et al. Thymic selection threshold defined by compartmentalization of Ras/MAPK signalling. Nature.

2006;444(7120):724-9.

46. Al-Aghbar MA, Jainarayanan AK, Dustin ML, Roffler SR. The interplay between membrane topology and mechanical forces in regulating T cell receptor activity. Commun Biol. 2022;5(1):40.

47. Liu Y, Blanchfield L, Ma VP, Andargachew R, Galior K, Liu Z, et al. DNA-based nanoparticle tension sensors reveal that T-cell receptors transmit defined pN forces to their antigens for enhanced fidelity. Proc Natl Acad Sci U S A. 2016;113(20):5610-5.

48. Ma R, Kellner AV, Ma VP, Su H, Deal BR, Brockman JM, et al. DNA probes that store mechanical information reveal transient piconewton forces applied by T cells. Proc Natl Acad Sci U S A. 2019;116(34):16949-54.

49. Man K, Miasari M, Shi W, Xin A, Henstridge DC, Preston S, et al. The transcription factor IRF4 is essential for TCR affinity-mediated metabolic programming and clonal expansion of T cells. Nat Immunol. 2013;14(11):1155-65.

50. Conley JM, Gallagher MP, Rao A, Berg LJ. Activation of the Tec Kinase ITK Controls Graded IRF4 Expression in Response to Variations in TCR Signal Strength. J Immunol. 2020;205(2):335-45.

51. Luckey CJ, Bhattacharya D, Goldrath AW, Weissman IL, Benoist C, Mathis D. Memory T and memory B cells share a transcriptional program of self-renewal with long-term hematopoietic stem cells. Proc Natl Acad Sci U S A. 2006;103(9):3304-9.

52. Best JA, Blair DA, Knell J, Yang E, Mayya V, Doedens A, et al. Transcriptional insights into the CD8(+) T cell response to infection and memory T cell formation. Nat Immunol. 2013;14(4):404-12.

53. White JT, Cross EW, Burchill MA, Danhorn T, McCarter MD, Rosen HR, et al. Virtual

memory T cells develop and mediate bystander protective immunity in an IL-15-dependent manner. Nat Commun. 2016;7:11291.

54. Kaech SM, Cui W. Transcriptional control of effector and memory CD8+ T cell differentiation. Nat Rev Immunol. 2012;12(11):749-61.

55. Alfei F, Kanev K, Hofmann M, Wu M, Ghoneim HE, Roelli P, et al. TOX reinforces the phenotype and longevity of exhausted T cells in chronic viral infection. Nature. 2019;571(7764):265-9.

56. Miyagawa F, Zhang H, Terunuma A, Ozato K, Tagaya Y, Katz SI. Interferon regulatory factor 8 integrates T-cell receptor and cytokine-signaling pathways and drives effector differentiation of CD8 T cells. Proc Natl Acad Sci U S A. 2012;109(30):12123-8.

57. Pollok KE, Kim YJ, Zhou Z, Hurtado J, Kim KK, Pickard RT, et al. Inducible T cell antigen 4-1BB. Analysis of expression and function. J Immunol. 1993;150(3):771-81.

58. Pollok KE, Kim SH, Kwon BS. Regulation of 4-1BB expression by cell-cell interactions and the cytokines, interleukin-2 and interleukin-4. Eur J Immunol. 1995;25(2):488-94.

59. Wong BR, Rho J, Arron J, Robinson E, Orlinick J, Chao M, et al. TRANCE is a novel ligand of the tumor necrosis factor receptor family that activates c-Jun N-terminal kinase in T cells. J Biol Chem. 1997;272(40):25190-4.

60. Snelgrove RJ, Goulding J, Didierlaurent AM, Lyonga D, Vekaria S, Edwards L, et al. A critical function for CD200 in lung immune homeostasis and the severity of influenza infection. Nat Immunol. 2008;9(9):1074-83.

61. Lutz-Nicoladoni C, Wolf D, Sopper S. Modulation of Immune Cell Functions by the E3 Ligase Cbl-b. Front Oncol. 2015;5:58.

62. Mandl JN, Liou R, Klauschen F, Vrisekoop N, Monteiro JP, Yates AJ, et al. Quantification

of lymph node transit times reveals differences in antigen surveillance strategies of naive CD4+ and CD8+ T cells. Proc Natl Acad Sci U S A. 2012;109(44):18036-41.

63. Elliot TAE, Jennings EK, Lecky DAJ, Rouvray S, Mackie GM, Scarfe L, et al. Nur77-Tempo mice reveal T cell steady state antigen recognition. Discov Immunol. 2022;1(1):kyac009.

64. Bending D, Prieto Martin P, Paduraru A, Ducker C, Marzaganov E, Laviron M, et al. A timer for analyzing temporally dynamic changes in transcription during differentiation in vivo. J Cell Biol. 2018;217(8):2931-50.

65. Ross JO, Melichar HJ, Au-Yeung BB, Herzmark P, Weiss A, Robey EA. Distinct phases in the positive selection of CD8+ T cells distinguished by intrathymic migration and T-cell receptor signaling patterns. Proceedings of the National Academy of Sciences. 2014;111(25):E2550-8.

66. Au-Yeung BB, Melichar HJ, Ross JO, Cheng DA, Zikherman J, Shokat KM, et al. Quantitative and temporal requirements revealed for Zap70 catalytic activity during T cell development. Nat Immunol. 2014;15(7):687-94.

67. Trefzer A, Kadam P, Wang SH, Pennavaria S, Lober B, Akcabozan B, et al. Dynamic adoption of anergy by antigen-exhausted CD4(+) T cells. Cell Rep. 2021;34(6):108748.

68. Nguyen TTT, Wang ZE, Shen L, Schroeder A, Eckalbar W, Weiss A. Cbl-b deficiency prevents functional but not phenotypic T cell anergy. J Exp Med. 2021;218(7).

69. Voisinne G, Garcia-Blesa A, Chaoui K, Fiore F, Bergot E, Girard L, et al. Co-recruitment analysis of the CBL and CBLB signalosomes in primary T cells identifies CD5 as a key regulator of TCR-induced ubiquitylation. Mol Syst Biol. 2016;12(7):876.

70. Qiao G, Li Z, Molinero L, Alegre ML, Ying H, Sun Z, et al. T-cell receptor-induced NF-

kappaB activation is negatively regulated by E3 ubiquitin ligase Cbl-b. Mol Cell Biol. 2008;28(7):2470-80.

71. Bachmaier K, Krawczyk C, Kozieradzki I, Kong YY, Sasaki T, Oliveira-dos-Santos A, et al. Negative regulation of lymphocyte activation and autoimmunity by the molecular adaptor Cbl-b. Nature. 2000;403(6766):211-6.

72. Odagiu L, May J, Boulet S, Baldwin TA, Labrecque N. Role of the Orphan Nuclear Receptor NR4A Family in T-Cell Biology. Front Endocrinol (Lausanne). 2020;11:624122.

73. Liu X, Wang Y, Lu H, Li J, Yan X, Xiao M, et al. Genome-wide analysis identifies NR4A1 as a key mediator of T cell dysfunction. Nature. 2019;567(7749):525-9.

74. Liebmann M, Hucke S, Koch K, Eschborn M, Ghelman J, Chasan AI, et al. Nur77 serves as a molecular brake of the metabolic switch during T cell activation to restrict autoimmunity. Proc Natl Acad Sci U S A. 2018;115(34):E8017-E26.

75. Hiwa R, Nielsen HV, Mueller JL, Mandla R, Zikherman J. NR4A family members regulate T cell tolerance to preserve immune homeostasis and suppress autoimmunity. JCI Insight. 2021.

76. Chen J, Lopez-Moyado IF, Seo H, Lio CJ, Hempleman LJ, Sekiya T, et al. NR4A transcription factors limit CAR T cell function in solid tumours. Nature. 2019;567(7749):530-4.

77. Bending D, Zikherman J. Nr4a nuclear receptors: markers and modulators of antigen receptor signaling. Curr Opin Immunol. 2023;81:102285.

78. Carpino N, Turner S, Mekala D, Takahashi Y, Zang H, Geiger TL, et al. Regulation of ZAP-70 activation and TCR signaling by two related proteins, Sts-1 and Sts-2. Immunity. 2004;20(1):37-46.

79. Mikhailik A, Ford B, Keller J, Chen Y, Nassar N, Carpino N. A phosphatase activity of Sts-1 contributes to the suppression of TCR signaling. Mol Cell. 2007;27(3):486-97.

80. Stanford SM, Rapini N, Bottini N. Regulation of TCR signalling by tyrosine phosphatases: from immune homeostasis to autoimmunity. Immunology. 2012;137(1):1-19.

81. Li JP, Yang CY, Chuang HC, Lan JL, Chen DY, Chen YM, et al. The phosphatase JKAP/DUSP22 inhibits T-cell receptor signalling and autoimmunity by inactivating Lck. Nat Commun. 2014;5:3618.

82. Wiede F, La Gruta NL, Tiganis T. PTPN2 attenuates T-cell lymphopenia-induced proliferation. Nat Commun. 2014;5:3073.

83. Tarakhovsky A, Kanner SB, Hombach J, Ledbetter JA, Muller W, Killeen N, et al. A role for CD5 in TCR-mediated signal transduction and thymocyte selection. Science. 1995;269(5223):535-7.

84. Pena-Rossi C, Zuckerman LA, Strong J, Kwan J, Ferris W, Chan S, et al. Negative regulation of CD4 lineage development and responses by CD5. J Immunol. 1999;163(12):6494-501.

85. Ju YJ, Lee SW, Kye YC, Lee GW, Kim HO, Yun CH, et al. Self-reactivity controls functional diversity of naive CD8(+) T cells by co-opting tonic type I interferon. Nat Commun. 2021;12(1):6059.

86. Huseby ES, Teixeiro E. The perception and response of T cells to a changing environment are based on the law of initial value. Sci Signal. 2022;15(736):eabj9842.

87. Grossman Z, Paul WE. Adaptive cellular interactions in the immune system: the tunable activation threshold and the significance of subthreshold responses. Proc Natl Acad Sci U S A. 1992;89(21):10365-9.

88. Elliot TAE, Jennings EK, Lecky DAJ, Thawait N, Flores-Langarica A, Copland A, et al. Antigen and checkpoint receptor engagement recalibrates T cell receptor signal strength. Immunity. 2021;54(11):2481-96 e6.

89. Buchholz VR, Schumacher TN, Busch DH. T Cell Fate at the Single-Cell Level. Annu Rev Immunol. 2016;34:65-92.

90. Wong HS, Germain RN. Robust control of the adaptive immune system. Semin Immunol. 2018;36:17-27.

91. Kadlecek TA, van Oers NS, Lefrancois L, Olson S, Finlay D, Chu DH, et al. Differential requirements for ZAP-70 in TCR signaling and T cell development. J Immunol. 1998;161(9):4688-94.

92. Wan YY, Flavell RA. Identifying Foxp3-expressing suppressor T cells with a bicistronic reporter. Proc Natl Acad Sci U S A. 2005;102(14):5126-31.

93. Koller BH, Marrack P, Kappler JW, Smithies O. Normal development of mice deficient in beta 2M, MHC class I proteins, and CD8+ T cells. Science. 1990;248(4960):1227-30.

94. Pircher H, Michalopoulos EE, Iwamoto A, Ohashi PS, Baenziger J, Hengartner H, et al. Molecular analysis of the antigen receptor of virus-specific cytotoxic T cells and identification of a new V alpha family. Eur J Immunol. 1987;17(12):1843-6.

95. Chiang YJ, Kole HK, Brown K, Naramura M, Fukuhara S, Hu RJ, et al. Cbl-b regulates the CD28 dependence of T-cell activation. Nature. 2000;403(6766):216-20.

96. Smith GA, Uchida K, Weiss A, Taunton J. Essential biphasic role for JAK3 catalytic activity in IL-2 receptor signaling. Nat Chem Biol. 2016;12(5):373-9.

97. Anderson KG, Sung H, Skon CN, Lefrancois L, Deisinger A, Vezys V, et al. Cutting edge: intravascular staining redefines lung CD8 T cell responses. J Immunol. 2012;189(6):2702-

6.

98. Kolawole EM, Andargachew R, Liu B, Jacobs JR, Evavold BD. 2D Kinetic Analysis of TCR and CD8 Coreceptor for LCMV GP33 Epitopes. Front Immunol. 2018;9:2348.

99. Evans E, Leung A, Heinrich V, Zhu C. Mechanical switching and coupling between two dissociation pathways in a P-selectin adhesion bond. Proc Natl Acad Sci U S A. 2004;101(31):11281-6.

100. Dobin A, Gingeras TR. Mapping RNA-seq Reads with STAR. Curr Protoc Bioinformatics. 2015;51:11 4 1- 4 9.

101. Jiang H, Lei R, Ding SW, Zhu S. Skewer: a fast and accurate adapter trimmer for next-generation sequencing paired-end reads. BMC Bioinformatics. 2014;15:182.

102. Lawrence M, Huber W, Pages H, Aboyoun P, Carlson M, Gentleman R, et al. Software for computing and annotating genomic ranges. PLoS Comput Biol. 2013;9(8):e1003118.

103. Robinson MD, McCarthy DJ, Smyth GK. edgeR: a Bioconductor package for differential expression analysis of digital gene expression data. Bioinformatics. 2010;26(1):139-40.

104. Gu Z, Eils R, Schlesner M. Complex heatmaps reveal patterns and correlations in multidimensional genomic data. Bioinformatics. 2016;32(18):2847-9.

105. Subramanian A, Tamayo P, Mootha VK, Mukherjee S, Ebert BL, Gillette MA, et al. Gene set enrichment analysis: a knowledge-based approach for interpreting genome-wide expression profiles. Proc Natl Acad Sci U S A. 2005;102(43):15545-50.

106. Wickham H. ggplot2 : Elegant Graphics for Data Analysis. Cham: Springer International Publishing : Imprint: Springer,; 2016.

107. Wherry EJ, Ha SJ, Kaech SM, Haining WN, Sarkar S, Kalia V, et al. Molecular signature of CD8+ T cell exhaustion during chronic viral infection. Immunity. 2007;27(4):670-84.

108. Parish IA, Rao S, Smyth GK, Juelich T, Denyer GS, Davey GM, et al. The molecular signature of CD8+ T cells undergoing deletional tolerance. Blood. 2009;113(19):4575-85.

109. Ahmed R, Salmi A, Butler LD, Chiller JM, Oldstone MB. Selection of genetic variants of lymphocytic choriomeningitis virus in spleens of persistently infected mice. Role in suppression of cytotoxic T lymphocyte response and viral persistence. J Exp Med. 1984;160(2):521-40.

Chapter 3: Discussion

Summary of main findings

Here, we utilized the Nur77-GFP system to investigate the functional implications of strong tonic TCR signaling in naive $CD8^+$ T cells. Nur77-GFP transgenic reporter mice enable visualization of T cell receptor (TCR) stimulation in T cells (1, 2). Moreover, T cells induce GFP expression even in response to weak agonist TCR signals (1). Hence, Nur77-GFP expression in the steady state reflects the weak tonic TCR signaling T cells experience from self-pMHC interactions (3). Such tonic TCR signals typically do not activate T cells but can influence the responsiveness to subsequent stimulation (4). Our study demonstrates that strong tonic TCR signaling in naive $CD8^+$ T cells (as indicated by high expression levels of Nur77-GFP) inversely correlated with the responsiveness to subsequent agonist TCR stimulation. Naive Nur77-GFP^{HI} $CD8^+$ T cells exhibited diminished upregulation of activation markers and reduced cytokine secretion upon stimulation relative to Nur77-GFP^{LO} cells. We further showed that strong tonic TCR signaling correlated with gene expression changes in naive $CD8^+$ T cells. Nur77-GFP^{HI} cells exhibited a gene expression profile associated with T cell activation and negative regulation. For instance, Nur77-GFP^{HI} naive $CD8^+$ T cells expressed higher protein levels of the E3 ubiquitin ligase, Cbl-b, an important negative regulator of T cell activation (5). Finally, we showed that Cbl-b-deficiency partly rescued the attenuated responsiveness observed in naive $CD8^+$ T cells that experience extensive tonic TCR signaling. Together, these results suggest that T cells that experience extensive TCR:self-pMHC signals induce adaptations that attenuate their responsiveness to subsequent agonist TCR stimulation. Hence, we propose a model where extensive tonic TCR signaling in naive $CD8^+$ T cells induces negative feedback mechanisms, which partly depends on the expression of Cbl-b (**Fig. 3.1**).

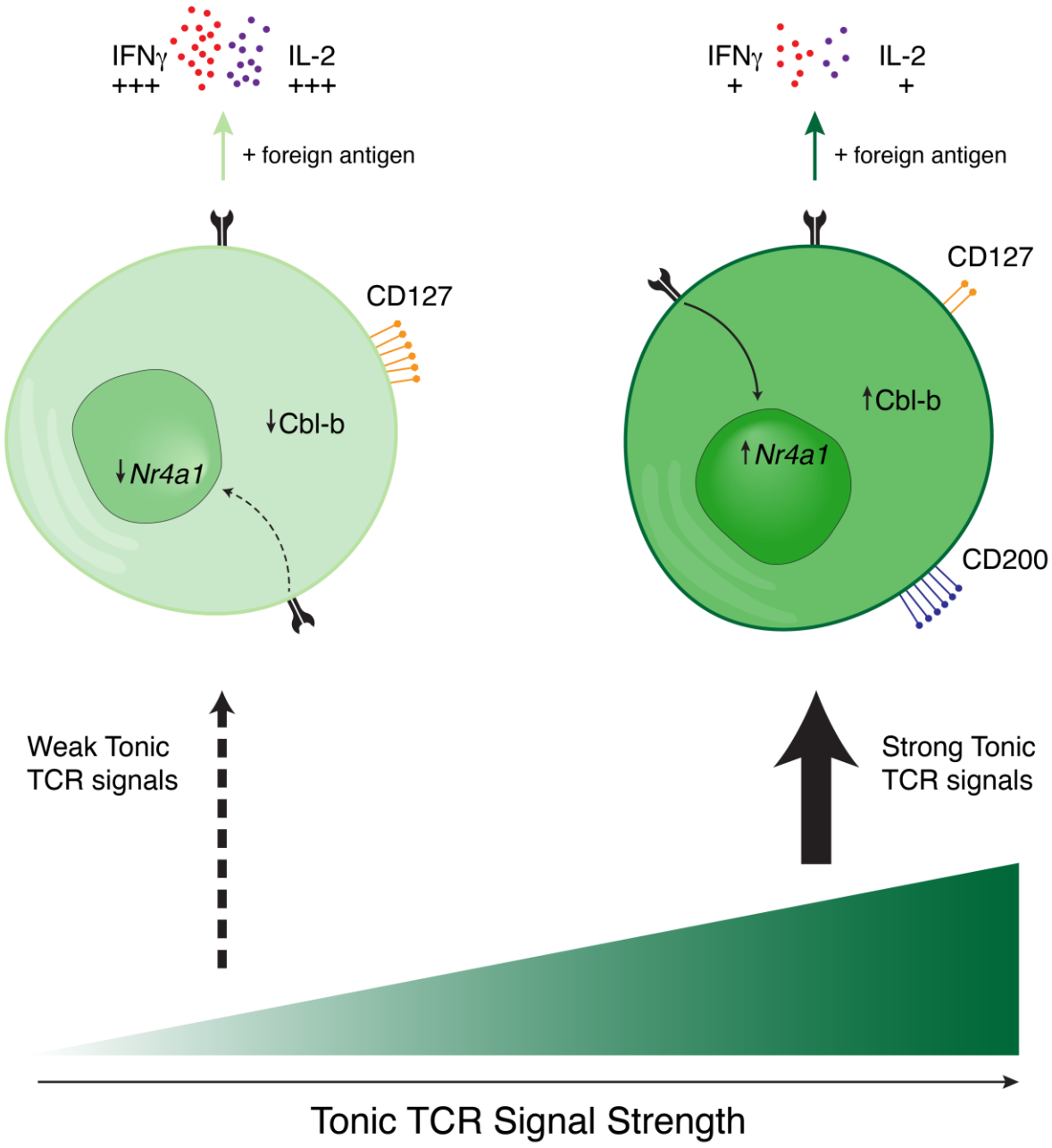

Fig. 3.1. Increased negative feedback in response to extensive tonic TCR signaling attenuates T cell responsiveness in naive CD8$^+$ T cells.

Extensive TCR:self-pMHC signals in naive CD8$^+$ T cells induce upregulation of *Nr4a1* and CD200 while downregulation of CD127 (right). Strong tonic signals are also associated with increased protein expression of Cbl-b, a negative regulator of T cell activation. Functionally, cells that experience stronger tonic TCR stimulation exhibit attenuated responsiveness upon subsequent

TCR agonist stimulation, manifested by diminished secretion of IFNγ and IL-2. The attenuated phenotype is partly rescued in the absence of Cbl-b, indicating that Cbl-b expression contributes to diminished responsiveness. Cells that experience weak tonic TCR signals express lower levels of *Nr4a1* and Cbl-b (left). However, weak tonic TCR signaling is associated with increased surface expression of CD127 and increased responsiveness to agonist TCR stimulation.

This thesis results in the context of the current paradigm

My results suggest that naive $CD8^+$ T cells that experience stronger TCR signals exhibit attenuated responsiveness even after several days of stimulation. Hence, the conclusion from our experiments using Nur77-GFP expression as a correlate marker of tonic TCR signaling in naive $CD8^+$ T cells is comparable to our previous studies on naive $CD4^+$ T cells (6, 7). However, our conclusion is vastly different from the current paradigm for $CD8^+$ T cells, which almost exclusively has relied on CD5 as a correlative marker of basal TCR signaling. It is important to point out that while there is a positive correlation between Nur77-GFP and CD5 expression on naive $CD8^+$ T cells, it is not a 1:1 correlation (**Fig. 2.S1 D**). In other words, the cellular composition of Nur77-GFP^{HI} cells differs from $CD5^{HI}$ cells, and Nur77-GFP^{LO} cells differ in composition from $CD5^{LO}$ cells. Therefore, our interpretation that these two markers solely reflect TCR signaling in a similar manner may be oversimplified. Thus, our understanding of hallmark studies utilizing these markers as correlate indicators of tonic TCR signaling could potentially change.

The factors that drive the underlying differences in cellular composition between Nur77-GFP^{HI} and $CD5^{HI}$ cells are unknown. One possibility is that external cues beyond TCR signals could influence Nur77-GFP or CD5 expression. Studies from Kristin Hogquist's laboratory established that Nur77-GFP expression in antigen-specific $CD8^+$ T cells is insensitive to the inflammatory environment of an infection in the absence of a cognate antigen (1). Moreover, IL-2 stimulation,

or transgenic expression of a constitutively active Stat5, did not induce increased expression of Nur77-GFP in T cells, suggesting that signaling from common γ-chain family cytokines does not contribute to Nur77-GFP expression (1). There is, however, evidence that cytokine signaling can modulate surface CD5 expression. Gagnon et al. showed that supplementing in vitro cultures with IL-7 alone or combined with IL-6 or IL-21 induces downregulation of CD5 surface levels on $CD8^+$ T cells after 24 hours (8). Studies also demonstrate that antibody-mediated ligation of CD5 can induce rapid endocytosis of surface CD5 on T cells in a clathrin-mediated manner (9). Hence, post-translational regulation of CD5 surface expression in $CD8^+$ T cells may occur independently of TCR signaling. On the other hand, GFP expression induced by the Nur77-GFP transgene may not undergo post-translational modifications. Therefore, in theory, the reason for some cells expressing high levels of Nur77-GFP but only intermediate levels of surface CD5 or why some Nur77-GFP^{MED} cells express low levels of surface CD5 could be due to CD5 downregulation induced by IL-7 signaling or CD5 ligand interactions, and thus independently of TCR signaling (**Fig. 2.S1 D**). It is also a possibility that cytokines and other proteins and ligands that induce signaling may indirectly affect cis-regulatory elements of CD5 and *Nr4a1,* which could induce transcription of these genes independently of TCR signaling in T cells and drive the Nur77-GFP^{MED} $CD5^{LO}$ phenotype.

A recent study highlighted the importance of dendritic cells (DCs) with a $CD5^{HI}$ surface phenotype for the antitumor response (10). Interestingly, depending on whether T cells were stimulated with cultures containing $CD5^+$ or CD5-deficient DCs, surface CD5 expression on the T cells correlated positively with CD5 expression on the DCs (10). Similarly, in a tumor model utilizing mice with CD5-deficient DCs, antigen-specific T cells expressed lower CD5 levels than in control mice (10). Hence, there is a possibility that surface CD5 on DCs might contribute to the regulation of CD5

expression in T cells. For instance, surface plasmon resonance studies suggested that CD5 can act as a homophilic ligand for itself (11). A careful characterization of the effects of cytokines and other stimuli on CD5 and Nur77 expression in $CD8^+$ T cells could shed light on whether cues beyond TCR stimulation can induce upregulation of these markers. For instance, culturing $CD5^{LO}$ naive $CD8^+$ T cells in the presence of anti-MHC I and $CD5^{HI}$ dendritic cells or recombinant CD5 protein could answer whether CD5 as a ligand can induce CD5 expression in the absence of TCR stimulation and could potentially explain why some naive $CD8^+$ T cells exhibit a Nur77-GFP^{LO} $CD5^{HI}$ phenotype (**Fig. 2.S1 D**). Such studies could tell us how functional heterogeneity is associated with TCR:self-pMHC signaling in the context of other contributing factors and may allow us to better predict the responsiveness of naive $CD8^+$ T cells based on cellular phenotype. A greater understanding of the underlying mechanisms that govern T cell responses might allow us to therapeutically influence desired T cell outcomes. For example, by understanding why naive Nur77-GFP^{LO} cells secrete more cytokines relative to GFP^{HI} cells, we could target those mechanisms therapeutically to increase cytokine secretion in T cells in the context of an infection or cancer and dampen cytokine secretion in T cells in the context of autoimmunity.

<u>The implications of tonic TCR signaling-induced negative feedback mechanisms on tolerance</u>

Central tolerance mechanisms prevent the selection of T cells bearing TCRs that react too strongly with self-pMHC during development (12). While central tolerance is efficient in deleting autoreactive thymocytes, it is not absolute (13). Peripheral T cell tolerance mechanisms, such as regulatory T cells and clonal deletion in the periphery or anergy, provide additional layers of defense (12). This dissertation describes a mechanism in naive $CD8^+$ T cells that may limit highly self-reactive naive T cells from responding inappropriately to self-pMHC by induced negative regulation.

Strong TCR:pMHC signals, without co-stimulation, induce T cell anergy (14). Moreover, upregulation of Cbl-b is apparent in anergic T cells and essential for their hyporesponsive state (15, 16). The fact that the Nur77-GFP distribution is unaffected by CD28 deficiency in $CD4^+$ and $CD8^+$ T cells suggests that tonic TCR signaling occurs independently of co-stimulation (1). Thus, TCR stimulation in the absence of co-stimulatory signals likely induces Cbl-b expression for both anergic and naive $CD8^+$ T cells that experience extensive tonic TCR signaling. At least for in vitro-generated anergic T cells, the hyporesponsiveness is reversible upon the addition of exogenous IL-2 (17). In this thesis, I detected a dramatically attenuated responsiveness of naive $CD8^+$ T cells that experienced extensive tonic TCR signaling in short-term in vitro assays but a much subtler difference during an in vivo response to a viral infection. Thus, it is possible that in an inflammatory environment with increased concentrations of cytokines such as IL-2, the hyporesponsiveness of naive $CD8^+$ T cells that experience strong tonic signals is reversed. Anergic T cells also exhibit attenuated IL-2 production (17). Furthermore, the IL-2 locus of anergized T cells is associated with altered chromatin modifications compared to effector T cells, such as diminished demethylation of the IL-2 promoter (18). Hypermethylation of the IL-2 promoter is also seen in recent thymic emigrants (RTEs) compared to mature naive T cells (19). RTEs have recently experienced strong TCR signals during development and exhibit attenuated IL-2 secretion upon stimulation (20). As hypermethylation of promoters correlates with transcriptional repression, strong TCR signaling may induce epigenetic modifications that limit IL-2 transcription in the context of anergic cells and RTEs (21). Considering these results, future studies could address whether strong tonic TCR signaling in naive T cells induce hypermethylation of cytokine loci, such as the IL-2 locus, resulting in diminished cytokine production upon activation.

The role of induced Cbl-b expression in response to chronic cognate antigen stimulation remains

incompletely described. Cbl-b-mediated negative regulation is not a typical mechanism associated with the functional impairment induced by chronic antigen stimulation (22). However, one study recently demonstrated the upregulation of Cbl-b mRNA in tumor-infiltrating lymphocytes that expressed the inhibitory receptors PD-1 and Tim-3 (23). Moreover, adoptive cell therapy using Cbl-b-deficient chimeric antigen receptor (CAR) T cells in a preclinical solid tumor model restored T cell function and promoted tumor regression (23). Our studies show that naive $CD8^+$ T cells that experience strong tonic TCR signals exhibit increased protein but similar transcript levels of Cbl-b, suggesting that TCR signaling can affect post-translational mechanisms of Cbl-b. Hence, Cbl-b upregulation in T cells that experience chronic antigen stimulation may thus be underappreciated in other models that solely characterized transcriptomic differences associated with exhausted T cells.

Our studies show that extensive tonic TCR signals in naive $CD8^+$ T cells can induce upregulation of Cbl-b under steady-state conditions and partly contributes to attenuated responsiveness. While naive $CD8^+$ TCR transgenic T cells that experience strong tonic TCR signals have a competitive disadvantage during the early phase of an immune response to a viral infection, the differences are subtle. Hence, the negative feedback mechanism induced by strong tonic TCR signaling may limit the autoreactive potential of T cell clones that were close to the self-reactivity threshold during development but escaped negative selection. At the same time, these self-reactive cells can seemingly participate in eliciting a robust protective immune response to a pathogen.

A shared functional feature between naive T cells that experience extensive tonic TCR signaling and anergic T cells is the reduced secretion of cytokines such as IL-2 and IFNγ upon TCR agonist stimulation (6, 17); (**Fig. 2.2** and **Fig. 2.3**). On the other hand, while anergic T cells exhibit almost complete proliferative impairment in response to agonist TCR stimulation and have a $CD44^{HI}$

surface phenotype, naive $CD44^{LO}$ T cells that encounter strong basal TCR signals can proliferate, although less extensively compared to naive T cells that experience weaker tonic TCR signaling (17, 24) and **Fig. 2.S2 G**). Hence, these results suggest that Nur77-GFP^{HI} cells are phenotypically different from anergic T cells, and the hypofunctional state of naive GFP^{HI} cells is less severe and more easily reversible than that of anergic T cells.

Implications of tonic TCR signaling on cell fate trajectories

In this thesis, I demonstrate that extensive tonic TCR signaling in naive $CD8^+$ T cells correlates with attenuated IL-2 secretion before cell division (**Fig. 2.2** and **Fig. 2.3**). If the bias in IL-2 secretion persists at later stages of the immune response, the level of basal TCR signaling naive $CD8^+$ T cells experience could have implications for effector T cell differentiation. For $CD4^+$ T cells, there is extensive evidence that tonic TCR signaling experienced by naive cells can influence lineage decisions of $CD4^+$ effector cells (4). For example, naive $CD4^+$ T cells encountering strong tonic TCR signals are more prone to differentiate into extrathymic regulatory T cells (6, 25, 26). Moreover, studies suggest tonic signaling in naive $CD4^+$ T cells affects the differentiation into $CD4^+$ follicular helper cells (T_{FH}) in viral infections (27, 28). Together, these studies suggest that tonic signaling can influence the diversification of the $CD4^+$ T cell response by shifting the probability of an individual T cell to differentiate into a specific T cell subset.

How tonic TCR signaling strength may influence the cell fate of naive $CD8^+$ T cells is less clear, but there is some evidence that tonic signaling may also diversify the $CD8^+$ T cell response. For instance, strong tonic signals and higher self-reactivity correlate with the differentiation of naive $CD8^+$ T cells into antigen-inexperienced memory-like T cells (AIMT) (29-33). Several studies demonstrate that AIMT cells can mediate immune protection in the absence of cognate antigens (30, 34, 35). Hence, strong tonic TCR signaling in $CD8^+$ T cells may modify the $CD8^+$ T cell

compartment by enhancing bystander T cell protection. Studies also show that the tonic signaling strength of naive $CD8^+$ T cells can affect antigen-specific T cell responses beyond the acute phase of the immune response. Ju et al. showed in a TCR transgenic system that $CD5^{LO}$ naive $CD8^+$ T cells that experienced weak tonic signaling persisted in greater frequencies and numbers relative to the $CD5^{HI}$ counterparts four months post an acute viral infection (36). The same study also showed a skewing of $CD5^{LO}$ cells toward central memory T cells (T_{CM}), whereas $CD5^{HI}$ cells were more likely to exhibit an effector memory (T_{EM}) phenotype (36). Therefore, the strength of tonic TCR signaling in naive $CD8^+$ T cells prior to activation may thus diversify both the composition and persistence of memory T cells.

While weak tonic TCR signals inversely correlate with an enhanced capacity of IL-2 secretion during the acute phase of an immune response, whether such biases persist during the later stages of the $CD8^+$ effector response remains unresolved. Although effector $CD8^+$ T cells produce robust levels of IFNγ during the peak of an acute viral infection, relatively few effector cells co-produce IL-2 (37). However, the transfer of $CD8^+$ effector cells from an acute immune response into secondary recipients subsequently challenged with a chronic viral infection revealed that $IL\text{-}2^+$ effectors were hyperfunctional relative to the $IL\text{-}2^-$ effector cells (37). Counterintuitively, IL-2 production in effector cells correlated with attenuated IL-2 signaling (37). IL-2 stimulation influences the $CD8^+$ T cell response by enhancing T cell effector differentiation (38). Moreover, continuous IL-2 signaling in mouse tumor models led to functional impairment of the $CD8^+$ T cell response (39). The resulting impairment depended on Stat5 as the knockdown of *Stat5* reversed the phenotype (39). Hence, persistent Stat5 activation seems detrimental to the $CD8^+$ T cell response during conditions of chronic antigen stimulation. If strong tonic signaling in naive $CD8^+$ T cells would also predict IL-2 production at later stages of the immune response, the resulting

attenuation of IL-2 signaling could potentially have implications for T cell functionality during chronic antigen stimulation. Future studies should thus address whether extensive tonic signaling in naive $CD8^+$ T cells may be detrimental to T cell outcomes during conditions of chronic antigen stimulation in vivo.

The implications of functional heterogeneity induced by tonic TCR signaling for adoptive cell therapy

Different adoptive T cell therapies have shown promising results in the context of cancer and in restoring T cell immunity against opportunistic viruses following allogeneic hematopoietic stem cell transplantation (40, 41). In both cases, isolated autologous or allogeneic T cells are generally expanded in vitro and reinfused into the patient (40, 41). An additional genetic manipulation step generating T cells expressing CARs targeting the B cell antigen CD19 has shown clinical success and has led to regulatory approval of multiple CAR T cell therapies against B cell malignancies (40). Most clinical studies of CD19 CAR T cell therapy have used a heterogenous mixture of isolated T cells as the starting point for downstream CAR transduction, expansion, and ultimately infusion (42). However, studies have demonstrated enhanced efficacy of CAR T cells in a humanized mouse model by modifying the cellular composition of the starting T cells (43). In this preclinical model, a cellular composition consisting of naive or T_{CM} $CD4^+$ T cells was superior over T_{EM} cells in inducing tumor regression (43). Using $CD8^+$ T cells as the starting material for CAR T cells showed that cell compositions of human $CD8^+$ T_{CM} cells were more efficacious than T_{EM} or naive cells (43). Furthermore, additional studies showed that CAR T cells from pre-enriched naive and memory T cells, rather than bulk T cells, were less likely to induce toxicities in a humanized mouse model (44).

Considering the favorable outcomes of using broad, defined T cell subsets as a starting material

for adoptive cell therapies in preclinical studies, it is tempting to speculate that more refined T cell compositions might be beneficial. Many studies demonstrate a correlation between weaker tonic TCR signals in $CD4^+$ T cells and enhanced responsiveness to TCR agonist stimulation (6, 7, 45, 46). Therefore, a potential strategy could be to pre-enrich naive or memory $CD4^+$ T cells that experience weaker tonic signaling and use these cells as the starting material for adoptive cell therapies instead of bulk T cells. Refining the cell composition by fluorescence-activated cell sorting based on the surface expression of markers that correlate with tonic signaling in human T cells would enable the strategy described above. It is unclear whether tonic TCR signals have such lasting effects on naive or memory T cells that they could impact the responsiveness of T cells after multiple rounds of clonal expansion. Nonetheless, since strong tonic signaling induces changes in chromatin accessibility in naive $CD4^+$ T cells, epigenetic modifications before the in vitro expansion of T cells may have long-lasting effects that could impact cell behavior in vivo (7, 28). Thus, my prediction would be that adoptive cell therapies using T cells that experience weaker tonic TCR signaling could exhibit enhanced effector functions and efficiency. Preclinical studies should, therefore, test whether such a hypothesis holds up.

Identifying new correlate markers of tonic TCR signaling in human T cells

Tonic TCR signaling induces phosphorylation of the CD3 ζ-chain, which enables recruitment of the signaling mediator ZAP-70 (47, 48). These events are evident in murine T cells isolated from secondary lymphoid organs where T cells experience TCR:self-pMHC signals but are non-detectable in T cells isolated from peripheral blood (49). Therefore, such biochemical analyses of human T cell subsets isolated from peripheral blood would likely fail in identifying cells that have experienced more extensive tonic TCR signaling. Studies have also aimed to investigate whether the expression of the correlate markers of TCR signaling in murine cells, Nur77 and CD5, can also

reflect TCR signaling in human T cells. TCR agonist stimulation induces Nur77 upregulation in human $CD4^+$ and $CD8^+$ T cells in a dose-dependent manner (50). However, the intracellular localization of Nur77 prevents isolating human T cell subsets based on Nur77 expression for functional assays. Recent studies have developed protocols to analyze the transcriptome of fixed T cells (51). Hence a reverse approach of sorting $Nur77^{LO}$ and $Nur77^{HI}$ cells to identify differentially expressed transcript levels of surface markers that correlate with TCR signaling in naive human T cells may be feasible. Likewise, single-cell transcriptomic analyses of naive human T cells could provide similar answers.

TCR ligation induces upregulation of surface CD5 on human $CD4^+$ T cells, indicating that CD5 expression can reflect TCR signaling in human T cells (52). $CD5^{HI}$ naive human $CD4^+$ T cells also express higher levels of Nur77 than $CD5^{LO}$ cells, albeit the difference is immensely subtle (52). Transcriptional analysis of naive human $CD4^+$ $CD5^{HI}$ and $CD5^{LO}$ cells revealed gene expression differences, but it is not clear that the transcriptome of $CD5^{HI}$ cells is indicative of increased TCR signaling (52). Hence, how well CD5 expression on naive human T cells reflects tonic TCR signaling is less clear. Another marker of interest to the field has been the chemokine receptor CXCR3, expressed on the surface of a subset of murine and human naive T cells (36, 53, 54). CXCR3 expression does not correlate with CD5 expression on naive human $CD8^+$ T cells, but $CXCR3^+$ cells exhibit a gene expression profile more similar to effector and memory T cells than $CXCR3^-$ cells (53). Hence, it is possible that increased TCR signaling in $CXCR3^+$ naive human $CD8^+$ T cells drives the expression of genes associated with T cell differentiation. Moreover, $CXCR3^+$ naive $CD8^+$ human T cells produce increased levels of IFNγ and IL-2 compared to the $CXCR3^-$ counterparts in response to acute stimulation, suggesting that the induced gene expression differences in $CXCR3^+$ cells may make them more poised to respond (53).

This dissertation shows that the expression of additional surface markers correlates with strong tonic TCR signaling in murine naive $CD8^+$ T cells. Nur77-GFP^{HI} cells exhibit increased CD200 expression and diminished expression of CD127. Moreover, I demonstrated that combining the two markers enhanced the separation between GFP^{LO} and GFP^{HI} naive $CD8^+$ T cells. Since human T cells express these surface proteins, they could potentially function as correlate markers of tonic TCR signaling in human T cells (55, 56).

A potential driver of the heterogeneity of tonic TCR signaling strength

I showed in this dissertation that the biases of Nur77-GFP expression in naive polyclonal $CD8^+$ T cells persist for at least seven days. This result is consistent with previous studies revealing that upon transferring $CD5^{LO}$ and $CD5^{HI}$ naive polyclonal $CD8^+$ or $CD4^+$ T cells into lymphoreplete recipients, cells maintain their skewed CD5 expression weeks post-transfer (57, 58). Hence, naive polyclonal T cells seemingly endure similar tonic TCR signaling strength over long periods. However, I also demonstrated that biases in Nur77-GFP expression in GFP^{LO} and GFP^{HI} TCR transgenic T cells do not persist for several weeks. One plausible explanation for these discording results is that TCR specificity is a primary driver of the levels of TCR signaling naive $CD4^+$ and $CD8^+$ T cells experience in the periphery. Hence, in a population of naive TCR transgenic $CD8^+$ T cells with identical TCR clonotypes, biases in tonic TCR signaling appear to be relatively short-lived. Previous studies by our laboratory showed that biases in Nur77-GFP expression of polyclonal CD4 single-positive (SP) thymocytes persist weeks later upon adoptive transfer to secondary recipients and maturation into naive T cells (7). Hence, perhaps due to TCR specificity, the level of TCR:self-pMHC signals that CD4 SP polyclonal thymocytes experience during development correlate with the level of tonic signaling mature naive cells experience in the periphery (7). Thus, the level of TCR signals that polyclonal $CD8^+$ T cells experience as CD8 SP

thymocytes may predict tonic TCR signaling levels in mature naive T cells. This hypothesis could be tested by adoptively transferring GFP^{LO} vs. GFP^{HI} CD8 SP polyclonal thymocytes into lymphoreplete recipients to investigate the Nur77-GFP distribution weeks later in naive T cells stemming from the GFP^{LO} or GFP^{HI} thymocytes. If biases in GFP distribution persist, it would suggest that TCR specificity is a primary driver of how much TCR:self-pMHC signaling T cells experience. Furthermore, it would indicate that the strength of those signals is set throughout a T cell's lifetime by the abundance of the self-antigens the T cell recognizes and/or the affinity of those TCR:self-pMHC interactions. If biases in GFP expression are non-existent, it would imply that TCR specificity is not an essential driver of tonic TCR signaling strength and that stochastic interactions with antigen-presenting cells and self-pMHC may drive Nur77-GFP heterogeneity.

Characterizing the effects of tonic TCR signaling in a polyclonal repertoire normalized for cognate pMHC affinity

Tetramer-based enrichment can facilitate the isolation of polyclonal antigen-specific T cells from the naive repertoire (59-61). Assuming that polyclonal $CD8^+$ T cells sustain a bias in the strength of tonic TCR signals, they experience as naive cells, TCR clonotypes experiencing weak or strong self-pMHC:TCR signals could potentially be isolated from Nur77-GFP mice for a given antigen using tetramers. We show in this dissertation that naive TCR transgenic $CD8^+$ T cells exhibit a wide range of Nur77-GFP fluorescent intensity, indicating that the strength of tonic signaling varies even in T cell populations that express identical TCRs. However, a primary driver of the heterogeneity of tonic TCR signals in the context of TCR transgenic cells could be that supraphysiological T cell frequencies lead to competition for self-antigens that generally do not occur for naive polyclonal T cells. A recent study compared the immune response in vivo of several T cell clones with similar specificity that exhibited differential self-reactivity, as measured by

surface CD5 expression in the naive state (33). However, whereas the TCR affinity to the cognate antigen correlated with the magnitude of the immune response, CD5 expression of naive T cells did not (33). Similarly, comparing three different T clones specific for the same *Toxoplasma gondii* epitope revealed that the affinity of the TCR/cognate pMHC ligand, as measured by surface plasmon resonance, was a better predictor of T cell expansion in response to infection compared to tonic TCR signaling strength indicated by steady-state CD5 and Nur77-GFP expression (62). These studies suggest TCR/cognate antigen affinity predicts the magnitude of the acute $CD8^+$ T cell response more reliably than tonic TCR signaling strength.

Hence, ideally, one would isolate numerous antigen-specific TCR clonotypes from the naive repertoire that exhibit similar affinity to cognate antigen but differential expression of steady-state Nur77-GFP. Such a study would be labor-intensive but is feasible by sequencing the naive TCR repertoire for a particular antigen, reexpressing the TCRs in retrogenic mice, and measuring the affinity to cognate pMHC by quantifying the dissociation rate of pMHC monomers (63-66). Moreover, fluorescent barcoding of T cells in retrogenic mice would allow tracking of the immune responses of distinct naive T cell clones co-transferred in small numbers into secondary recipients (67, 68). Assuming that naive $CD8^+$ T cells experience a bias in tonic TCR signaling that persists in the context of physiological precursor frequencies, such an experiment could allow the characterization of a "polyclonal" naive repertoire with similar affinity to cognate pMHC, but that experiences different levels of tonic signaling. Hence, such a system could ask how adaptations induced by tonic signaling shape the immune response while normalizing cognate pMHC affinity, which is an effective predictor of T cell responsiveness (69, 70). Based on the slight competitive advantage of Nur77-GFP^{LO} over GFP^{HI} TCR transgenic cells at the acute phase of a viral infection (**Fig. 2.S2 H** and **I**), my prediction would be that naive $CD8^+$ T cells that experience extensive

tonic TCR signaling but similar cognate pMHC affinity, would expand slightly less during a primary response. Furthermore, recent studies suggest that naive TCR transgenic $CD8^+$ T cells that experience weaker tonic TCR signaling exhibit enhanced self-renewal capacity as memory cells one month post an acute viral infection and also persist in increased numbers in secondary lymphoid organs four months post-infection relative to the naive cells that experience strong tonic signals (36). Therefore, $CD8^+$ T cell clones that encounter extensive tonic signaling as naive cells may mount a less robust secondary response than the naive counterparts that experience weaker tonic signaling due to reduced frequencies of persisting memory cells following an acute infection.

Conclusion

This dissertation aimed to determine the functional implications of tonic TCR signaling in naive $CD8^+$ T cells. By utilizing transgenic Nur77-GFP mice that visualize TCR signaling from self-pMHC interactions, I showed that strong tonic signaling correlates with an attenuated responsiveness of naive $CD8^+$ T cells that is partly dependent on Cbl-b, a negative regulator of TCR signaling. This study illustrates that extensive tonic TCR signals in naive $CD8^+$ T cells induce adaptations that mitigate T cell activation and early responsiveness but raises the question of how long such adaptations persist. The findings in this dissertation challenge the current paradigm that strong tonic TCR signals enhance the responsiveness of naive $CD8^+$ T cells to subsequent stimulation.

References

1. Moran AE, Holzapfel KL, Xing Y, Cunningham NR, Maltzman JS, Punt J, et al. T cell receptor signal strength in Treg and iNKT cell development demonstrated by a novel fluorescent reporter mouse. J Exp Med. 2011;208(6):1279-89.
2. Zikherman J, Parameswaran R, Weiss A. Endogenous antigen tunes the responsiveness of

naive B cells but not T cells. Nature. 2012;489(7414):160-4.

3. Myers DR, Zikherman J, Roose JP. Tonic Signals: Why Do Lymphocytes Bother? Trends Immunol. 2017;38(11):844-57.
4. This S, Rogers D, Mallet Gauthier E, Mandl JN, Melichar HJ. What's self got to do with it: Sources of heterogeneity among naive T cells. Semin Immunol. 2022;65:101702.
5. Lutz-Nicoladoni C, Wolf D, Sopper S. Modulation of Immune Cell Functions by the E3 Ligase Cbl-b. Front Oncol. 2015;5:58.
6. Zinzow-Kramer WM, Weiss A, Au-Yeung BB. Adaptation by naive CD4(+) T cells to self-antigen-dependent TCR signaling induces functional heterogeneity and tolerance. Proc Natl Acad Sci U S A. 2019;116(30):15160-9.
7. Zinzow-Kramer WM, Kolawole EM, Eggert J, Evavold BD, Scharer CD, Au-Yeung BB. Strong Basal/Tonic TCR Signals Are Associated with Negative Regulation of Naive CD4(+) T Cells. Immunohorizons. 2022;6(9):671-83.
8. Gagnon J, Chen XL, Forand-Boulerice M, Leblanc C, Raman C, Ramanathan S, et al. Increased antigen responsiveness of naive CD8 T cells exposed to IL-7 and IL-21 is associated with decreased CD5 expression. Immunol Cell Biol. 2010;88(4):451-60.
9. Lu X, Axtell RC, Collawn JF, Gibson A, Justement LB, Raman C. AP2 adaptor complex-dependent internalization of CD5: differential regulation in T and B cells. J Immunol. 2002;168(11):5612-20.
10. He M, Roussak K, Ma F, Borcherding N, Garin V, White M, et al. CD5 expression by dendritic cells directs T cell immunity and sustains immunotherapy responses. Science. 2023;379(6633):eabg2752.
11. Brown MH, Lacey E. A ligand for CD5 is CD5. J Immunol. 2010;185(10):6068-74.

12. Xing Y, Hogquist KA. T-cell tolerance: central and peripheral. Cold Spring Harb Perspect Biol. 2012;4(6).

13. Gallegos AM, Bevan MJ. Central tolerance: good but imperfect. Immunol Rev. 2006;209:290-6.

14. Goronzy JJ, Weyand CM. T-cell co-stimulatory pathways in autoimmunity. Arthritis Res Ther. 2008;10 Suppl 1(Suppl 1):S3.

15. Jeon MS, Atfield A, Venuprasad K, Krawczyk C, Sarao R, Elly C, et al. Essential role of the E3 ubiquitin ligase Cbl-b in T cell anergy induction. Immunity. 2004;21(2):167-77.

16. Nguyen TTT, Wang ZE, Shen L, Schroeder A, Eckalbar W, Weiss A. Cbl-b deficiency prevents functional but not phenotypic T cell anergy. J Exp Med. 2021;218(7).

17. Beverly B, Kang SM, Lenardo MJ, Schwartz RH. Reversal of in vitro T cell clonal anergy by IL-2 stimulation. Int Immunol. 1992;4(6):661-71.

18. Thomas RM, Saouaf SJ, Wells AD. Superantigen-induced CD4+ T cell tolerance is associated with DNA methylation and histone hypo-acetylation at cytokine gene loci. Genes Immun. 2007;8(7):613-8.

19. Berkley AM, Hendricks DW, Simmons KB, Fink PJ. Recent thymic emigrants and mature naive T cells exhibit differential DNA methylation at key cytokine loci. J Immunol. 2013;190(12):6180-6.

20. Fink PJ. The biology of recent thymic emigrants. Annu Rev Immunol. 2013;31:31-50.

21. Suzuki MM, Bird A. DNA methylation landscapes: provocative insights from epigenomics. Nat Rev Genet. 2008;9(6):465-76.

22. McLane LM, Abdel-Hakeem MS, Wherry EJ. CD8 T Cell Exhaustion During Chronic Viral Infection and Cancer. Annu Rev Immunol. 2019;37:457-95.

23. Kumar J, Kumar R, Kumar Singh A, Tsakem EL, Kathania M, Riese MJ, et al. Deletion of Cbl-b inhibits CD8(+) T-cell exhaustion and promotes CAR T-cell function. J Immunother Cancer. 2021;9(1).

24. Kalekar LA, Schmiel SE, Nandiwada SL, Lam WY, Barsness LO, Zhang N, et al. CD4(+) T cell anergy prevents autoimmunity and generates regulatory T cell precursors. Nat Immunol. 2016;17(3):304-14.

25. Martin B, Auffray C, Delpoux A, Pommier A, Durand A, Charvet C, et al. Highly self-reactive naive CD4 T cells are prone to differentiate into regulatory T cells. Nat Commun. 2013;4:2209.

26. Henderson JG, Opejin A, Jones A, Gross C, Hawiger D. CD5 instructs extrathymic regulatory T cell development in response to self and tolerizing antigens. Immunity. 2015;42(3):471-83.

27. Bartleson JM, Viehmann Milam AA, Donermeyer DL, Horvath S, Xia Y, Egawa T, et al. Strength of tonic T cell receptor signaling instructs T follicular helper cell-fate decisions. Nat Immunol. 2020.

28. Rogers D, Sood A, Wang H, van Beek JJP, Rademaker TJ, Artusa P, et al. Pre-existing chromatin accessibility and gene expression differences among naive CD4(+) T cells influence effector potential. Cell Rep. 2021;37(9):110064.

29. Rudd BD, Venturi V, Li G, Samadder P, Ertelt JM, Way SS, et al. Nonrandom attrition of the naive CD8+ T-cell pool with aging governed by T-cell receptor:pMHC interactions. Proc Natl Acad Sci U S A. 2011;108(33):13694-9.

30. White JT, Cross EW, Burchill MA, Danhorn T, McCarter MD, Rosen HR, et al. Virtual memory T cells develop and mediate bystander protective immunity in an IL-15-dependent

manner. Nat Commun. 2016;7:11291.

31. Drobek A, Moudra A, Mueller D, Huranova M, Horkova V, Pribikova M, et al. Strong homeostatic TCR signals induce formation of self-tolerant virtual memory CD8 T cells. EMBO J. 2018;37(14).

32. Miller CH, Klawon DEJ, Zeng S, Lee V, Socci ND, Savage PA. Eomes identifies thymic precursors of self-specific memory-phenotype CD8(+) T cells. Nat Immunol. 2020;21(5):567-77.

33. Paprckova D, Niederlova V, Moudra A, Drobek A, Pribikova M, Janusova S, et al. Self-reactivity of CD8 T-cell clones determines their differentiation status rather than their responsiveness in infections. Front Immunol. 2022;13:1009198.

34. Chu T, Tyznik AJ, Roepke S, Berkley AM, Woodward-Davis A, Pattacini L, et al. Bystander-activated memory CD8 T cells control early pathogen load in an innate-like, NKG2D-dependent manner. Cell Rep. 2013;3(3):701-8.

35. Lin JS, Mohrs K, Szaba FM, Kummer LW, Leadbetter EA, Mohrs M. Virtual memory CD8 T cells expanded by helminth infection confer broad protection against bacterial infection. Mucosal Immunol. 2019;12(1):258-64.

36. Ju YJ, Lee SW, Kye YC, Lee GW, Kim HO, Yun CH, et al. Self-reactivity controls functional diversity of naive CD8(+) T cells by co-opting tonic type I interferon. Nat Commun. 2021;12(1):6059.

37. Kahan SM, Bakshi RK, Ingram JT, Hendrickson RC, Lefkowitz EJ, Crossman DK, et al. Intrinsic IL-2 production by effector CD8 T cells affects IL-2 signaling and promotes fate decisions, stemness, and protection. Sci Immunol. 2022;7(68):eabl6322.

38. Pipkin ME, Sacks JA, Cruz-Guilloty F, Lichtenheld MG, Bevan MJ, Rao A. Interleukin-2

and inflammation induce distinct transcriptional programs that promote the differentiation of effector cytolytic T cells. Immunity. 2010;32(1):79-90.

39. Liu Y, Zhou N, Zhou L, Wang J, Zhou Y, Zhang T, et al. IL-2 regulates tumor-reactive CD8(+) T cell exhaustion by activating the aryl hydrocarbon receptor. Nat Immunol. 2021;22(3):358-69.

40. Hiltensperger M, Krackhardt AM. Current and future concepts for the generation and application of genetically engineered CAR-T and TCR-T cells. Front Immunol. 2023;14:1121030.

41. Papadopoulou A, Alvanou M, Karavalakis G, Tzannou I, Yannaki E. Pathogen-specific T Cells: Targeting Old Enemies and New Invaders in Transplantation and Beyond. Hemasphere. 2023;7(1):e809.

42. Busch DH, Frassle SP, Sommermeyer D, Buchholz VR, Riddell SR. Role of memory T cell subsets for adoptive immunotherapy. Semin Immunol. 2016;28(1):28-34.

43. Sommermeyer D, Hudecek M, Kosasih PL, Gogishvili T, Maloney DG, Turtle CJ, et al. Chimeric antigen receptor-modified T cells derived from defined CD8+ and CD4+ subsets confer superior antitumor reactivity in vivo. Leukemia. 2016;30(2):492-500.

44. Arcangeli S, Bove C, Mezzanotte C, Camisa B, Falcone L, Manfredi F, et al. CAR T cell manufacturing from naive/stem memory T lymphocytes enhances antitumor responses while curtailing cytokine release syndrome. J Clin Invest. 2022;132(12).

45. Milam AAV, Bartleson JM, Donermeyer DL, Horvath S, Durai V, Raju S, et al. Tuning T Cell Signaling Sensitivity Alters the Behavior of CD4(+) T Cells during an Immune Response. J Immunol. 2018;200(10):3429-37.

46. Milam AAV, Bartleson JM, Buck MD, Chang CH, Sergushichev A, Donermeyer DL, et

al. Tonic TCR Signaling Inversely Regulates the Basal Metabolism of CD4(+) T Cells. Immunohorizons. 2020;4(8):485-97.

47. van Oers NS, Tao W, Watts JD, Johnson P, Aebersold R, Teh HS. Constitutive tyrosine phosphorylation of the T-cell receptor (TCR) zeta subunit: regulation of TCR-associated protein tyrosine kinase activity by TCR zeta. Mol Cell Biol. 1993;13(9):5771-80.

48. van Oers NS, Killeen N, Weiss A. ZAP-70 is constitutively associated with tyrosine-phosphorylated TCR zeta in murine thymocytes and lymph node T cells. Immunity. 1994;1(8):675-85.

49. Stefanova I, Dorfman JR, Germain RN. Self-recognition promotes the foreign antigen sensitivity of naive T lymphocytes. Nature. 2002;420(6914):429-34.

50. Ashouri JF, Weiss A. Endogenous Nur77 Is a Specific Indicator of Antigen Receptor Signaling in Human T and B Cells. J Immunol. 2017;198(2):657-68.

51. Nicolet BP, Guislain A, van Alphen FPJ, Gomez-Eerland R, Schumacher TNM, van den Biggelaar M, et al. CD29 identifies IFN-gamma-producing human CD8(+) T cells with an increased cytotoxic potential. Proc Natl Acad Sci U S A. 2020;117(12):6686-96.

52. Sood A, Lebel ME, Dong M, Fournier M, Vobecky SJ, Haddad E, et al. CD5 levels define functionally heterogeneous populations of naive human CD4(+) T cells. Eur J Immunol. 2021;51(6):1365-76.

53. De Simone G, Mazza EMC, Cassotta A, Davydov AN, Kuka M, Zanon V, et al. CXCR3 Identifies Human Naive CD8(+) T Cells with Enhanced Effector Differentiation Potential. J Immunol. 2019;203(12):3179-89.

54. Jergovic M, Coplen CP, Uhrlaub JL, Besselsen DG, Cheng S, Smithey MJ, et al. Infection-induced type I interferons critically modulate the homeostasis and function of CD8(+)

naive T cells. Nat Commun. 2021;12(1):5303.

55. Elshal MF, Aldahlawi AM, Saadah OI, McCoy JP. Expression of CD200R1 and its Ligand CD200 on T-helper Lymphocytes of Pediatric Patients with Ulcerative Colitis and Crohn's Disease. Clin Lab. 2016;62(8):1521-9.

56. Appay V, van Lier RA, Sallusto F, Roederer M. Phenotype and function of human T lymphocyte subsets: consensus and issues. Cytometry A. 2008;73(11):975-83.

57. Mandl JN, Monteiro JP, Vrisekoop N, Germain RN. T cell-positive selection uses self-ligand binding strength to optimize repertoire recognition of foreign antigens. Immunity. 2013;38(2):263-74.

58. Fulton RB, Hamilton SE, Xing Y, Best JA, Goldrath AW, Hogquist KA, et al. The TCR's sensitivity to self peptide-MHC dictates the ability of naive CD8(+) T cells to respond to foreign antigens. Nat Immunol. 2015;16(1):107-17.

59. Altman JD, Moss PA, Goulder PJ, Barouch DH, McHeyzer-Williams MG, Bell JI, et al. Phenotypic analysis of antigen-specific T lymphocytes. Science. 1996;274(5284):94-6.

60. Hataye J, Moon JJ, Khoruts A, Reilly C, Jenkins MK. Naive and memory CD4+ T cell survival controlled by clonal abundance. Science. 2006;312(5770):114-6.

61. Obar JJ, Khanna KM, Lefrancois L. Endogenous naive CD8+ T cell precursor frequency regulates primary and memory responses to infection. Immunity. 2008;28(6):859-69.

62. Swee LK, Tan ZW, Sanecka A, Yoshida N, Patel H, Grotenbreg G, et al. Peripheral self-reactivity regulates antigen-specific CD8 T-cell responses and cell division under physiological conditions. Open Biol. 2016;6(11).

63. Holst J, Szymczak-Workman AL, Vignali KM, Burton AR, Workman CJ, Vignali DA. Generation of T-cell receptor retrogenic mice. Nat Protoc. 2006;1(1):406-17.

64. Nauerth M, Weissbrich B, Knall R, Franz T, Dossinger G, Bet J, et al. TCR-ligand koff rate correlates with the protective capacity of antigen-specific CD8+ T cells for adoptive transfer. Sci Transl Med. 2013;5(192):192ra87.

65. Hebeisen M, Schmidt J, Guillaume P, Baumgaertner P, Speiser DE, Luescher I, et al. Identification of Rare High-Avidity, Tumor-Reactive CD8+ T Cells by Monomeric TCR-Ligand Off-Rates Measurements on Living Cells. Cancer Res. 2015;75(10):1983-91.

66. Nauerth M, Stemberger C, Mohr F, Weissbrich B, Schiemann M, Germeroth L, et al. Flow cytometry-based TCR-ligand Koff -rate assay for fast avidity screening of even very small antigen-specific T cell populations ex vivo. Cytometry A. 2016;89(9):816-25.

67. Grassmann S, Sun JC, Buchholz VR. Retrogenic Color-Barcoding for Fate Mapping of Single Innate Lymphocytes. Methods Mol Biol. 2022;2463:117-27.

68. Grassmann S, Pachmayr LO, Leube J, Mihatsch L, Andrae I, Flommersfeld S, et al. Distinct Surface Expression of Activating Receptor Ly49H Drives Differential Expansion of NK Cell Clones upon Murine Cytomegalovirus Infection. Immunity. 2019;50(6):1391-400 e4.

69. Zhong S, Malecek K, Johnson LA, Yu Z, Vega-Saenz de Miera E, Darvishian F, et al. T-cell receptor affinity and avidity defines antitumor response and autoimmunity in T-cell immunotherapy. Proc Natl Acad Sci U S A. 2013;110(17):6973-8.

70. Hombrink P, Raz Y, Kester MG, de Boer R, Weissbrich B, von dem Borne PA, et al. Mixed functional characteristics correlating with TCR-ligand koff -rate of MHC-tetramer reactive T cells within the naive T-cell repertoire. Eur J Immunol. 2013;43(11):3038-50.